Master Thesis, Department of Geosciences

Development and distribution of palsas in Finnmark, Northern Norway, for the period 1950s to 2010s

Amund Frogner Borge

UNIVERSITY OF OSLO

FACULTY OF MATHEMATICS AND NATURAL SCIENCES

Development and distribution of palsas in Finnmark, Northern Norway, for the period 1950s to 2010s

Amund Frogner Borge

Master Thesis in Geosciences

Discipline: Physical Geography

Department of Geosciences

Faculty of Mathematics and Natural Sciences

University of Oslo

1. June 2015

Supervisor(s): **Sebastian Westermann (UiO) – Bernd Etzelmüller (UiO).**

Front page: Fellow student Kenneth Bahr sitting on top of a palsa in Áidejávri, Finnmark. Photo by Amund F. Borge.

This work is published digitally through DUO – Digitale Utgivelser ved UiO

http://www.duo.uio.no

It is also catalogued in BIBSYS (http://www.bibsys.no/english)

Abstract

Palsas are permafrost mounds in mires with a core of ice, widespread situated in the sporadic permafrost zone. A tendency towards decay of palsa mires since the second half of the 20th century has been observed in Fennoscandia. This thesis is investigating the lateral changes and the distribution of palsas in Finnmark by utilizing multiple aerial images from 1950s onwards and by Geomorphological Distribution Modelling. Aerial images in a north-south transect from Lakselv, Suossjavri and Goatheluoppal reveal a total decrease in areas of palsas by 48 %, 33 % and 71 %, respectively, wherease the rate of degradation has increased since the start of 2000. Signs of degradation on aerial images from the 1950s suggest that the tendency of decay started at latest in the 1950s, and probably already from the warming period in the 1920s-1930s. The most important factors for the increase in rate of degradation are most likely the increase in both temperature and precipitation observed in the last few decades.

By utilizing Generalized Linear Model, the probability of presence of palsas increase with 1) decreasing freezing degree days, 2) a humped (nonlinear) curve of thawing degree days, 3) decreasing mean annual precipitation, 4) increasing mean summer precipitation, 5) increasing area of mire and 6) a humped (nonlinear) curve of area of water. Hierarchical Partitioning indicates that the climate variables are the most important group of variables to independently explain the distribution of palsas. The total area of palsas in Finnmark in 2010 based on GDM and aerial images is estimated to be roughly 0.3 % of the total area of Finnmark. By utilizing the degradation rate and the total area of palsas in Finnmark, the total amount of potential carbon gas release in form of CH_4 from decay of palsas from 1960 to 2010 was estimated to be less than three times as much as the human emissions of CH_4 in Finnmark for one year (2010), and thus of rather minor importance in the global carbon cycle.

Acknowledgements

First of all, I want to thank my supervisors Sebastian Westermann and Bernd Etzelmüller for all help with my thesis. Thank you Sebastian, for introducing me to palsas when I wanted to study glaciers. Palsas were much more fascinating than I thought! You have always time to explain stuff when I show up at your office. Thanks both of you for memorable trips to Finnmark, Troms, Finland and of course Sapporo! Bernd, you are definitely the coolest prof. I know, and when I am done with my master degree, I am finaly going to watch all of the Star Wars movies.

Thanks to Kristin Sæterdal Myhra and Celinè Steiger for help with fieldwork in Suossjavri in August 2014. A special thanks to Celinè who I was so lucky to be field assistant for in Lyngsalpene in Troms. Steindalen was amazing and we had a fun trip, even if I made you frustrated because I was driving so slow when we was heading back to Oslo :P

Furthermore, a special thank goes to my superb field assistant Kenneth Bahr who was with me in the mires at Suossjavri and around for five days in August 2014. Lot`s of beer, but even more mosquitos and heavy walking in mires. Never any complaints and with a lot of guts, that's you Kenneth boy! Also thanks for all your comments and corrections when reading through my long thesis.

My uncle Bjørn Frogner has been so kind of correcting my hopeless English grammar. Thank you for all your help, I have really appreciated it!

Thanks to Trond Eiken for all technical help with GPS equipment and ordering of aerial images, and for tips about georeferencing of the images.

Thanks to all of my fellow students at room 219. We`ve had a lot of fun and helped each other, good luck with the future! ☺

I am greatful of all the nice experiences and new friendships I have got on courses in Troms/Finland, Svalbard and Japan. Thanks to my travelling companion Ingvild Solheim for some great days in crazy Tokyo and to both Celine and Ingvild for some nice days of skiing in Niseko.

Thanks to Kjersti Gisnås who offered some of the climate data for me that she had processed based on the SeNorge climate data.

Thanks to Ingvild and Irene Brox Nilsen for reading through my thesis and giving comments and corrections.

A last thank goes to my mum and dad who always have their home open to me when I don't have any money left because I was quiting my part-time work so I could have more time to work with my master thesis.

Table of contents

1. Introduction

1.1 Permafrost, palsas and climate

According to the Intergovernmental Panel on Climate Change (IPCC, 2014), it is today unequivocal that the climate system is warming. Especially Arctic and subarctic regions are considered to be vulnerable to climatic changes, and the largest temperature increase has been observed at high latitudes (IPCC, 2014). The increase in temperature has resulted in increasing permafrost temperatures in most regions since the early 1980s (Vaughan et al., 2013), with increasing permafrost temperatures in most of North America (Smith et al., 2010), Russia (Romanovsky et al., 2010) and central Asia (Zhao et al., 2010) for the last few decades. Warming of permafrost in the Nordic area has been evident since the beginning of 2000 (Christiansen et al., 2010)

Permafrost is by the International Permafrost Association (IPA, 2014) defined as *"ground (soil or rock and included ice or organic material) that remains at or below 0 °C for at least two consecutive years"*. Since permafrost is a thermal condition of the ground, permafrost landforms are highly dependent on climatic conditions. In Fennoscandia, four landforms indicate current of former permafrost conditions: palsas, rock glaciers, ice wedge polygons and ice-cored moraines (Lilleøren and Etzelmüller, 2011). Of these landforms, palsas are by far the most common in Fennoscandia, with widespread abundance in the sporadic permafrost zone in Northern Norway, Finland and Sweden (Seppälä, 1986). A palsa is a subarctic permafrost landform in mires defined by van Everdingen (1998) as *"a peaty permafrost mound possessing a core of alternating layers of segregated ice and peat or mineral soil material"*. Normally, palsas demarcate the outer limit for permafrost in a given area (Sollid and Sørbel, 1998) and are found in a narrow climate envelope (Parviainen and Luoto, 2007). Thereby, the permafrost temperature in palsas is relatively warm, with a mean annual ground temperature close to 0 °C in Fennoscandia (Christiansen et al., 2010). Therefore, several studies predict palsas to be vulnerable to future climatic conditions (e.g. Aalto et al., 2014; Fronzek et al., 2006; Parviainen and Luoto, 2007). In this quantitative study, the lateral development from 1950s to 2010s and the distribution of palsas in Finnmark are investigated by interpretation of aerial images and by Geomorphological Distribution Modelling (GDM).

Further, potential emissions of CH_4 and CO_2 from thawing palsas are roughly estimated and discussed.

In Fennoscandia, degradation of some palsa mires related to an increase in temperature have been observed in northern Sweden (Zuidhoff and Kolstrup, 2000), Dovrefjell (Matthews et al., 1997; Sollid and Sørbel, 1974, 1998) and Ferdesmyra in western Finnmark (Hofgaard and Myklebost, 2014) . Degradation of palsas will potentially affect local wildlife, vegetation and hydrology, and possibly be a substantial carbon source. Around 50 % of the organic carbon stored below ground is situated in the northern hemisphere permafrost zone (Tarnocai et al., 2009). Thus, earlier recognized as a carbon sink, an increase in carbon fluxes (especially CH_4) to the atmosphere from the decomposition of carbon when organic–rich permafrost thaws, is expected to turn the subarctic to a carbon source (Koven et al., 2011; Schaefer et al., 2011). Furthermore, palsa mires have a biologically distinct and heterogeneous environment and are especially known for their rich bird life (Luoto et al., 2004b). Thawing palsas may affect the bird populations, as the environment in the palsa mires become more homogenous (Luoto et al., 2004b). In river hydrology, several studies suggest permafrost thawing as one contributing reason to an widely observed increase in river low-flow for subarctic rivers (e.g. Bense et al., 2012; St Jacques and Sauchyn, 2009; Walvoord and Striegl, 2007). An increase in river low-flow has also been observed in Fennoscandia (Sjöberg et al., 2013; Wilson et al., 2010).

In this context, more knowledge about the rate of degradation and the distribution of palsas are essential to quantify the consequences of decaying palsas.

1.2 Previous research on palsas in Fennoscandia

Most of the palsa mires in Fennoscandia are located in northern Norway. Still, little research have/has been conducted on palsas in Norway, compared to both Sweden and Finland. Most of the research on palsas in Norway are from the few palsa mires in Dovrefjell, in southern part of Norway (e.g. Matthews et al., 1997; Sollid and Sørbel, 1974, 1998). The first investigations of palsa mires in northern Norway were mainly by Swedish researchers (e.g. Svensson, 1961; Åhman, 1977). An exception is the biologist Karl-Dag Vorren who performed stratigraphical analyses and dating of palsas (e.g. K. Vorren, 1972; K. D. Vorren, 1979; K. D. Vorren and Vorren, 1975). In 2004, the Norwegian Institute for Nature Research (NINA) started a surveillance program of palsa mires in Norway (Hofgaard, 2004). This

surveillance program monitors six selected palsa mires in both southern and northern Norway. In northern Norway, this surveillance includes the palsa mires Osteojaggi in Troms and Goatheluoppal and Ferdesmyra in Finnmark (Hofgaard, 2004).

Swedish researchers had a dominance of investigations of palsas and related forms in Fennoscandia in the 1950s and 1960s (e.g. Lundqvist, 1951, 1953; Svensson, 1961, 1969; Wramner, 1965). From the 1980s onwards, the dominance of palsa research has been conducted in Finland. In particular, the Finnish geographer Matti Seppälä has dedicated his life to palsas with numerous studies concerning the effect of snow cover (Seppälä, 1982, 1990a, 1994), surface abrasion by wind action (Seppälä, 2003) the concept of cyclic development (Seppälä, 1986), dating of palsas (Seppälä, 2005) and the role of buoyancy in the formation of palsas (Seppälä and Kujala, 2009).

In geomorphology, statistically based modelling has a relatively short history compared with biological research (Hjort and Luoto, 2013). Since the mid-1990s, the use of geographical information systems and statistical modelling in geomorphology has increased rapidly. In periglacial research, simple statistical methods such as multiple logistic regression with the use of topographic and/or land cover variables were common in the early 2000 (e.g. Gruber and Hoelzle, 2001; Lewkowicz and Ednie, 2004; Luoto and Seppälä, 2002, 2003). As the accuracy of climate data has increased, there has been an increasing number of studies in recent years that include climate variables. However, in periglacial research, most of the studies included only climate variables (e.g. Fronzek et al., 2006; Luoto et al., 2004a) as they influence on a larger scale than topographic and land cover variables. Recently, integrating climate variables together with topographic and land cover variables for prediction of different earth surface processes (including palsa mires) have been successfully implemented (Aalto and Luoto, 2014).

In later years, the statistical models used in GDMs have become increasingly more advanced and sophisticated (e.g. Aalto and Luoto, 2014; Hjort et al., 2014; Luoto and Hjort, 2005; Marmion et al., 2008, 2009) Thus, statistical modelling has increased the knowledge of the complex interaction between palsas and the environment.

1.3 Objectives

The objectives of this thesis are as follows:

1. Quantify the degradation of palsas in Finnmark from the 1950s until the 2010s.
2. Quantify today's distribution of palsas in Finnmark.
3. Relate the distribution and degradation of palsas with climatic, topographic and land cover variables.
4. Give a rough estimate of potential gas release of CH_4 and CO_2 from palsa mires in Finnmark between 1960 until 2010.

Based on these objectives, an overview of today's situation of palsas in Finnmark is presented, with some consequences of the degradation relevant for other research fields. To address the first objective, multiple aerial images from four (only from 1959 and 2008 for Lakselv) time periods (1950s, 1980s, 2003 and 2010s) are utilized to delineate the area of palsas in three study sites in a north-south transect in Finnmark. These study sites are (from north to south): Lakselv, Suossjavri and Goatheluoppal (see Figure 3 for position of the study sites).

As few ground surveys have been conducted, the term palsas used in this thesis usually includes all types of palsas (including peat plateaus) and lithalsas. Exceptions are when simple palsas (such as dome palsas) are compared to peat plateaus or lithalsas.

The second objective is addressed by GDM, using the statistical method of Generalized Linear Model (GLM). This method gives also indications of the significance of the different environmental variables. Because of problems with multicollinearity when using GLM (Hjort and Luoto, 2013), Hierarchial Partitioning (HP) is also utilized as a complementary method to reveal the independent effect of the different variables to the distribution of palsas.

Furthermore, climate data from nearby meteorological stations of the three study sites is analyzed to investigate which climate variables could be the driving agent of the lateral changes of palsas.

To address the last objective, rough estimates of the potential CH_4 and CO_2 release for the period 1960-2010 are estimated with a simple model by knowing the quantity of palsas and the degradation rate.

1.4 Thesis structure

The first part of Chapter 2 gives an overview of general theory about palsas, which factors that control the distribution of palsas and the hypothesis of the "cyclicity" of palsas. The concepts of GDM are presented in Section 2.2, together with theory about GLM and HP.

The study area is described in Section 3, with an overview of the geographic and climatic setting of Finnmark, including knowledge on the extent of permafrost in the region.

All methodologies utilized in this thesis are outlined in Chapter 4. Thus, the process of delineation of palsas by aerial images in a Geographical Information System (GIS) framework (4.1), the process of GDM and HP (4.2) and the process of estimating a rough estimate of carbon gas release from thawing palsas (4.3) are explained in this chapter.

Chapter 5 contains all the results of the work with this thesis. Processed meteorological data obtained from meteorological stations in Finnmark are presented in Section 5.1. Observations from fieldwork in Suossjavri during summer 2014 are given in Section 5.2. Section 5.4 starts with some contemporary results from the GDM process, continuing with the results of HP, the final GLM and the probability map of palsas. The final GLM and the probability map are evaluated at the end of the chapter, and the total area of palsas in Finnmark is estimated. The results of the simple model of carbon gas release are given in Section 5.5.

Discussion of the methodology and the results are found in Chapter 6. Section 6.1 discusses the methodological aspect and the results of the delineation process, while Section 6.2 concerns the process of GDM, including discussion of input data, the final GLM and the probability map, the importance of variables and the results of HP. The end of Section 6.2 gives a short evaluation of the plausibility of the estimated total area of palsas. The results of the simple model of carbon gas release are discussed in Section 6.3.

Chapter 7 summarizes the main results and the conclusions drawn from the discussion.

Information about aerial images utilized in this thesis is presented in the Appendix.

2. Theoretical background

The theoretical background consists of general theory about permafrost and palsas (2.1) and statistical prediction of landforms (2.2). Section 2.1 includes concepts and definitions relevant for permafrost, with information about some important factors influencing the permafrost temperature (2.1.1). Furthermore, it contains the morphology of palsas, lithalsas and peat plateaus (2.1.2), the distribution of palsas and controlling factors (2.1.3) and the origin, development and degradation of palsas (2.1.4). Section 2.2 contains the proper procedure in GDM (2.2.1), the general theory of GLMs (2.2.2), evaluation measures of GDM (2.2.3) and a simple explanation of HP (2.2.4).

2.1 Permafrost and palsas

2.1.1 Permafrost and climate – concepts, definitions and important factors

Permafrost is by definition totally controlled by the thermal regime in the ground, which is influenced by air temperature, thermal properties of the ground, and the geothermal heat flux from below. Permafrost has a slow response to climatic changes at the surface, and the present state of permafrost is thus partly a function of former climatic conditions (C. Harris et al., 2009). According to C. Harris et al. (2009) the propagation of a warming trend through the entire permafrost thickness is typically measured in decades to centuries, even in thin discontinuous permafrost. Since parts of the ground thaws during summer in regions that experience temperatures above 0 °C, an active layer (AL) is apparent above the permafrost table. The active layer is defined as the upper part of the ground that experiences seasonally thawing and freezing (van Everdingen, 1998).

Figure 1 by Smith and Riseborough (2002) illustrates the link between air temperature and ground temperature. The difference in temperature between the mean annual air temperature (MAAT) and the mean annual ground surface temperature (MAGST) is termed the surface offset, a result of the vegetation in the summer and the snow cover during winter (Smith and Riseborough, 2002). Vegetation has several effects on the surface temperature, with different effects due to different types of vegetation. During summer, dense vegetation decreases the

radiation reaching the ground surface and thereby depressing the temperature (vegetation offset). During winter, vegetation plays a crucial role in controlling the depth and persistence of the snow cover (Smith and Riseborough, 2002).

As a result of the low thermal conductivity of snow, a snow layer insulate the ground from cold winter temperatures, resulting in higher ground-surface temperatures than air temperatures. This offset in temperature during winter is called the nival offset (Smith and Riseborough, 2002). The total annual effect of vegetation and nival offsets are termed the surface offset. It is usually positive (e.g. higher temperatures at the ground surface than in the air – see Figure 1) due to the importance of snow (Smith and Riseborough, 2002).

The temperature in the upper parts of the ground is sometimes decreasing with depth, as visible on Figure 1. This difference in temperature between MAGST and the temperature at the top of the permafrost (TTOP) is called the thermal offset (Smith and Riseborough, 2002). This difference is apparent due to a different conductivity in water-rich ground between summer and winter. Water in its liquid state has a relatively low thermal conductivity compared with its solid state (Smith and Riseborough, 2002). Thus, water-rich sediments, peat or soils have the possibilities of permafrost conditions even when MAGST is > 0 °C. A measure of the difference between summer and winter conductivity is the conductivity ratio, which is the ratio of summer conductivity by winter conductivity (Smith and Riseborough, 2002). A low conductivity ratio indicate a possible thermal offset. While organic soils have a great range in conductivity ratio (from less than 0.3 to 1) from saturated to dry conditions, conductivity ratio is usually close to 1 for bedrock (Smith and Riseborough, 2002). Thus, usually no thermal offset exist for bedrock.

The mean annual ground temperature (MAGT) is the temperature in the ground at an unspecified depth, but often at the depth where there are practically no annual fluctuations in ground temperature: depth of the zero annual amplitude (DZAA) (van Everdingen, 1998). Below the DZAA, the ground temperature is increasing as a response to the geothermal heat flow from below. The temperature gradient downward from this point is termed the geothermal gradient (see Figure 1).

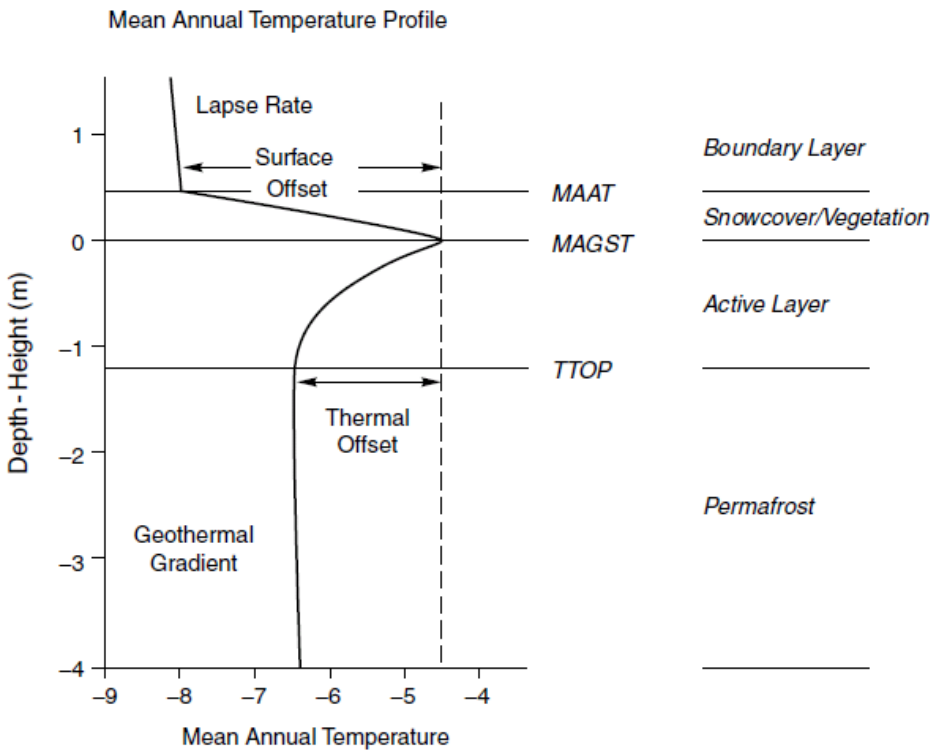

Figure 1: A general mean annual temperature profile through air, surface layer and the ground, reflecting the relationship between air temperature and permafrost. Figure from Smith and Riseborough (2002).

2.1.2 Palsas, peat plateaus and lithalsas – morphology

The morphology of palsas has a huge variety. Different types of palsas described in the literature are e.g. esker palsas, string palsas, cluster palsas, dome shaped palsas, conical palsas, palsa complexes and palsa/peat plateaus (Pissart, 2013). Furthermore, palsas are distinguished by content of minerals or peat in the cover: mineral palsas (without any peat cover) and organic palsas (with a peat cover) (Dionne, 1978). Today, the term lithalsas proposed by S. Harris (1993, references therein Pissart, 2013) has replaced the term of mineral palsas, as the definition of palsas originally included the cover of peat.

The height of palsas is normally between 0.5 m up to 7 m in Fennoscandia (Matti Seppälä, 2006). Peat plateaus, as a special case of palsas, are flat, wide and only elevated 1-2 m above the surrounding mire (Sollid and Sørbel, 1998). The length of single palsas can be of several

hundred meters. In the case of peat plateaus, an area of a square km can be covered (Matti Seppälä, 2006).

2.1.3 Distribution of palsas and controlling factors

In Fennoscandia, the main region of palsa mires are in a relatively narrow belt in a southwest-northeast direction between roughly 67° N and 70° N latitudes (Luoto et al., 2004a). According to Luoto et al. (2004a), the Scandinavian mountain range controls the climate and the distribution of palsa mires in the region, as over 90 % of the palsa mires are located east of the mountain range where a rain shadow is present. In Norway, palsas are particularly abundant in the inland regions of Troms and Finnmark (J. L. Sollid and Sørbel, 1998). In continuous permafrost zones, no palsas are present as no water from below can feed the ice lenses (Pissart, 2013).

According to Sollid and Sørbel (1998), The upper boundary for palsa formation in Dovrefjell is controlled by the lack of peat for insulation, while the lower limit is primarily dependent on temperature variation. This is supported by Luoto and Seppälä (2002), who argue that the thickness of the peat layer in mires is one of the primary controlling factors of palsa formation in the coldest part of the distribution of palsa mires. According to Pissart (2013) the thickness of the peat layer is not as important as the snow cover which limits the loss of heat from the ground during winter. But, vegetation is also important, as analysis by Zuidhoff and Kolstrup (2005) revealed that the height of vegetation usually correlates with the thickness of snow cover.

According to Washburn (1980), palsas are in general restricted to areas with MAAT no higher than 0 °C. In Sweden, Lundqvist (1962, references therein Seppälä, 2011) concluded that palsas occurred mainly in a zone with mean annual temperatures of -2 °C to -3 °C and less than 300 mm precipitation during November to April. Luoto et al. (2004a) found by spatial analysis that the distribution of palsas in northern Fennoscandia is favorably in areas with a MAAT between -3 °C and -5 °C and with precipitation below 450 mm. According to Sollid and Sørbel (1998), a colder climate is required to initiate the formation of palsas than is necessary for their survival.

2.1.4 Cyclicity of palsas – origin, development and degradation

How palsas initiate is not fully understood. By definition, a peat layer is necessary. Peat is important since the thermal conductivity of unfrozen peat is much lower than the thermal conductivity of frozen peat (Kujala et al., 2008), giving a low conductivity ratio. The peat thickness necessary for the formation of palsas are dependent on different climatic factors, and especially the summer temperature (Seppälä, 1988). According to Seppälä (1982), small differences in the drifting of snow may explain the beginning of the formation of palsas before any upheaval takes place. When the snow cover is thin, the frost can penetrate deep into the peat (Seppälä, 1986). A small man-made palsa was made in an experimental study by Seppälä (1982), where an area of 5x5 m of wet mire was cleared of snow several times during three consecutive winters. This experiment demonstrates that if the frost penetrates deeper than the thawing in the summer for a few years, a frost mound can appear. Wind is then able to redistribute the snow away from the mound and to lower grounds, thereby accelerating the growing phase (Seppälä, 1986).

There are still uncertainties regarding how ice accumulates in the frozen core. According to Pissart (2013), the growth of palsas is due to the formation of lenses of segregation ice in the mineral core. Previously, it was believed that palsas consisted of ice-rich peat only. The existence of a frozen mineral core was first discovered in the 1960s and 1970s (Pissart, 2013). Most ice accumulates in the silty mineral core, due to the fact that peat is not frost susceptible (Kujala et al., 2008). As ice layers also have been observed in palsas without a silty core, an alternative explanation on the formation of ice layers has been explained by Seppälä and Kujala (2009) with the effect of buoyancy. Because of differences in the density between the frozen core and the wet mire around, the core is lifted up during summers, floating like an island. This process creates a void underneath the core where water accumulates. Furthermore, when this water freezes during the next winter, thin ice layers are forming. Only when the frozen core gets in contact with the silt layer at the bottom of the mire, ice segregation starts to play an important role in the formation of palsas (Seppälä and Kujala, 2009).

What controls the size of a palsa? According to Seppälä (1986), the size of a palsa is already decided in the initial phase when a small “pillow-like” frost body forms in the peat during the

first few years. This frost body grows primarily in thickness (Seppälä, 1986). Localized growth is limited when the palsas have developed high and steep slopes that can accumulate enough snow to inhibit any further frost penetration (Seppälä, 1994).

The extension of the overlying peat will give radiation cracks, causing an increase in thawing as high temperatures and water more easily penetrate into the inner core. Therefore, the palsa enters its degradation phase where the primary processes are block erosion (Seppälä, 1986), thermal erosion from water (Sollid and Sørbel, 1998), and thawing from underneath (Seppälä, 1986) or from the surface by solar radiation (Matthews et al., 1997). Block erosion is a process where blocks of peat collapse along cracks (Seppälä, 1986). Block erosion removes the insulating layer of peat, thus making the ice-rich inner core vulnerable to high temperatures, solar radiation and latent heat from the freezing of water.

There is also evidence of palsas decreasing in thickness because of slowly thawing from underneath resulting in small mounds sinking in thermokast ponds (Seppälä, 1986). According to Sollid and Sørbel (1998), the morphology of palsas is affecting the relative importance of degradation processes: block erosion is common for high dome palsas, while erosion in connection with water accumulation (thermal erosion) is the most common form of erosion in low peat plateaus. Another direct degradation process is abrasion of the uppermost peat layer by strong winter winds containing snow- and ice crystals (M. Seppälä, 2003). M. Seppälä (2003) found the removal of a peat layer up to more than 40 cm thick in palsas in western Utsjoki, Finnish Lapland. The abrasion destroys the vegetation, and many palsas observed by M. Seppälä (2003) was almost bare of vegetation as a result.

When the degradation phase finally ends, thermokarst ponds are often evident (Seppälä, 1986). After a phase of peat formation, a new palsa can develop in the same area, starting a new palsa-cycle (Seppälä, 1986), as observed by Matthews et al. (1997). Because all stages of development can be found in the same mire, Seppälä (1982) suggest that changes in climate are not necessarily the reason for the collapse of individual palsas, but a natural part of their cyclic development. Studies by Zoltai (1993) and Matthews et al. (1997) support this view. Studies that show a general pattern of degradation of palsas (Sollid and Sørbel, 1998; Zuidhoff and Kolstrup, 2000) or evidence of more palsas in the past (Luoto and Seppälä, 2003) indicate, however, that the climate has the primary control on the distribution of palsas.

2.2 Statistical prediction of landforms

2.2.1 Geomorphological distribution modeling

According to Riseborough et al. (2008), a model is a conceptual or mathematical representation of a phenomenon. In permafrost modelling, two main modelling approaches dominate: process-based models and empirical-statistical models. Empirical-statistical models presume static conditions (equilibrium models) (Hjort and Luoto, 2013), while process-based models may be either equilibrium models or they may include the transient evolution of permafrost conditions from some initial state to a modelled current or future state (transient models) (Riseborough et al., 2008). As the thermal condition in the ground is affected by former temperature fluctuations, equilibrium models are a simplification of the dynamic nature.

There is a large diversity of statistical techniques that have been used to study landforms and processes at the surface (Hjort and Luoto, 2013). In geomorphology, GDM is an empirical/numerical model that relates observations of different geomorphologic features (e.g. palsas) to explanatory variables (Hjort and Luoto, 2013) such as different terrain parameters, climate variables or land cover types. Thus, GDMs can be used to simplify complex systems, to better understand the relationship between processes and to predict distributions in space and/or time (Hjort and Luoto, 2013).

Statistical analysis can be performed across different spatial scale (Hjort and Luoto, 2013). According to Harris et al. (2009), groups of environmental variables have different impact on the distribution of permafrost on the basis of scale. Weather and climate controlled by oceanic and atmospheric patterns operate on a continental scale, while terrain parameters are more important at regional and local scale as it controls local differences in, for example, radiation. Furthermore, surface and subsurface properties (e.g. land cover) work on an even smaller scale, as it influences how, for example, the temperature-signal from the atmosphere propagates into the ground (Harris et al., 2009). According to Harris et al. (2009), linking continental and local scales is a major problem in permafrost distribution modelling.

A benefit of statistical modelling is the possibility of detailed investigation of the shapes of response functions for different explanatory variables (see e.g. Hjort and Luoto, 2011). In

order to improve our knowledge about the relationship between response and explanatory variables, such response curves need to be well understood and analyzed (Hjort and Luoto, 2013). Nevertheless, for very complex geomorphological systems, statistical techniques have difficulties of capturing the true relationships between geomorphological processes and environmental variables (Hjort and Luoto, 2013).

There is a distinction between direct (i.e. causal variables as temperature and humidity) or indirect (i.e. noncausal variable as elevation and coordinates) environmental variables according to their effects on geomorphological features (Hjort and Luoto, 2013). Hjort and Luoto (2013) recommend avoiding indirect variables as surrogates of environmental determinants, as the extrapolation potential (i.e. the robustness) of the model increases with more process-oriented (direct) environmental variables.

Hjort and Luoto (2013) recommend certain steps when practicing GDM, represented in Figure 2. After the study objective(s) is known (first step), a conceptual model should be planned based on theory (second step) (Hjort and Luoto, 2013). The third step of data compilation is a time consuming (and sometimes difficult) task, where the variables can be gathered from fieldwork, remote sensing, maps and processing Digital Elevation Models (DEMs). In the fourth step, the data needs to be investigated in several ways (e.g. by histograms, correlation matrix and scatterplots) in an explorative analysis. For instance, highly correlated explanatory variables need to be removed (Hjort and Luoto, 2013). In the step of statistical formulation, the most suitable statistical approach based on the modelling setting (such as input data, expert knowledge, objective of study etc.) is selected. Furthermore, in calibration of the final model, environmental variables are selected and the model parameters estimated (Hjort and Luoto, 2013). The selection of explanatory variables has earlier mostly been based on *p*-values, but in the last few years, there has been a transition towards using information theories like Akaike`s information criterion (AIC) (Anderson and Burnham, 2002). AIC was developed by the Japanese statistician Hirotogu Akaike in the 1970s, and is a method of model selection based on an extension of the maximum likelihood principle (Akaike, 1998). More detailed, AIC measures the relative quality of a statistical model for a given set of data as it quantifies the discrepancy between the estimated and the true probability distribution (Akaike, 1998). Furthermore, it deals with the trade-off between the goodness of fit and the complexity of the model.

The final model needs to be evaluated in form of an assessment of the realism of the response functions, the models fit to data and predictive performance on evaluation data (Hjort and Luoto, 2013). Hjort and Luoto (2013) recommend using spatially independent areas as evaluation data, but cross-validation and split-sample approaches are frequently used due to data constraints. In the last step, either the final model is used to map the prediction or renewed knowledge from the procedure is used in an iterative process to improve the model (Hjort and Luoto, 2013).

There are several challenges related to the process of GDMs. Several subjective choices need to be made when it comes to select explanatory variables, statistical model and type of evaluation. There are also often uncertainties concerning the quality of explanatory variables (e.g. quality of DEM and interpolated climate data), which may have a crucial effect on the results, depending on the scale of the model.

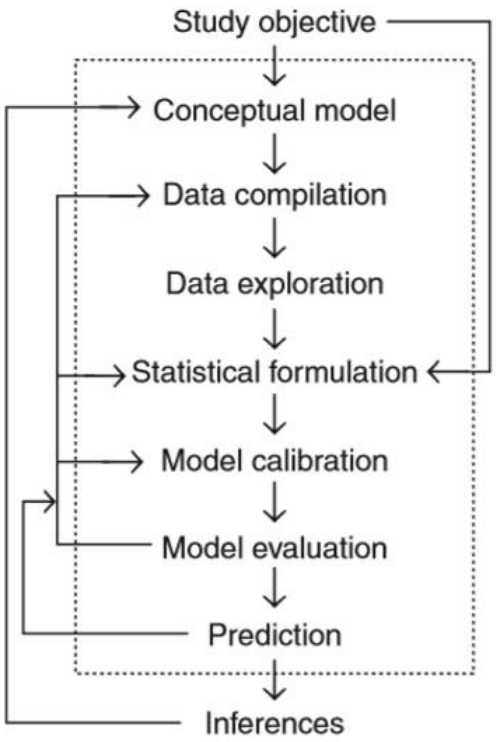

Figure 2: Presentation of the modelling steps recommended by Hjort and Luoto (2013) for statistical modelling of geomorphological features. Figure from Hjort and Luoto (2013).

2.2.2 Generalized linear models

GLMs are a mathematical extension of general linear models that allows for nonlinearity and nonconstant variance structures in the data, and is thus better suited for analyzing geomorphological relationships than its predecessor (Hjort and Luoto, 2013). A large range of different types of spatial data (e.g. discrete, ordinal and continuous data) is all handled by GLMs (Hjort and Luoto, 2013). Thus, GLMs are useful for testing the shapes of the response curves and the significance of explanatory variables (Hjort and Luoto, 2013). In geomorphology, GLMs have mostly been used in research of landslides and periglacial phenomena (Hjort and Luoto, 2013).

There are three main components in the mathematical description of GLMs: (1) the response variables, (2) a set of parameters α and β and explanatory variables, and (3) a link function g (McCullagh et al., 1989, references therein Hjort and Luoto, 2013). The link function relates the predictors to the mean of the response variable, and it allows transformation to linearity and maintenance of the predictions within the range of coherent values for the response variable (Luoto and Hjort, 2005). By doing so, GLMs can handle a large range of distributions (Hjort and Luoto, 2013). The model in GLMs are built through a reduction in deviance, like ordinary LS regression models (Hjort and Luoto, 2013).

Of different types of GLMs, logistic regression models have especially been fruitful in geomorphology. The reason is the simplicity of gathering response variables in a binary form, where geomorphological features are either present or absent (Hjort and Luoto, 2013). In logistic regression, the relationships between the response and the explanatory variables are expressed as a probability surface and a logit link function (g) is applied to the data (Hjort and Luoto, 2013) . With the logit link function, the probability of a positive response (e.g. the presence of palsas) is a logistic s-shaped function for first order polynomial predictors and an approximation of a bell-shaped function for second order polynomial (quadratic) predictors (Luoto and Hjort, 2005).

Weaknesses of GLMs include the assumptions that all explanatory variables are measured without error, problems dealing with multicollinearity, and inflexibility compared to more sophisticated models (Hjort and Luoto, 2013). Multicollinearity is intercorrelation between explanatory variables, and is not handled by GLMs. Spatial autocorrelation can thus inhibit

the attempt to detect the true relationship between the explanatory variables and the response variable. Furthermore, the consequences of multicollinearity might be to reject true important factors from the model (Luoto and Hjort, 2005).

For complex relationships between environmental and response variables, GLMs may not be flexible enough to detect the true shape of the response function (Hjort and Luoto, 2013). Nonetheless, GLMs may capture most of the same variation and have a more realistic explanation than more sophisticated nonparametric methods (Hjort and Luoto, 2013). Furthermore, GLMs are relatively robust against the risk of over-fitting and a rather low level of knowledge is needed to utilize the method.

2.2.3 Evaluation measures

When using binary data in a presence/absence model, there are four possible outcome of the prediction: true positive (TP), true negative (TN), false positive (FP) and false negative (FN). The two last outcomes are the two possible prediction errors (Fielding and Bell, 1997). Table 1 is a error matrix that summarizes and explains these outcomes. Positive values imply either a probability above a set threshold (test outcome) or a real observation of a response variable (e.g. presence of palsas). Negative values conversely imply a probability below the same threshold (test outcome) or that there are no real observation of a response variable (e.g. absence of palsas). For instance, true positive values are values where both the real observation and the test outcome are positive (i.e. presence of palsas and a probability above a set threshold).

Table 1: Explain the concepts of true positive, false negative, false positive and true negative values, when comparing results from a test (in this case from the final GLM) with real observations (e.g. presence/absence of palsas). Modified from Fielding and Bell (1997).

		Real observations	
		Positive	**Negative**
Test outcome	**Positive**	True positive	False positive
	Negative	False negative	True negative

A variety of different measures of error and accuracy can be calculated based on the four possible outcomes. Relevant measures for this thesis include the measures of *sensitivity* (true

positive rate), *specificity* (true negative rate) and *correct classification rate* (overall accuracy). *Sensitivity* (eq. 2.1) is the conditional probability that case X is correctly classified positive, whereas *specificity* (eq. 2.2) is the inverse case (Fielding and Bell, 1997):

$$\boldsymbol{Sensitivity} = \frac{\boldsymbol{TP}}{\boldsymbol{TP} + \boldsymbol{FN}} \tag{2.1}$$

$$\boldsymbol{Specificity} = \frac{\boldsymbol{TN}}{\boldsymbol{TN} + \boldsymbol{FP}} \tag{2.2}$$

The correct classification rate is the overall accuracy of the model by calculating the ratio of true positive and true negative values of the total dataset (eq. 2.3):

$$\boldsymbol{Correct\ classification\ rate} = \frac{\boldsymbol{TP} + \boldsymbol{TN}}{\boldsymbol{TP} + \boldsymbol{FN} + \boldsymbol{TN} + \boldsymbol{FN}} \tag{2.3}$$

The above method to evaluate a model is dependent on choosing an appropriate probability threshold that decides whether an outcome is positive or negative. Thus, although dichotomous classifications can be convenient when making decisions, this method fails to use all of the available information (Fielding and Bell, 1997). Hence, a threshold independent method developed in signal processing has received increasingly attention: receiver operating characteristic (ROC) curves (Fielding and Bell, 1997). A ROC curve is obtained by plotting all sensitivity values on the *y*-axis against specificity values for all available thresholds on the *x*-axis. The area under the ROC curve (AUC) is recognized as an important index because it provides a single measure of overall accuracy that is not dependent on a particular threshold (DeLeo, 1993). The value of the AUC is between 0.5 and 1. Swets (1988) classified the level of performance of the AUC-values into failed (0.50-0.60), poor (0.61-0.70), fair (0.71-0.80), good (0.81-0.90) and excellent (0.91-1.00).

2.2.4 Hierarchial Partitioning

There is a need in many multivariate studies to understand the individual importance of factors in a quantitative and simple way (Chevan and Sutherland, 1991). Hierarchial Partitioning (HP), developed by Chevan and Sutherland (1991), can handle the problem of multicollinearity in multivariate settings and has therefore been highlighted as valuable in complementing GDMs (Hjort and Luoto, 2009). HP is an analytical method of multiple

regression to determine the relative importance of independent (explanatory) variables based on hierarchies where all orders of variables are used. Furthermore, the method is applicable to all regression methods, including ordinary least squares, logistic, probit, and log-linear regression (Chevan and Sutherland, 1991). In more detail, HP conducts goodness-of-fit measures (e.g. R^2) for each of the 2^k possible models for k independent variables. The variances are partitioned in such a way that for each independent variable, the explanatory power is segregated into the average independent (i) and jointly contribution (j) (Mac Nally, 2000). Thus, the explanatory variable can be investigated in sense of both the individual effect the variables have on a response and the shared effect the variables have together with other variables, revealing possibly new understandings of complex relationships between variables (Chevan and Sutherland, 1991).

3. Area of study

3.1 Geographical setting

The area of study is Finnmark county, the largest and northernmost county in Norway, covering an area of 48,618 km^2 (SNL, 2015). Finnmark extends from roughly 68° N to 71° N and is thus north of the polar circle. Finnmark shares border with Russia in the east, Finland in the south and with the neighboring county Troms in the west.

Figure 3 illustrates the position of Finnmark in northern Europe (a), and the positions of the three study sites for the delineation process and the calibration and evaluation areas for the GDM process (b). It also contains the position of the three nearest meteorological stations for the study sites (b).

The calibration area for the GDM process cover 2016 km^2 of central Finnmark. This area include parts of the Gaissene mountains in northeast, with some mountain tops exceeding 1000 m a.s.l., Finnmarksvidda in south (with elevations of around 300 – 500 m a.s.l.) and with Norway`s 6th largest lake, Iesjavri, in the centre. The two evaluation areas are located in northeast Finnmark around Varangerfjorden and in southwest Finnmark close to the Finnish border, with areas of 2705 km^2 and 780 km^2, respectively.

The three study sites for the delineation process, Lakselv, Suossjavri and Goatheluoppal, are situated in a roughly north-south transect in Finnmark (Figure 3). Lakselv (70° N) is located in the inner part of Porsangerfjorden almost at sea level. Suossjavri (69° 23′ N) is situated in the centre of Finnmarksvidda, with elevations of around 300 – 350 m a.s.l. Goatheluoppal (68° 54′ N) is located southeast of Kautokeino, approximately 5 km from the border of Finland and with an elevation of around 440 m a.s.l.

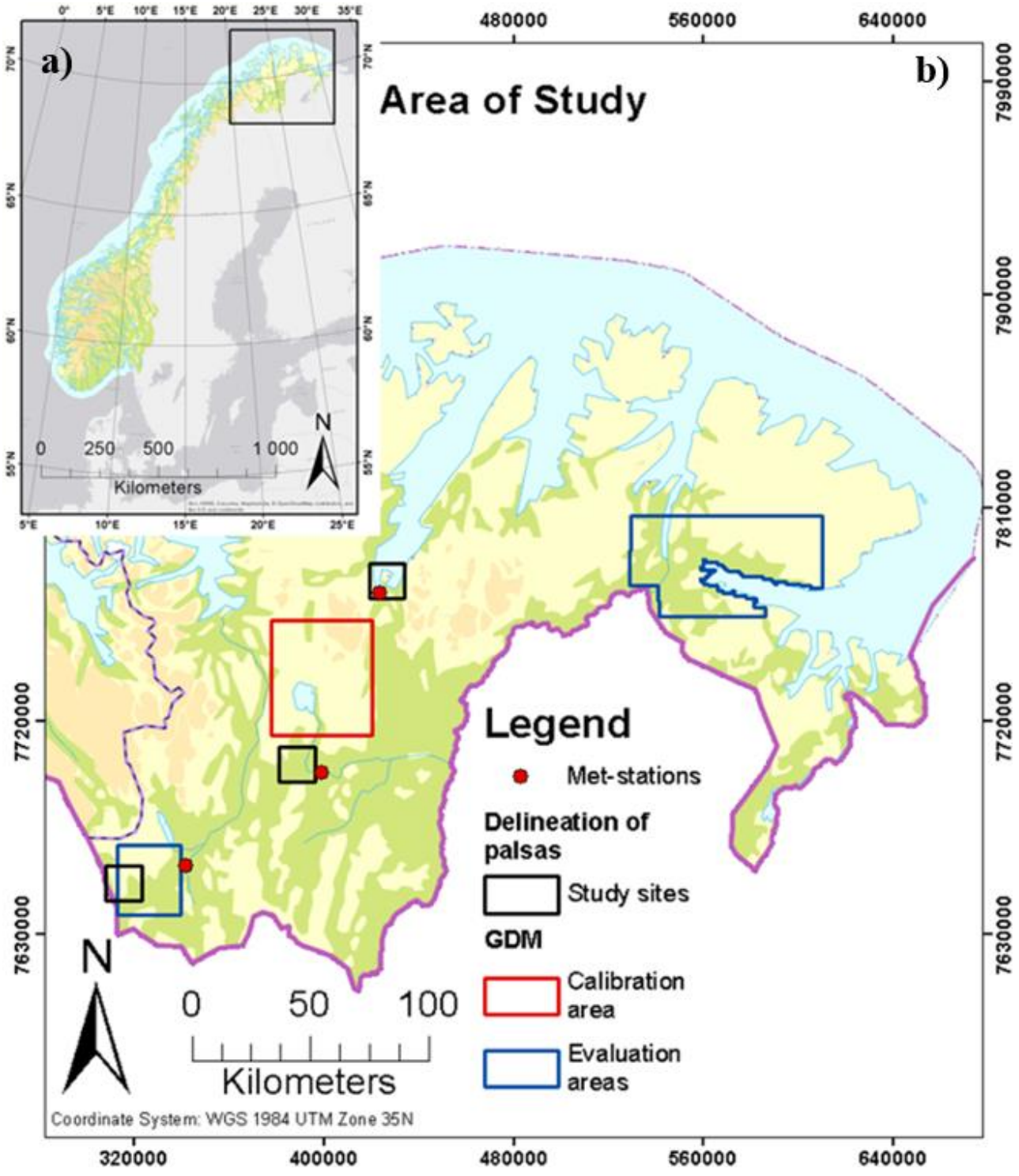

Figure 3: Maps of the study area, with Finnmark's position in northern Europe (a) and the location of the study sites for the delineation process, the position of meteorological stations nearby the study sites and the calibration and evaluation areas for the GDM process (b).

3.2 Geomorphology and Geology

Just as the rest of Norway, the geomorphology of Finnmark is highly impacted by the glaciations in the Pleistocene Epoch (2.6 million years to 11.7 thousand years ago), with several long and wide fjords, rounded mountains, long eskers and huge fields of flutes, drumlines and other types of moraines as the result. The large Finnmarksvidda dominates the centre of Finnmark. With an area of more than 22,000 km^2, the plateau is almost half the size of entire Finnmark and the largest plateau in Norway (SNL, 2014). The plateau is made up of old basement, consisting of mostly old granites and gneisses from the Precambrium Eon (4,6 billion years to 541 million years ago) (Askheim, 2013). The landscape is smoothly undulating with small hills and plains at an elevation of about 300 – 500 m a.s.l., and most of the landscape covered with till and moraines. The vegetation on the plateau is sparse, with scrubland, low birch trees or bare mountains (SNL, 2014). Thousands of wet mires have filled the concavities in between the moraines and ridges.

Further north is the mountain chain Gaissene, which makes an almost continuous wall of mountains from Stabbursdalen in the west to Laksefjordvidda in the east, separating Finnmarksvidda from Porsangerfjorden and Laksefjorden (SNL, 2009). Gaissene is made up of nearly horizontal layers of the resistant bedrock Sparagmitt, which has been pushed over the basement under the late Precambrium Eon (SNL, 2009).

The northwest part of Finnmark has an alpine landscape with peaks, cirques and a few small glaciers (Askheim and Thorsnæs, 2015). The bedrock here belongs to the Caledonides from the Caledonian Orogenese (approx. 750 – 400 million years ago) with mostly magmatic bedrocks (Askheim and Thorsnæs, 2015).

3.3 Climate

Due to Finnmark's vast area, the climate varies widely from a maritime climate on the relatively wet and warm coast in the northwest, to a dry and cold environment on Finnmarksvidda (Dannevig, 2009). Of great importance for the climate at the coast is the temperate water brought by the Norwegian Atlantic current. This current ensures an ice-free coast at the northwest during the winter (Dannevig, 2009). Figure 4 shows maps of the

normal annual temperature (1961-1990), the normal annual precipitation (1961-1990) and the normal maximum snow depth (1961-1990) for Finnmark (MET, 2015a, 2015b).

The normal annual temperature (1961-1990) close to the coast in north and northwest was mostly between -1 °C to 2 °C, while inner parts of Finnmark and the Gaissene mountains had temperatures between -2 °C to -5 °C. February was the coldest month at the coast, with normal temperatures (1961-1990) from -2 °C to -7 °C. The normal temperature (1961-1990) at the coast in July was 10 °C to 12 °C (Dannevig, 2009), only around 15°C higher than in February. In comparison, the climate in Finnmarksvidda was highly continental with a much larger temperature span from winter to summer than the coast. Often, the coldest winter temperatures measured in Europe are at Finnmarksvidda (Dannevig, 2009). The normal winter temperature (1961-1990) for this area was around -16°C, and it is not unusual with temperatures lower than -40 °C (MET, 2015c). In summer (June – August), Finnmarksvidda has a normal temperature at around 10 °C, with maximum temperatures often exceeding 20 °C (MET, 2015c). According to Dannevig (2009), the normal temperature (1961-1990) for July goes up to roughly 14 °C in inner parts of Finnmark.

Finnmark is the county in Norway with the lowest amount of precipitation per year. The normal annual precipitation (1961-1990) was mostly between 300 mm to 500 mm in the continental parts of Finnmark (Figure 4). The coast in north and northwest and the mountains of Gaissene had a higher normal annual precipitation with between 600 mm to 1000 mm (Figure 4). Most of the precipitation from November to April falls as snow in Finnmark. At Finnmarksvidda, the snow usually stays to the end of May or even later (MET, 2015c). Continental parts of Finnmark have the highest amount of precipitation during summer, while the coast gets most precipitation during fall and early winter (Dannevig, 2009). During winter, Finnmarksvidda has the lowest amount of precipitation: normally only 50 mm in inner parts (Dannevig, 2009). Thus, Finnmarksvidda had a low normal maximum snow depths (1961-1990) with large areas less than 0.4 m of snow (Figure 4). The northern part of Finnmark had a much higher maximum snow depths of mostly between 0.8-1.8 m. Interestingly; Lakselv has a very low maximum depth of snow, with less than 0.4 m of snow according to Figure 4.

Continental parts of Finnmark are mostly characterized by a low wind speed, while the coast in January has strong breezes or more at 30-40 % of the time (Dannevig, 2009). Near the

coast, the wind speed is lowest during summer. In winter, the wind is usually blowing from the plains down valleys to the coast due to heavy cold air masses (Dannevig, 2009).

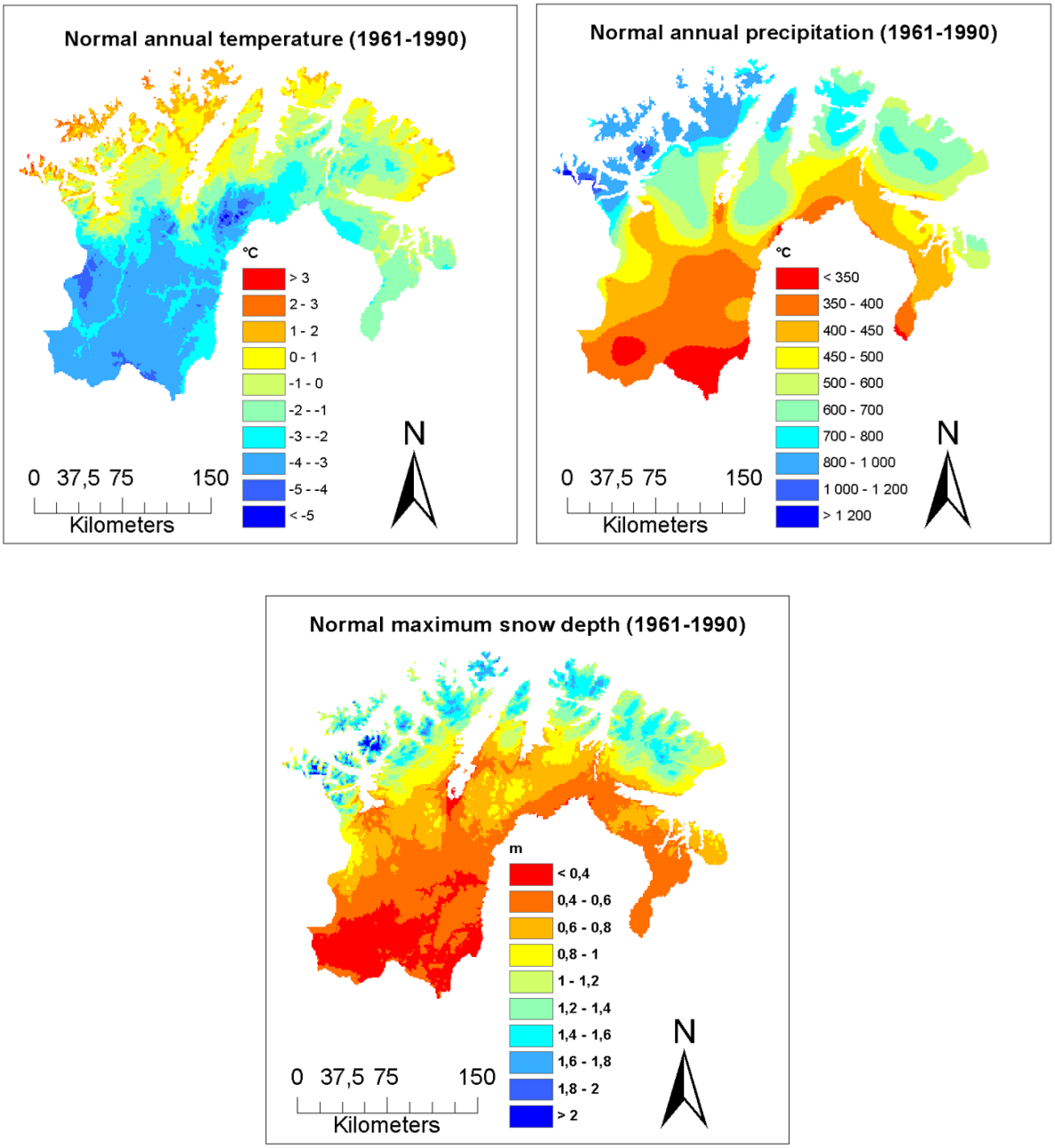

Figure 4: Maps of the normal annual temperature (1961-1990), normal annual precipitation (1961-1990) and the normal maximum snow depth (1961-1990) for Finnmark. Data of normal annual temperature and precipitation is downloaded from the Norwegian Meteorological Institute (MET, 2015a, 2015b). Data of normal maximum snow depth are gathered from Kjersti Gisnås (PhD research fellow at University of Oslo).

3.4 Permafrost in Finnmark

According to the spatial equilibrium model CryoGRID 1.0 (see Gisnås et al., 2013), approximately 19 % of the land surface in Troms and Finnmark had permafrost during the period from 1981 to 2010 (Farbrot et al., 2013). In Finnmark, permafrost in palsas is the dominating permafrost feature (Farbrot et al., 2013). Some relict rock glaciers and a few active rock glaciers are apparent in northern Finnmark (Lilleøren and Etzelmüller, 2011). The permafrost is mostly warm, with MAGT above -3 °C (Farbrot et al., 2013). The elevation of the lower limit of permafrost is above 500-700 m a.s.l. in continental areas of Finnmark, except for sporadic permafrost in palsa mires (Farbrot et al., 2013) which exists down to almost sea level in a few places, e.g. in Lakselv and inner part of Varangerfjorden. In the Gaissene Mountains, permafrost is usually present above 350-450 m a.s.l. For this area, the presence of coarse openwork blocks reduces the ground surface temperatures substantially (Farbrot et al., 2008).The permafrost in the summit areas at about 1000 m a.s.l. have possibly been present since the last interglaciation (Farbrot et al., 2008). According to Isaksen et al. (2008), permafrost is widespread in Finnmark in areas above the timberline having MAAT lower than -3 °C. As a result of the negative temperature and precipitation gradient from the coast towards Finnmarksvidda, a NW-SE lowering of the permafrost limit is reasonable for this region. This continental effect with lowering of the permafrost limit inland is well known from south of Norway (Etzelmüller et al., 2003).

According to Farbrot et al. (2013), the effects of snow depth and vegetation cover are the two most critical factors for the existence of permafrost in northern Norway. Birch and pine forests in Finnmark appear to correspond with areas without permafrost, as trees cause snow to accumulate and insulate against strong ground cooling (Isaksen et al., 2008). Above the timberline, and apart from the palsa mires, the formation of permafrost is possible at Finnmarksvidda at local exposed sites where snow does not accumulate (Isaksen et al., 2008).

4. Methodology

This chapter describes all the different methodologies utilized in this thesis. The chapter is divided into three main sections – (4.1) delineation of palsas by multitemporal aerial images, (4.2) statistical prediction of palsas and (4.3) a simple model of carbon gas release. The overall structure of the methodologies, and how the different methodologies are related to each other in order to reach the main objectives of this thesis, is presented by a flowchart in Figure 5.

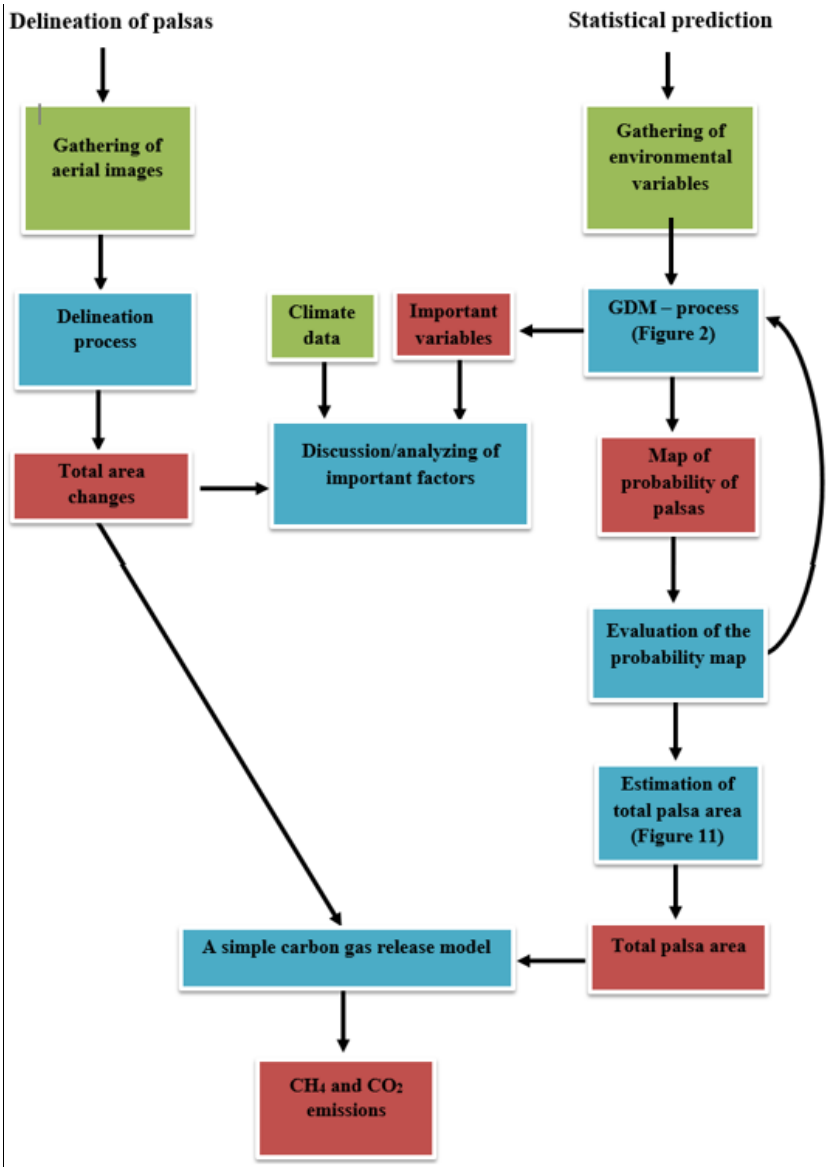

Figure 5: Flowchart of the overall structures of the methodologies and how they are related to reach the main goals of this thesis. Green boxes represent input data, blue boxes processes and red boxes results.

4.1 Delineation of palsas by aerial images

4.1.1 Choice of study sites

The choice of study sites was decided by a trade-off between the following factors:

- Geographical position of the study sites
- Availability of images
- Availability of climate data
- Access of study sites for fieldwork
- Amount and type/form of palsas.

First, a north-south transect through mid-Finnmark was desired. Two of the study sites, Lakselv and Suossjavri, have good coverage of climate data as nearby meteorological stations are situated very close to the mires (Figure 3). These two study sites are also easily accessible through roads. Goatheluoppal is more remote and situated further away from meteorological stations. The geographical position of Goatheluoppal is slightly more east than desirable. Nonetheless, the Goatheluoppal study site has very distinct palsas with clear palsa edges surrounded by numerous small thermokarst ponds making delineation of palsas easy and accurate. Other areas of large palsa fields more south in Finnmark have a more complex and chaotic degradation that are difficult to delineate. Lakselv is dominated by large peat plateaus that have experienced a chaotic degradation more difficult to delineate than the distinct palsas in Goatheluoppal. In return, the geographical position of Lakselv is favourable.

4.1.2 Aerial images

The aerial images used in this thesis are extracted from two different sources. First, the Norwegian webpage Norgeibilder.no (Norgeibilder, 2015) contains aerial images of the entire Norway. The webpage is thre result of a collaboration between the Norwegian Forest and Landscape Institute, the Norwegian Public Roads Administration and the Norwegian Mapping Authority. Most of the images are from after 2000, and multiple images from different years are available for many areas. The images are ortorectified and freely available by using Web Map Service (WMS) in a GIS-framework.

Another way to get aerial images is to order them from the Norwegian Mapping Authority who operates a webpage with an archive of aerial images in Norway (Kartverket, 2015a). These images are not orthorectified or georeferenced. Detailed information about all of the aerial images used in this thesis is presented in the tables A.1, A.2 and A.3 in the Appendix following this thesis. The images are from four different times for the Goatheluoppal and Suossjavri study sites: the end of 1950s, the 1980s, 2003 and the 2010s.

The year of capturing the images differs slightly for the different study sites. The images from end of 1950s and 1980s are ordered from the Norwegian Mapping Authority (Kartverket, 2015a), while the images from 2003 and 2010s are from Norgeibilder (2015). For the Lakselv study site, only images from 1959 (ordered from the Norwegian Mapping Authority) and 2008 (Norgeibilder, 2015) have been used. Images covering the Lakselv site for the early 2000s were unfortunately not available. Images from 1975 for the Lakselv study site were ordered, but the images were not of sufficient quality. Therefore, these images were not utilized. A few palsa mires in the Lakselv study site are not delineated due to unavailability of some classified aerial images (military restrict area).

4.1.3 Georeferencing

Due to the nature of palsas being situated in flat mires, orthorectification of the images is decided to not be of necessity in this thesis. Orthorectification of this large amount of old images is time consuming, and it is doubtful if orthorectification improves much compared to just doing georeferencing. For the georeferencing process, the *Georeferencing tool* in *ArcMap 10.2* (part of the *ArcGIS Platform* from *Esri*) was used.

Usually, control points (CPs) for georeferencing should be evenly distributed on the images, preferably with every corner covered. However, this thesis is only interested in the part of the images where the palsa mires are situated. Thereby, the CPs were focused around the palsa mires. To ensure a low radial displacement, it is preferable to utilize images where the palsa mires are situated close to the image centre. Figure 6 illustrates an example of the distribution of control points around a palsa mire in Suossjavri on one image from 1982. As a consequence of this method, some images had to be georeferenced several times for different palsa mires. It is important to note that the Root Mean Square Error (RMSE) is only valid for the area in between the control points.

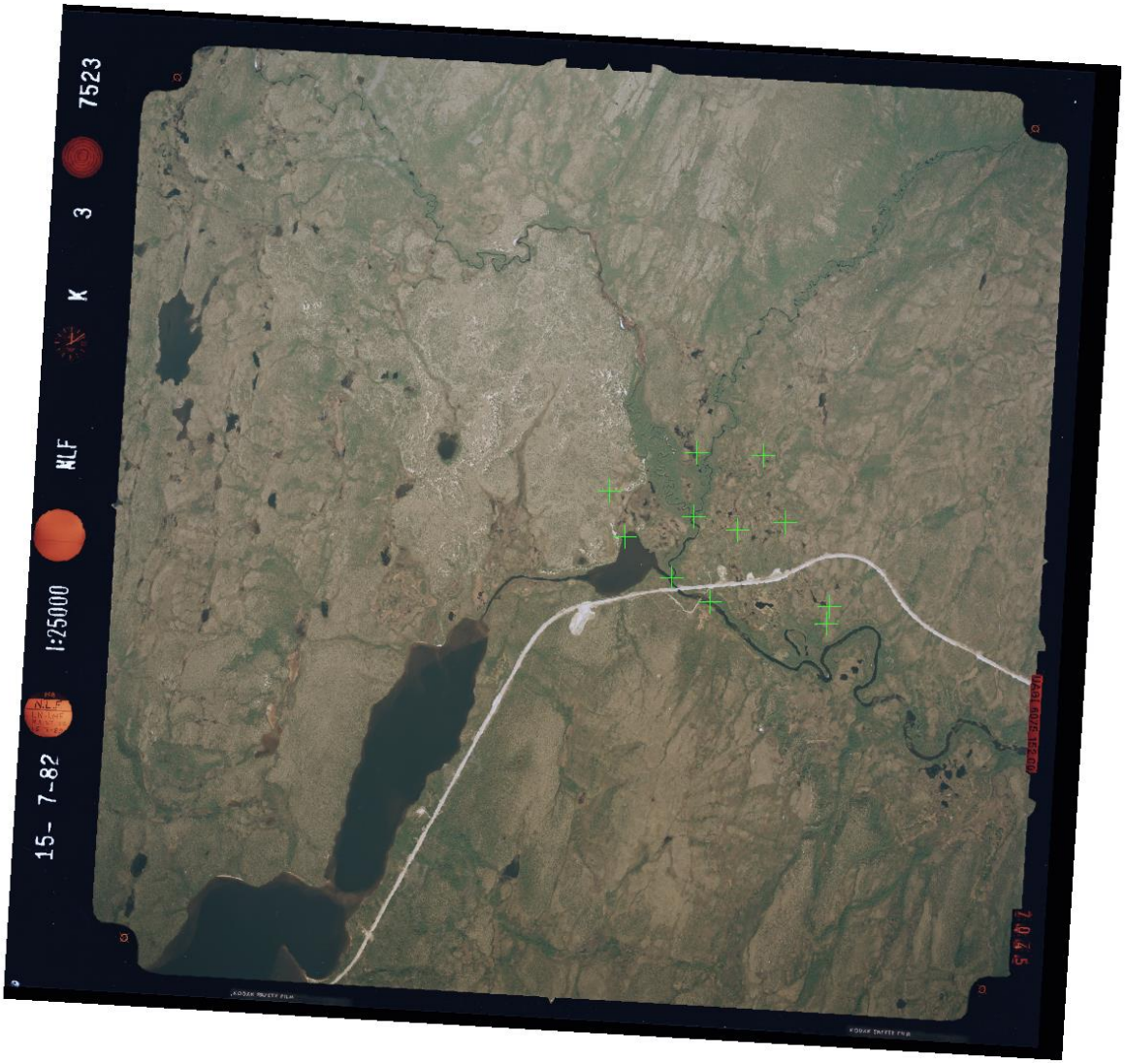

Figure 6: Example of the distribution of control points (represented by green crosses) for a palsa mire in Suossjavri on one image from 1982 (image K-3, coverage number NLF-7523).

4.1.4 Delineation

The delineation of palsas was a manual task where polygons that matched the individual palsas were produced. The polygons were produced by using the *Draw Toolbar* in *ArcMap*. This step was achieved by following the edges of the palsas by visual interpretation of the aerial images. The information of all polygons was exported from *ArcMap* in text files for further analysis in *Microsoft Excel* by *Microsoft Corporation.* By summarizing the area of all

the polygons for each individual period, the development in the total area between the different periods could be analysed.

In the delineation process, some techniques were performed to recognize and separate palsas from the rest of the landscape. Furthermore, knowledge obtained from fieldwork was beneficial in this process (see 5.2). When doing observations in the field, I have compared what I have seen on the ground with what I observe on aerial images. Thus, observations from the field have been of value to better understand the nature of palsa mires on aerial images. Flickering between different years revealed area changes of palsas, and was of importance to notice palsas at the brink of moraines. Flickering between years can give a history in the development of palsas, thereby helping to understand where the edges are. Furthermore, differences in vegetation between dry palsas and wet mires gives different albedo that make it possible to separate these land covers on aerial images. It is especially easy to delineate the edge of palsas where the dominant degradation form is block erosion into dark thermokarst ponds.

The palsas that are most difficult to delineate are palsas situated at the brink of moraines. For these palsas, there are often a diffuse transition between the moraines and the palsas making accurate delineation difficult. Consequently, several palsas in this situation have not been delineated.

4.1.5 Accuracy, uncertainties and difficulties

The accuracy of the final polygons of palsas is a result of a mix between the ground spatial resolution of the aerial images, the subjective delineation and the accuracy of the georeferencing (Table 6). In general, the accuracy of each individual polygons of palsas is low. However, the total accuracy will increase with numbers of polygons, assuming that no great systematic errors are present.

Depending on time of day and time of year the images were captured, shadows and shades at the palsa edges are slightly different. Shadows and shades are of importance in the interpretation of the edges, and these differences may affect the difference in the delineation of the edges between the years.

The interpretation of the exact pathway for palsa edges could be slightly different from black/white-images and RGB-images, which may influence the results and give systematic errors. For Suossjavri and Goatheluoppal, the images between the periods are every other panchromatic- (black/white) and RGB-images (Table 2). Thereby, if the observed changes have a clear trend, this influence is of less importance.

4.1.6 Climate data

Since fieldwork only was lasted conducted once, meteorological data was not gathered. Therefore, for the discussion of which climate variables that could be a driving agent of the area changes of palsas, climate data from nearby meteorological stations of the study sites has been downloaded through the webpage eklima.met.no. This webpage gives free access to the Norwegian Meteorological Institutes (MET, 2015d) climate database. This database contains data of all present and past meteorological stations by MET, also including meteorological stations owned and operated by other institutions (MET, 2015d).

The available climate data of interest are temperature, precipitation, maximum snow depth and mean wind speed. Climate data from three meteorological stations has been downloaded: Banak in Lakselv, Cuovddatmohkki close to Suossjavri and Kautokeino in Kautokeino. The position of the meteorological stations are showed in Figure 3. The meteorological station Banak (5 m a.s.l.) is 2 to 6 km from the palsa mires, Cuovddatmohkki (286 m a.s.l) is roughly 6 to 12 km away from the palsa mires, while Kautokeino (307 m a.s.l.) is around 30 km away from the palsa mires in Goatheluoppal. The locations of the meteorological stations are shown in Figure 3. The climate data is processed using *Microsoft Excel*. Because permafrost in general has a slow response to the climate at the surface (Harris et al., 2009), long-term time series are desirable.

4.2 Statistical Prediction of palsas

The occurrence and distribution of palsas in central Finnmark are statistically analysed and predicted by GLM in the absence/presence of a grid-based approach at meso-scale (1x1 km of spatial resolution). The choice of using GLM is due to its user-friendliness, the relatively low overfitting risk, and because the method has shown to be useful in geomorphology (Hjort and

Luoto, 2013). In the general process of statistical prediction, I have tried to follow the modelling steps recommended by Hjort and Luoto (2013) (Figure 2).

The GLM is based on a calibration area of observations, and evaluated by two spatially independent evaluation areas (see Figure 3), as recommended by Hjort and Luoto (2013). Based on the final GLM, a prediction map of the probability of presence of palsas is produced.

4.2.1 Data compilation

Data for the response variable have been gathered for three different regions (Figure 3): one calibration area in centre of Finnmark (1994 km^2, with 352 grid cells of palsas) and two evaluation areas named *Varanger* (2705 km^2, with 176 observations of palsas) and *Southwest* (780 km^2, with 182 observations of palsas). Data for the environmental explanatory variables have been gathered for the whole area of Finnmark County. Below follows a more detailed description about the gathering of data for the response and the explanatory variables.

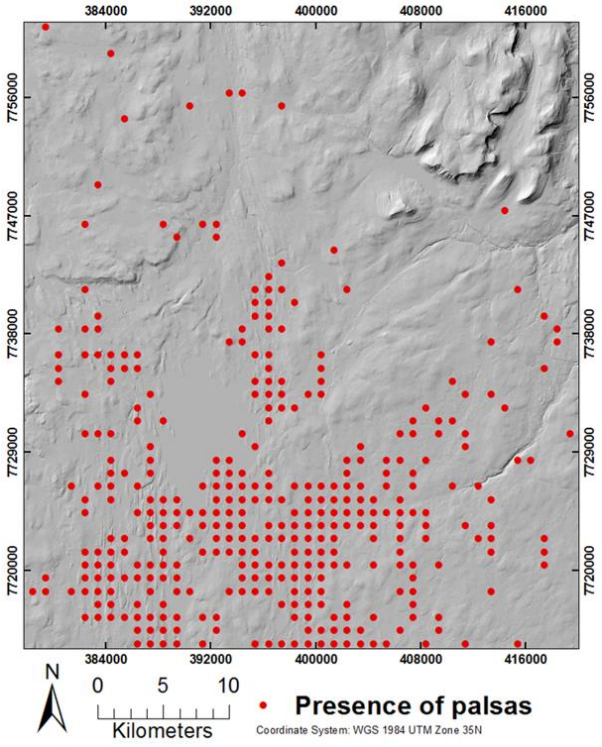

Figure 7: The presence of palsas is overlaid a shaded relief (hillshade) of the calibration area. The hillshade is based on the DEM from the Norwegian Mapping Authority (Kartverket, 2015b).

The response variable of palsas is based on visual interpretation of orthorectified aerial images from 2008-2012 with commonly ≤ 0.5 m in spatial resolution from Norgeibilder.no. If the grid cell of 1x1 km had occurrence of one or more palsas with diameter of at least 10 m, the grid cell was assigned the value 1. If the grid cell had no occurrence of palsas with diameter of at least 10 m, the cell was assigned the value 0. The threshold of 10 m is used as a matter of convenience: A palsa with diameter of less than 10 m is difficult to detect and correctly interpret due to the quality of the aerial images. Because no ground surveys have been conducted to validate the presence and absence of palsas, other frost mounds as lithalsas might be included as present. Nonetheless, this study are interested in sporadic permafrost, and distinguishing between palsas and lithalsas are not of interest.

Some methods/knowledge helped with the identification of palsas: (a) palsas have relatively low albedo due to dry vegetation, (b) flickering between years shows changes, (c) occurrence of thermokarst lakes and other signs of degradation of palsas, (d) no (or almost no) larger trees on the palsa surface, and (e) sometimes very green vegetation around palsas, especially where palsas degrade fast. The number of grid cells with occurrence of palsas are probably slightly underestimated, as it is easier to overlook some palsas than to interpret a feature wrongly as palsas. As previously mentioned in 4.1.4, it is especially difficult to discover palsas that are situated at the brink of moraines as a continuation of the landform. In these cases, flickering between years to detect changes are necessary to interpret the landform as a palsa.

The explanatory variables – 12 environmental explanatory variables have been gathered for the entire Finnmark (Table 2). The explanatory variables consists of six climate variables, two land cover variables, and four topography variables. The variables were selected based on theory and earlier statistical modelling studies of palsas. For instance, the significance of *MinElevation*, *Flat*, *Mire* and *Water* was highlighted in a prediction study of palsas by Luoto and Hjort (2002), while different climate variables of temperature and precipitation has been recognized as important by Luoto et al. (2004) and Aalto and Luoto (2014). The important influences of snow, summer precipitation and temperature on palsas are widely recognized in the literature (e.g. Matthews et al., 1997; Seppälä, 1982; Sollid and Sørbel, 1998; Zuidhoff, 2002). Further, *TWI* and *Slope* have been recognized as important topographic variables in periglacial research concerning solifluction and patterned ground (Hjort, 2014; Ridefelt et al.,

2010)). Examples of gridded versions of the explanatory variables *FDD* and *Flat* for the calibration area are given in Figure 8.

The climate variables *MaxSnow*, *FDD* and *TDD* were obtained from Kjersti Gisnås (PhD research fellow at University of Oslo) who used gridded climate data from the Norwegian Meteorological Institute to produce these variables. Freezing and thawing degree-days are the total sum of all negative and all positive degrees during a defined period with a defined frequency, respectively. *FDD* and *TDD* are here computed as the sum of the mean daily negative and positive temperatures during a year.

The other climate variables (*MAAT*, *MSP*, *MAP*) were gathered from the Norwegian Meteorological Institute (MET, 2015a, 2015b). All the climate variables were in raster format and with 1x1 km spatial resolution. The land cover variables (*Water* and *Mire*) were extracted from the map AR5 (vector format) which is a national map dataset for Norway that describes land resources, produced by the Norwegian Forest and Landscape Institute (Skog og landskap, 2015). The topography variables (*MinElevation*, *Slope*, *Flat* and *TWI*) were derived by using the national covered raster DEM with originally 10x10 m spatial resolution from the Norwegian Mapping Authority (Kartverket, 2015b).

The flow chart in Figure 9 and Figure 10 presents the process of modifying the layers of land cover and topographic variables in *ArcMap 10.2*, to fit the format used in the prediction. The climate variables were originally of whole Norway in UTM 33N, but was projected to UTM 35N in *ArcMap 10.2* with the data of Finnmark extracted from the dataset. For the variable *Flat*, flat areas of water bodies are excluded from the layer.

TWI is based on both slope (in radians) and flow accumulation by the following equation:

$$TWI = \frac{a}{\tan(b)} \tag{4.1}$$

Where *a* is the local upslope area draining through a certain point per unit contour length and *tan(b)* is the local slope in radians. To convert slope from degrees to radians, the layer of slope is multiplied with 180°/π.

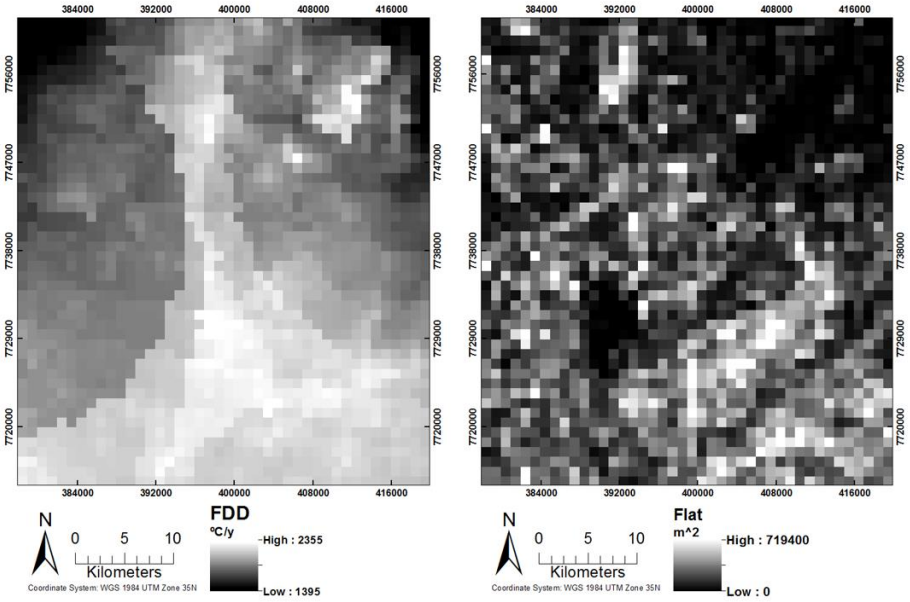

Figure 8: Examples of the gridded explanatory variables of FDD and Flat for the calibration area. Note the unnatural pattern of FDD reflecting the problems of accuracy of meteorological data in this area.

Table 2: Overview of all 12 environmental explanatory variables, divided in six climate variables, four topography variables and two land cover variables. The mean, standard deviation (stdv.), minimum (min) and maximum (max) values of the variables are for the calibration area.

Category	Variable	Description	Unit	Mean ± stdv. [min, max]
Climate	*MAP*	Normal annual precipitation (1961-1990)	mm	458±74 [358, 651]
	MSP	Normal annual summer precipitation (1961-1990)	mm	159±5.55 [146, 172]
	MaxSnow	Normal maximum snow depth (1961-1990)	m	0.60±0.09 [0.43, 1.04]
	MAAT	Normal annual air temperature (1961-1990)	°C	-3.12±0.50 [4.97, -0.31]
	TDD	Normal annual thawing degrees day (1961-1990)	$°Cy^{-1}$	948±98 [103, 1273]
	FDD	Normal annual freezing degrees day (1961-1990)	$°Cy^{-1}$	2068±162 [1395, 2355]
Topography	*MinElevation*	Minimum elevation above sea level	m.a.s.l.	441±84 [80, 975]
	Slope	Mean slope angle	°	4±4.53 [0, 41]
	Flat	Area of flat topography (slope ≤ 0,2°)	m^2	162951±130489 [0, 719400]
	TWI	Mean Topographic wetness index		5.26±0.58 [1, 8.61]
Land cover	*Water*	Area covered by water	m^2	88278±166860 [0, 997200]
	Mire	Area covered by mire	m^2	51755±70614 [0, 522600]

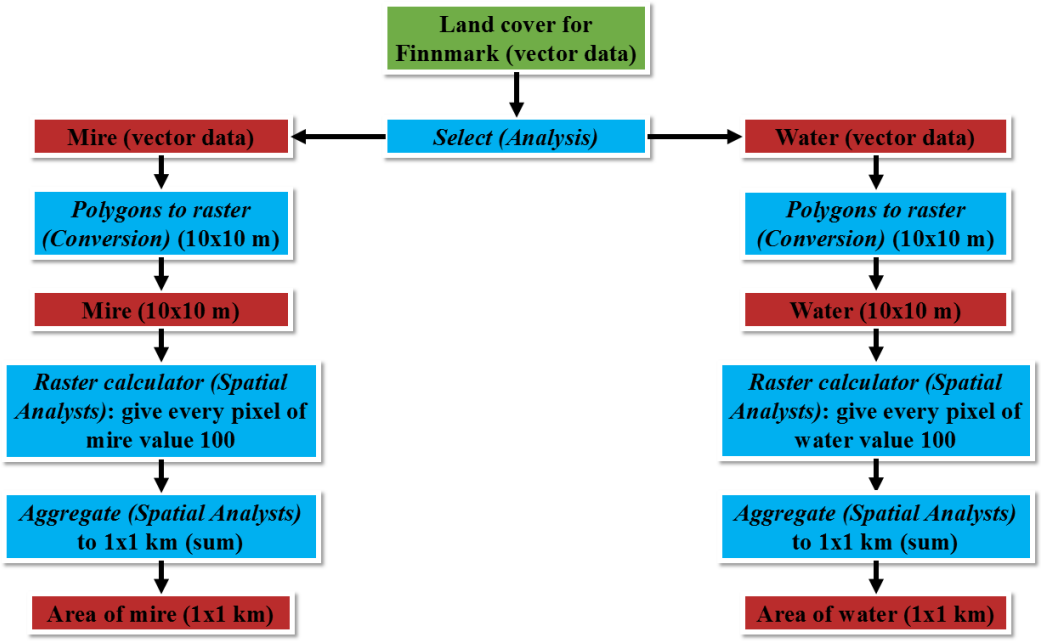

Figure 9: Flowchart illustrate the process of deriving the land cover variables of Water and Mire (description of the variables in Table 2) from a land cover map by the Norwegian Forest and Landscape Institute. All operations are performed by using ArcMap 10.2. All tools in italic. Green boxes represent input data, blue boxes processes and red boxes results.

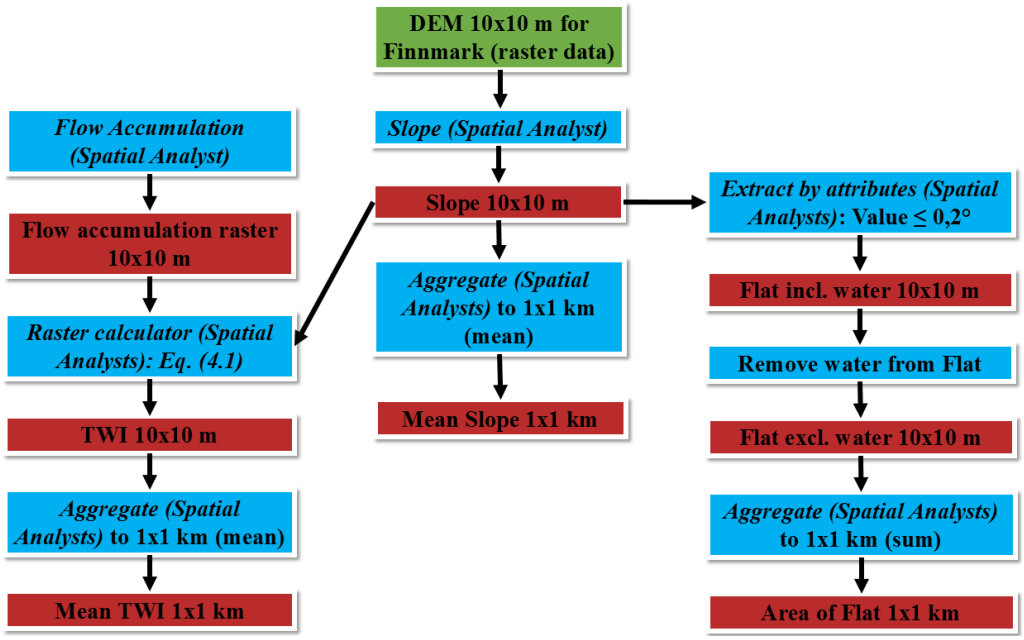

Figure 10: Flowchart illustrate the process of deriving the topographic variables of Slope, Flat and TWI (description of the variables in Table 2) from the national 10x10 m DEM from the Norwegian Mapping Authority. All operations are performed by using ArcMap 10.2 and all tools are in italic. Green boxes represent input data, blue boxes processes and red boxes results.

4.2.2 Data exploration and calibration of GLM

All statistical exploration and calibration of the GLM were done by using the statistical software *R* (R Core Team, 2014) and the package *R Commander* (*Rcmdr*) (Fox, 2005). Exploration of the explanatory variables and the relation between the response variable and the explanatory variables were investigated by means of correlation matrix, boxplots (by using the default box plot tool in R), histograms and response curves.

To prevent the final model against multicollinearity, the first step after data exploration is to exclude predictors with a high degree of correlation by producing a correlation matrix (using Spearman`s rank order because of non-normal data). The correlation threshold for exclusion is set to $R_s > 0.7$, same threshold used by Hjort et al. (2010).

In the model building process, both backward and forward selection were explored to find the best combination of variables, based on *p*-values ($p < 0.01$) and Akaike`s information criterion (AIC). The linearity of the variables was explored by looking at response curves in a univariate setting. Also, changes in AIC when using nonlinear variables compared with linear variables were investigated for potential nonlinear explanatory variables. It was decided to have explanatory variables as nonlinear if they had a clear nonlinear response and at the same time a satisfying empirical explanation for this nonlinearity.

4.2.3 Evaluation of the model

The evaluation of the final GLM is based on AUC-values for both the calibration and the evaluation areas, using package *pROC* (Robin et al, 2011) in *R*. A way to assess the stability of the model is to use a formula termed AUC-stability:

$$\boldsymbol{AUC_{stability}} = \frac{\boldsymbol{AUC_{evaluation}}}{\boldsymbol{AUC_{calibration}}} \qquad (4.2)$$

An AUC-stability of close to one indicates that the model is robust, and might be transferable to other regions. Furthermore, the direction of the variables in the final model gives information about the validity of the variables when compared with theory.

4.2.4 Prediction

In the end, the regression coefficients for the explanatory variables in the final GLM are used to predict the occurrence of palsas in whole Finnmark by using the raster layers of the explanatory variables. This is achieved by using the tool *Raster Calculator* in *ArcMap 10.2*. In GLMs with binary data, the combination of explanatory variables is related to the expected value (i.e. the prediction of probability) through a logit link function (Hjort and Luoto, 2013):

$$\boldsymbol{Prediction} = \frac{\mathbf{1}}{(\mathbf{1} + \left(\boldsymbol{Exp}\left(-(\boldsymbol{\alpha} + (\boldsymbol{\beta_1} * \mathbf{x_{1i}}) + (\boldsymbol{\beta_2} * \mathbf{x_{2i}}) + \cdots + (\boldsymbol{\beta_k} * \mathbf{x_{ki}})\right)\right))} \quad (4.3)$$

Where α is constant (i.e. intercept), β_k are regression coefficients and x_{ki} are explanatory variables.

Finally, the prediction map needs to be evaluated by visual interpretation and by comparing the results with current theory and knowledge. Does the result look realistic? In this process, the prediction map will be compared with Sollid and Sørbels (1998) map of the distribution of palsas in Fennoscandia. This map is revised from Sollid and Sørbel (1974), which again is based on the work of several researchers and by studies of aerial images for certain areas in Norway by the authors.

4.2.5 Estimation of total area of palsas

The flowchart in Figure 11 illustrates the main steps in the process of estimating the total area of palsas in Finnmark. First, a reasonable threshold must be selected. In this thesis, the threshold is based on how the final model fits the evaluation areas and by interpretation of the final map of prediction of palsas. To evaluate whether the final GLM overestimate or underestimate the probability of palsas, I carried out investigations of how the sensitivity (2.2), specificity (2.3) and the overall correct classification rate of the model (2.4) changed with different thresholds.

When a reasonable threshold is selected, all of the grid cells in Finnmark at or above this threshold are extracted from the map using the function *Extract by Attributes* in *ArcMap.* Since palsas need to be situated in mires, the first step to estimate the total area of palsas is by calculating the total area of mire in these grid cells. Using the explanatory variable *Mire*, the

total area of mire is calculated by the function *Aggregate* in *ArcMap 10.2*. When the total area of mire in the grid cells at or above the threshold is known, the proportion of palsas covering this area of mire has to be estimated. To avoid qualified guessing, the results of the delineation of palsas in the study sites Lakselv, Suossjavri and Goatheluoppal have been utilized to find the proportion of palsas by mire. To best simulate the final calculation of the total area of palsas, the polygons of palsas in these study sites are divided into grid cells. Only grid cells where a large fraction of all palsas is delineated are used for the estimation. Then the area of mire and area of palsas are calculated for each grid cell, and the proportion of palsas by mire is calculated. The same proportion is in the end extrapolated to all grid cells at or above the set threshold, and a total area of palsas is calculated.

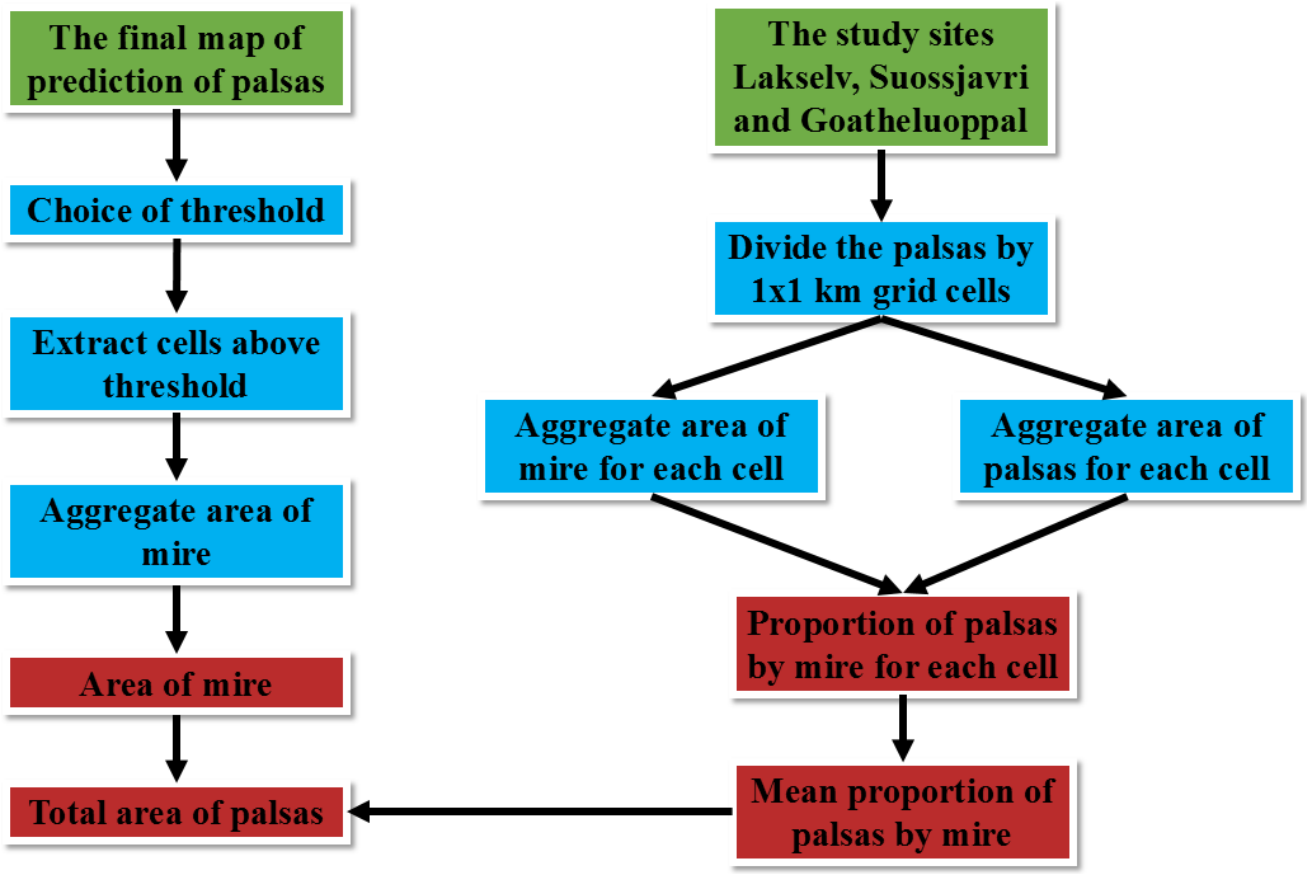

Figure 11: Flowchart of the main steps in the process of estimate the total area of palsas. Green boxes represent input data, blue boxes processes and red boxes results. The green box with the study sites Lakselv, Suossjavri and Goatheluoppal means the delineated palsas in these study sites.

4.2.6 Hierarchial Partitioning

HP for the explanatory variables for the calibration area are performed by using the package *hier.part* (Walsh and Nally, 2013) in *R*. This method gives the independent effect of all variables to explain the distribution of palsas for the calibration area (further details about HP in 2.2.4). According to the documentation of the package by Walsh and Nally (2013), HP produces a rounding error when the model consist of more than nine explanatory variables. Further, a detailed study of this "rounding" error by Olea et al. (2010) reveal that this rounding error is significant and produce considerable inconsistency for analyses with more than nine variables. Thus, they recommend avoiding more than nine explanatory variables when utilizing HP in *hier.part*. On the basis of this information, there was decided to produce three independent HPs:

1. HP of all topography and land cover variables together.
2. HP of all climate variables together.
3. HP of the four most important variables from (1) and (2) in the same model

Thus, a comparison between the most important variables from topography, land cover and climate variables are possible in HP 3. The result is further compared with the significance of the variables from the final GLM, and used to evaluate the final model. Further, HP is of importance when discussing the relative independent importance of the explanatory variables.

4.3 A simple carbon gas release model

The idea is to use inputs from the results of this thesis to produce a simple model of the potential release of CO_2 and CH_4 from the degradation of palsas for whole Finnmark for the period 1960 to 2010 (50 years). The main steps in this simple model are presented in Figure 12. The two most important numbers for this model are the rate of degradation and the total area of palsas in 2010. An estimate of the total area of palsas are explained in 4.2.5. An estimate of degradation from 1960 to 2010 is based on the results of the delineation of palsas in Lakselv, Suossjavri and Goatheluoppal. In addition, key figures that the model need are an estimate of the proportion of peat in the frozen core, the density of peat, a mean height of palsas and mean carbon content in peat. According to M. Seppälä and Kujala (2009), 80 - 90 % of the volume of frozen peat in the permafrost core is ice. Thereby, 10 - 20 % of the

volume is peat. The middle value of 15 % is used in this model. Loisel et al. (2014) found that the average carbon content for 56 peat cores located north of 45° was 47 %, while the dry organic matter (OM) bulk density from 184 peat cores averaged 0.11 g/cm^3. Of all peat cores, 40 % were collected in peatlands affected by permafrost (Loisel et al., 2014). Oksanen (2005) found a average carbon content of 51 % for peat in palsa mires across Fennoscandia. Thus, a carbon content of 50 % and a dry OM bulk density of 0.11 g/cm^3 are selected for the model.

This model estimates only the volume of palsas above the mire. As we know that the permafrost core in palsas extends below the rest of the mire, this underestimation of volume of palsas will give more conservative results of the potential release of CO_2 and CH_4 from thawing palsas. A mean height of 2 m for palsas is used in the model for the computation of the volume. As the active layer is neglected in this model, the estimate of mean height of 2 m of palsas is thus really the mean height of the permafrost core.

This thesis will not investigate whether the potential gas release from thawing palsas will be in form of CO_2 or CH_4, but will model the individual potential release of both CO_2 and CH_4 on the basis that all the carbon in the degraded peat will form a component of either CO_2 or CH_4.

The final estimates of gas release from thawing palsas are compared with human emissions of CO_2 and CH_4 in Finnmark for 2010.

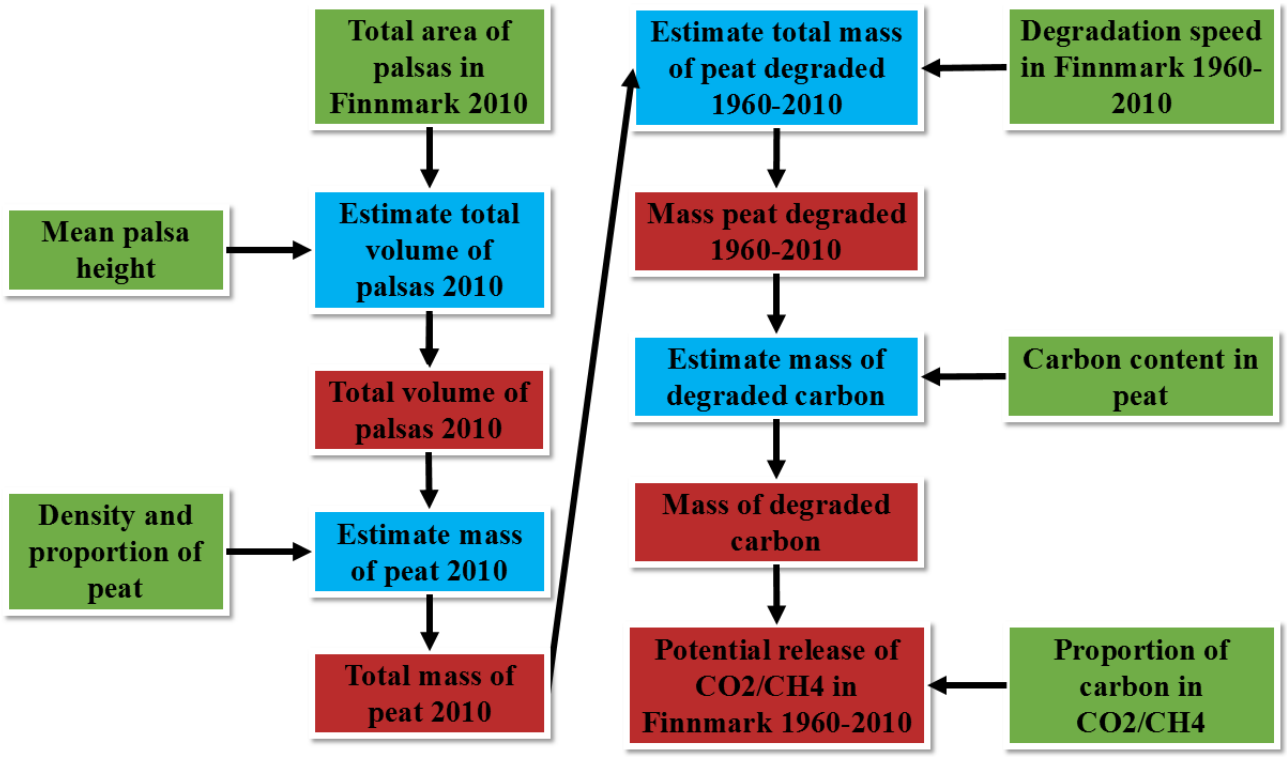

Figure 12: Flowchart of the main steps towards a rough estimate of the potential release of CO_2 and CH_4 in Finnmark for 1960-2010 from thawing palsas. Green boxes represent input data, blue boxes processes and red boxes results.

5. Results

This chapter includes the results from the processing of meteorological data (5.1), from observations in the field (5.2), from the delineation of palsas (5.3) from the GDM process (5.4) and from the simple model of carbon gas release (5.5). Section 5.1 contains time series of climatic data from meteorological stations close to the study sites. Section 5.2 include some examples of recent degradation in two palsa mires in Suossjavri, and some observations relevant to understanding how to interpret palsas on aerial images. Section 5.3 consist of the accuracy of the georeferencing process and the results of the delineation of palsas in Lakselv, Suossjavri and Goatheluoppal. Furthermore, Section 5.3 includes examples of images from the 1950s demonstrating the occurrence of thermokarst lakes and degrading palsas. The results in 5.4 begin with some results that highlight the importance's of the different variables, continuing with presenting the final GLM and a map of the probability of palsas in Finnmark. The final GLM and the probability map are evaluated at the end of the chapter. Based on this probability map and the evaluation, a total area of palsas in Finnmark for 2010 is estimated. Section 5.5 presents the result of the simple model of potential carbon gas release from thawing palsas in Finnmark, including a comparison with emissions of CH_4 and CO_2 in Finnmark by different sources.

5.1 Meteorological data

5.1.1 Lakselv

Banak meteorological station in Lakselv has available data of temperature, precipitation and mean wind speed. These data have been used to make plots of MAAT (Figure 13), MAP (Figure 14) and mean wind speed (Figure 15) for the period 1966 to 2014. Information of snow cover was not available. There are unfortunately some gaps of missing data for the time series. Table 3 shows MAAT, MAP, maximum snow depth and the mean wind speed for different periods (naturally divided by the data gaps). Because of slightly different data gaps between the variables, the mean is calculated for different periods. Some minor data gaps are also evident in the periods.

The results show an increase in both MAAT and MAP, while mean wind speed is quite stable until the last ten years when there was a notably higher wind speed (Figure 13, 14 and 15). MAAT was as high as 1.57 °C for the period 1998-2014, 1 °C warmer compared with 1966-1983 (Table 3). MAP increased with over 60 mm, from 339 mm to 403 mm, for the same period (Table 3).

Table 3: Mean temperature, precipitation, maximum snow depth and mean wind speed for different periods at Banak meteorological station. Because of the difference in data gaps between the climate variables, the mean is calculated for different periods. Some minor data gaps are also evident in the periods.

Mean for the period:	**1966-2014**	**1966-1996**	**1966-1983**	**1985-1996**	**1998-2014**
MAAT [°C]	0.96	-	0.51	0.91	1.57
MAP [mm]	359.77	-	339.48	335.65	403.41
Mean wind speed [m/s]	4.81	4.69	-	-	5.17

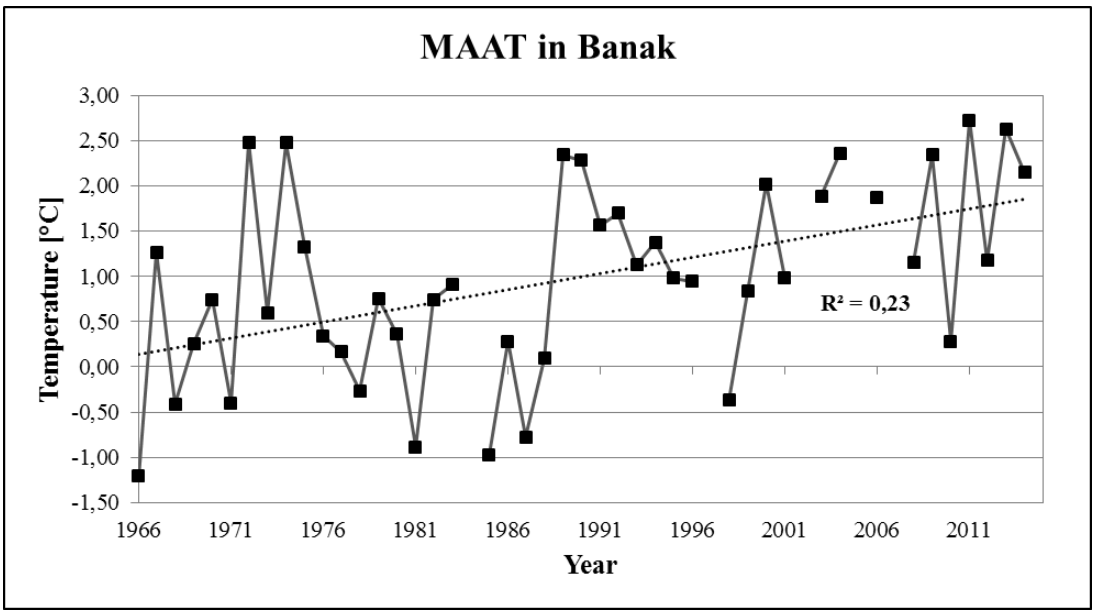

Figure 13: MAAT at the meteorological station Banak in Lakselv, from 1966 to 2014, including linear trend line and R-squared value for this trend line.

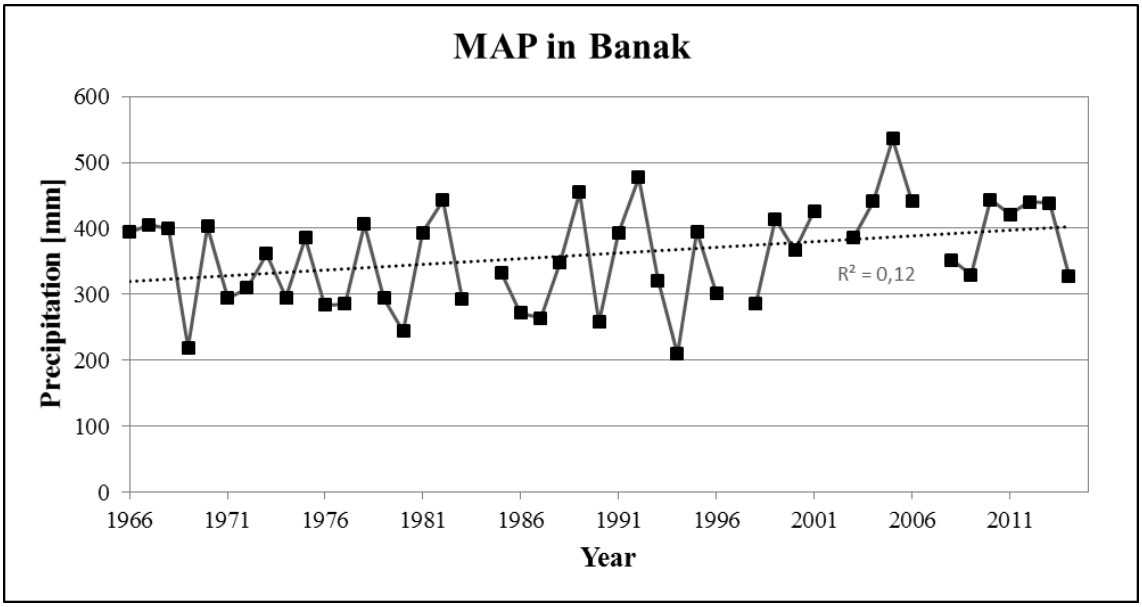

Figure 14: MAP at the meteorological station Banak in Lakselv, from 1966 to 2014, including linear trend line and R-squared value for this trend line.

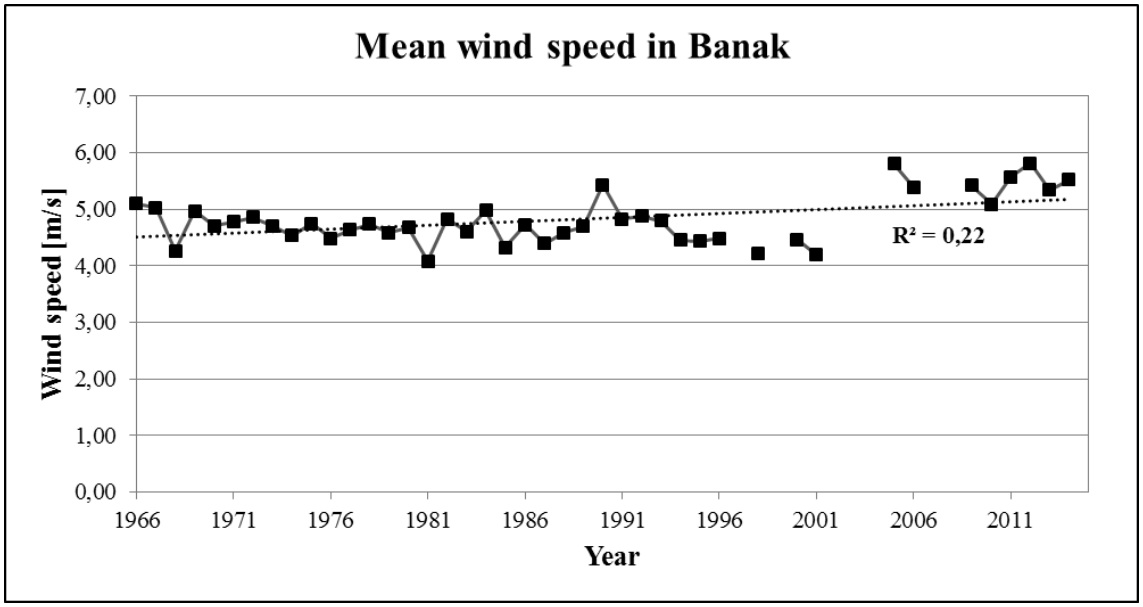

Figure 15: Mean wind speed at the meteorological station Banak in Lakselv, from 1966 to 2014, including linear trend line and R-squared value for this trend line.

5.1.2 Suossjavri

Cuovddatmohkki meteorological station in Suossjavri has data of temperature, precipitation, snow depth and mean wind speed. These data have been used to make plots of MAAT (Figure 16), MAP (Figure 17), maximum snow depth (Figure 18) and mean wind speed (Figure 19) for the period 1967 to 2014. Unfortunately, there exist some gaps of missing data for the time series. Table 4 shows MAAT, MAP, maximum snow depth and the mean wind speed for different periods (naturally divided by the data gaps). Because of slightly different data gaps between the variables, the mean is calculated for different periods. Some minor data gaps are also evident in the periods.

Like Banak, there has been an increase in both MAAT and MAP during the period (Figure 16 and 17). MAAT has increased by more than 1 °C up to -1.51 °C for the period 1995-2014 compared with the period 1967-1980 (Table 4). MAP increased with 61 mm, from 359 mm to 420 mm, for the same period (Table 4). No trend is observed for the maximum snow depth (Figure 18). The most distinct trend in Cuovddatmohkki is the increase in mean wind speed (Figure 19), whereas the mean wind speed for the period 1995-2014 was 1 m/s higher compared with the period 1967-1980 (Table 4).

Table 4: Mean temperatures, precipitation, maximum snow depth and mean wind speed for different periods at Kautokeino meteorological station. Because of the difference in data gaps between the climate variables, the mean is calculated for different periods. Some minor data gaps are also evident in the periods.

Mean for the period:	**1967-2014**	**1967-1980**	**1982-1993**	**1984-1992**	**1995-2014**
MAAT [°C]:	-1.97	-2.59	-	-	-1.51
MAP [mm]:	391.62	358.51	-	-	420.02
Max snow depth [cm]:	61.39	60.57	63.00	-	61.00
Mean wind speed [m/s]:	1.42	0.96	-	1.04	2.00

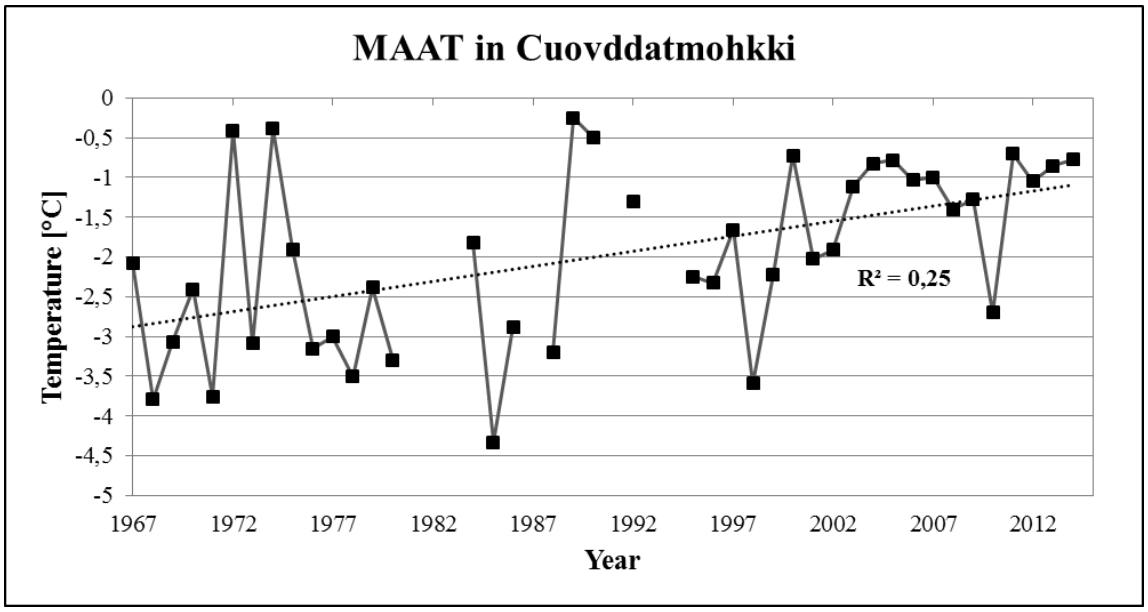

Figure 16: MAAT at the meteorological station Cuovddatmohkki in Suossjavri, from 1967 to 2014, including linear trend line and R-squared value for this trend line.

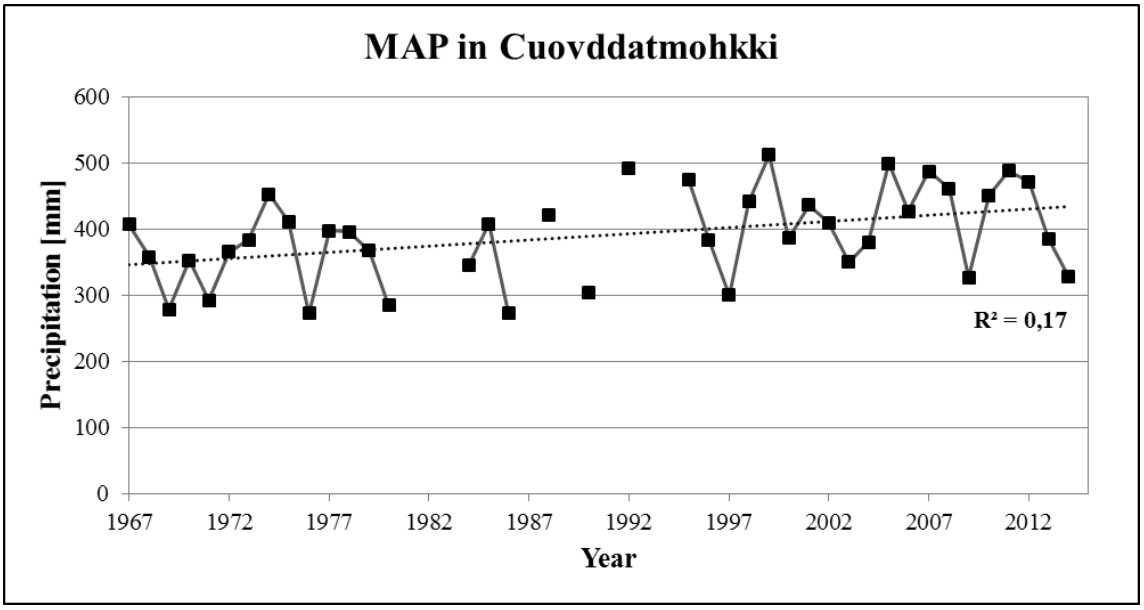

Figure 17: MAP at the meteorological station Cuovddatmohkki in Suossjavri, from 1967 to 2014, including linear trend line and R-squared value for this trend line.

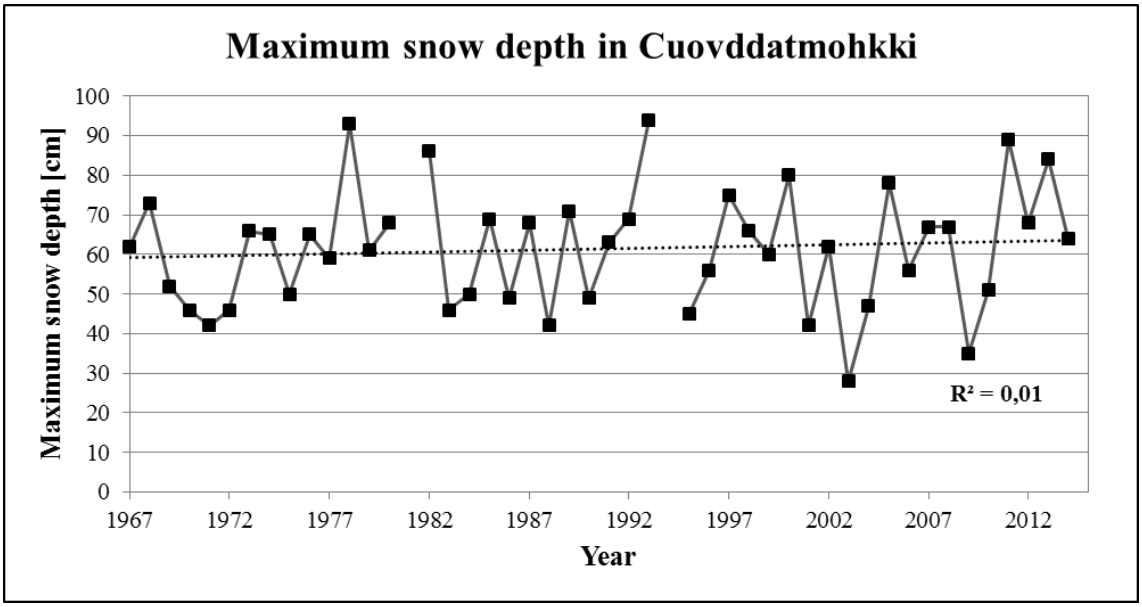

Figure 18: Maximum snow depth at the meteorological station Cuovddatmohkki in Suossjavri, from 1967 to 2014, including linear trend line and R-squared value for this trend line.

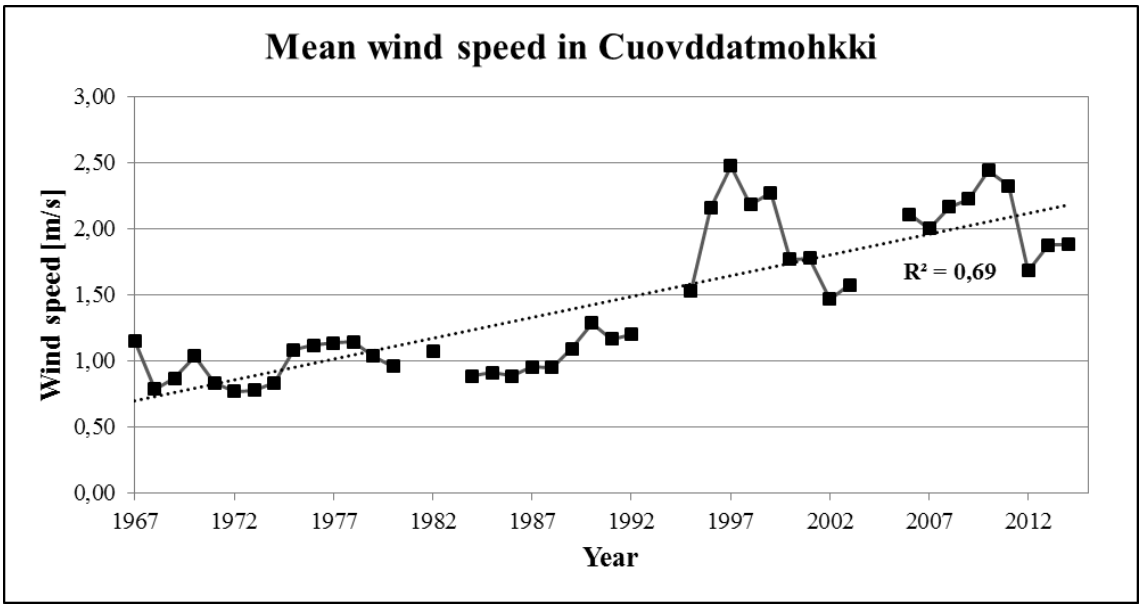

Figure 19: Mean wind speed at the meteorological station Cuovddatmohkki in Suossjavri, from 1967 to 2014, including linear trend line and R-squared value for this trend line.

5.1.3 Goatheluoppal

Kautokeino meteorological station in Kautokeino has data of temperature, precipitation, snow depth and mean wind speed. The data has been used to make plots of MAAT (Figure 20), MAP (Figure 21), maximum snow depth (Figure 22) and mean wind speed (Figure 23) for the time period 1922 (1957 for the mean wind speed) to 2013. There is unfortunately a large gap of missing data for all the meteorological variables for the period from 1970s to mid-1990s, a total of about 25 years. Table 5 shows MAAT, MAP, maximum snow depth and the mean wind speed for different periods (naturally divided by the gap of data). Because of different data gaps between the variables, the mean is calculated for different periods. Some minor data gaps are also evident in within the periods.

There is no clear trend during the whole period for MAAT (Figure 20). Nonetheless, several shorter trends can be observed from the plot. From 1922-1938, there was a clear positive trend. From 1939 to 1970, there was a colder period with a large variety in temperatures. From 2000 onwards, there was again a trend of increasing temperatures. The period 1997-2013 was the warmest, with MAAT of -1.47 °C (Table 5).

While MAP has increased during the period, with an increase of over 100 mm in 1997-2013 compared with 1922-1969 (Table 5), there is no clear trend for the maximum snow depth (Figure 22). There are large gaps in the data of mean wind speed; nonetheless, the available data suggest a positive trend (Figure 23).

Table 5: Mean temperatures, precipitation, maximum snow depth and mean wind speed for different periods at Kautokeino meteorological station. Because of the difference in data gaps between the climate variables, the mean is calculated for different periods. Some minor data gaps are also evident in the periods.

Mean for the period:	**1922-2013**	**1922-1969/1970***	**1922-1938**	**1939-1970**	**1957-1969**	**1997-2013**
MAAT [°C]	-2,00	-	-1,69	-2,45	-	-1,47
MAP [mm]	352,95	326,84	-	-	-	433,99
Max snow depth [cm]	67,52	68,72	-	-	-	64,18
Mean wind speed [m/s]	2,91	-	-	-	2,47	3,24

*1969 applies to MAP, 1970 applies to maximum snow depth.

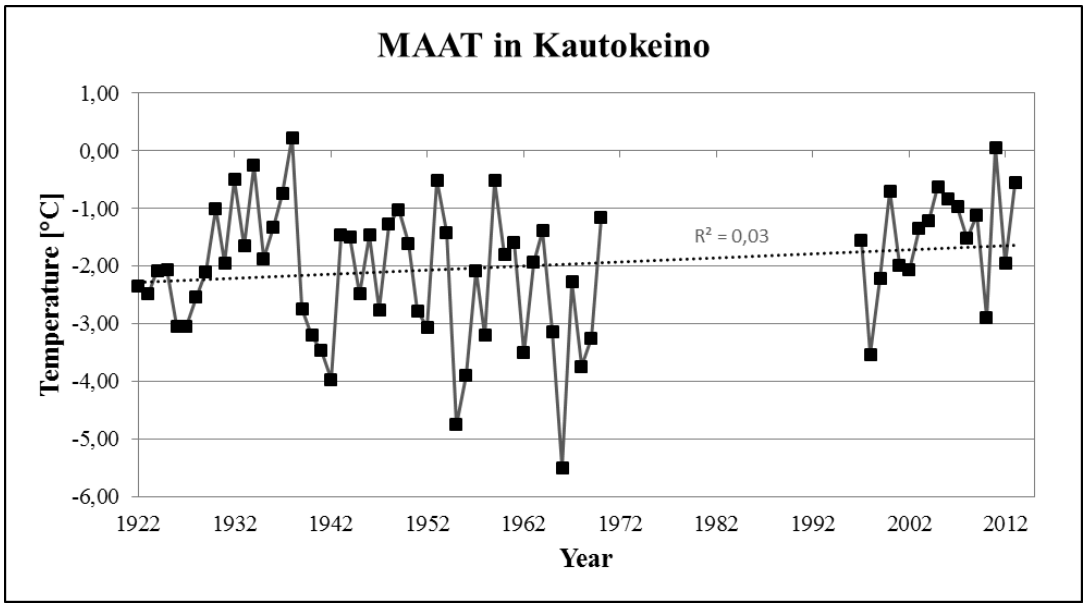

Figure 20:: MAAT at the meteorological station Kautokeino in Kautokeino, from 1922 to 2013, including linear trend line and R-squared value for this trend line. There are a large gap of missing data from the start of 1970s to mid- 1990s.

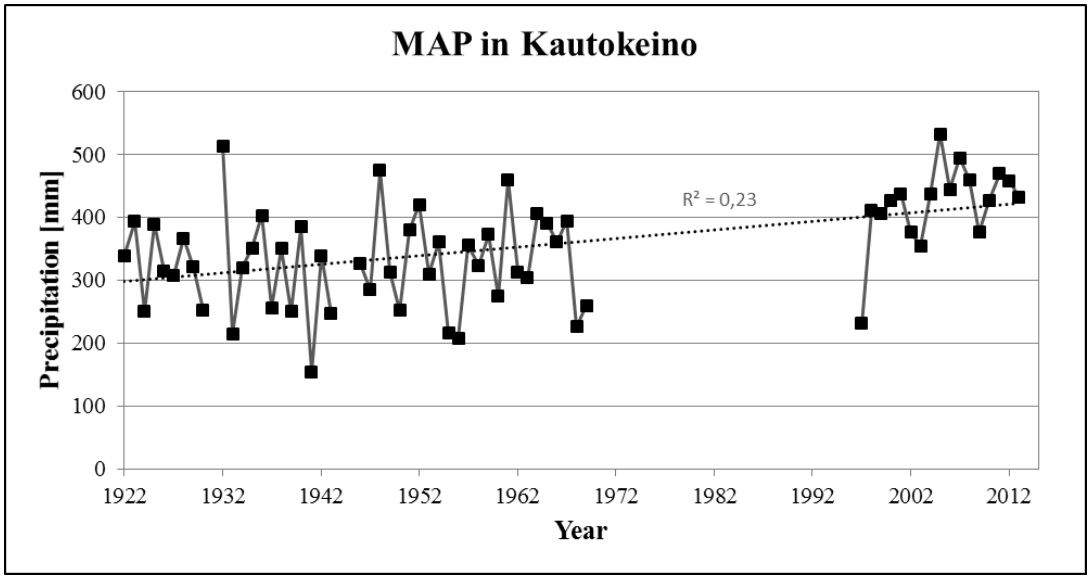

Figure 21: MAP at the meteorological station Kautokeino in Kautokeino, from 1922 to 2013, including linear trend line and R-squared value for this trend line. There are a large gap of missing data from the start of 1970s to mid- 1990s.

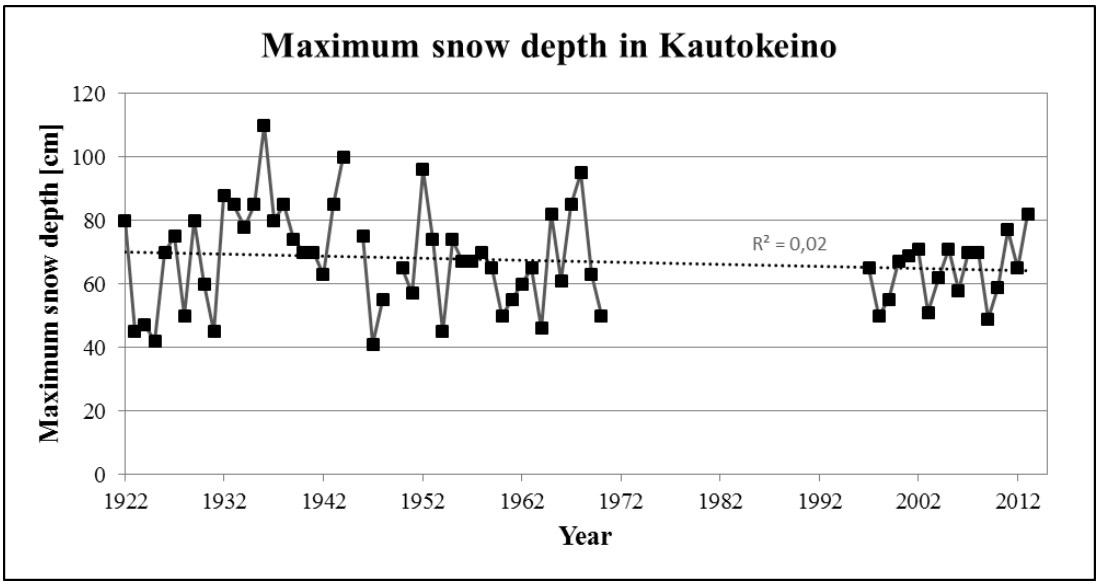

Figure 22: Maximum snow depth at the meteorological station Kautokeino in Kautokeino, from 1922 to 2013, including linear trend line and R-squared value for this trend line. There are a large gap of missing data from the start of 1970s to mid- 1990s.

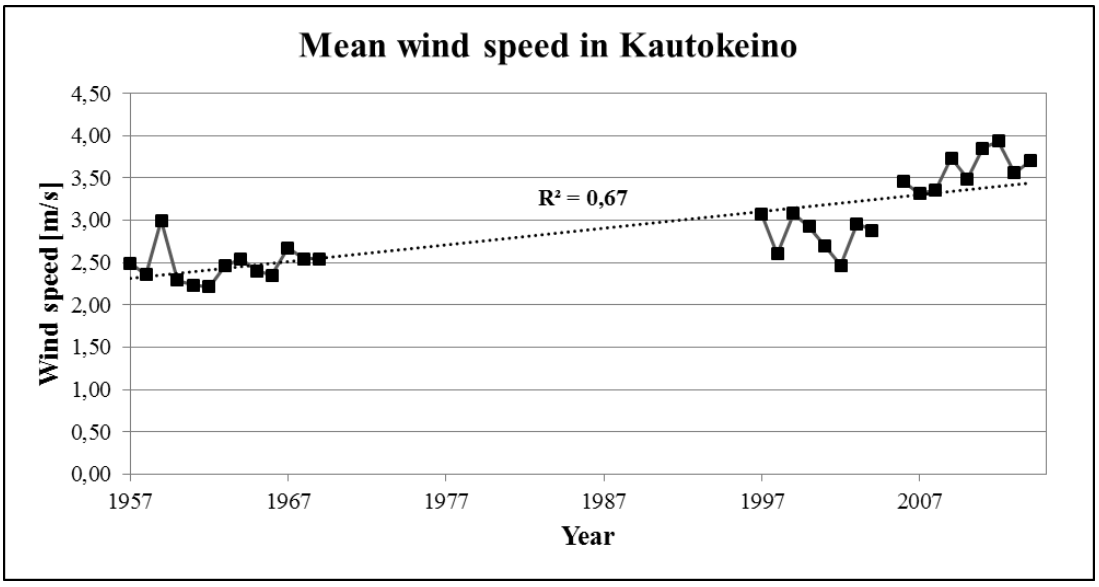

Figure 23: Mean wind speed at the meteorological station Kautokeino in Kautokeino, from 1922 to 2013, including linear trend line and R-squared value for this trend line. There are a large gap of missing data from the start of 1970s to mid- 1990s.

5.2 Observations from fieldwork August 2014

Five days of fieldwork was conducted in Suossjavri in mid of August 2014. This section is divided in general observations from the fieldwork (5.2.1) and in observations of continued degradation from the fieldwork (5.2.2). The general observations have been of value for the delineation process and to better understand what is` what on aerial images. When doing observations in the field, I compared what I have seen on the ground with what I observed on aerial images. Several valuable indicators helped to differentiate between wet mire and palsas. Furthermore, several observations have given some insight into where the real edges (i.e. containing permafrost core) of the palsas are situated. Also, for some of the palsa mires in the Suossjavri area, the observations have validated my results that the features mapped in the aerial images really are permafrost mounds in form of either palsas, peat plateaus or lithalsas. Information about peat/mineral content in the active layer was also investigated during the fieldwork. The results showed that the active layer of 14 palsas in palsa mire 3 and 6 (see Figure 36) were mainly consisting of peat, while two were consisting of a mix of layers of peat and silt/sand.

5.2.1 General observations

"Buffer vegetation" and rim ridges

The vegetation is differently due to where it is situated on a palsa. High vegetation is common in concave areas and at the edges, probably because of a relatively high snow cover. At convex areas on the top of the palsas, the vegetation is low, probably because of low snow cover and sometimes as a result of wind erosion (Seppälä, 2003) Also, the vegetation in the wet mire around the palsa is different, doing delineation of palsas by aerial images possible. The vegetation at the edges is like "buffer vegetation", as it is situated in the zone between the dry elevated palsa and the flat and wet mire, with an often diffuse boundary in between. The image in Figure 14 illustrates a situation of such a diffuse boundary of "buffer vegetation" for a 1.5 m high palsa in Suossjavri (69.3823 N, 24.1041 E). In this example, permafrost is evident where the stick is penetrating the "buffer vegetation", with an AL of 0.55 m. Notice almost no vegetation on the top of the palsa, probably due to wind erosion. In comparison, on the other side of the same palsa, a "buffer vegetation" is evident (Figure 15), but this buffer vegetation is situated to the side of the edge, and is not part of the real edge like in Figure 14.

In this buffer vegetation, no permafrost (AL > 1.1 m) was found. The sketch in Figure 16 illustrates both examples: permafrost is evident where the "buffer vegetation" form the real edge, while when the "buffer vegetation" is situated to the side of the real edge as a rampart, in between the wet mire and the edge, no permafrost is evident. When the palsa in Figure 15 degrade further and a gap is created between the palsa and the "buffer vegetation", a "ring" of peat and high vegetation are created around the degrading palsas. These rim ridges are according to Seppälä and Kujala (2009) created by block erosion, where blocks of peat have collapsed along the frost table. According to Pissart (2013), only the ridges from lithalsas remains for a longer time period after the palsas thaw, while palsas leave almost no trace. However, Svensson 1969 relate the observation of some circular to oval lakes in Northern Norway to the collapse of e.g. palsas, because the lakes are enclosed by low rim ridges.

During the fieldwork, a few rim ridges around degrading palsas were investigated for evidence of permafrost (e.g. Figure 17), but no permafrost was found (AL < 1.1 m).

In this master thesis, the problem arises when rim ridges with "buffer vegetation" are just outside the present edge of the palsas, as is illustrated in Figure 15 and 16. In aerial images, such rim ridges are often observed in close connection with the real edge, making delineation more difficult.

Figure 14: High buffer vegetation in between the bare surface of the palsa and the wet mire around. Where is the edge of the palsa? Permafrost is evident where the iron stick penetrate, with AL = 0.55 m. Photo from August 2014, by Amund F. Borge.

Figure 15: Elevated peat and high "buffer vegetation" (in the centre of the photo) to the side of the real edge of the palsa. No permafrost is evident in this "buffer vegetation". Photo from August 2014, by Amund F. Borge.

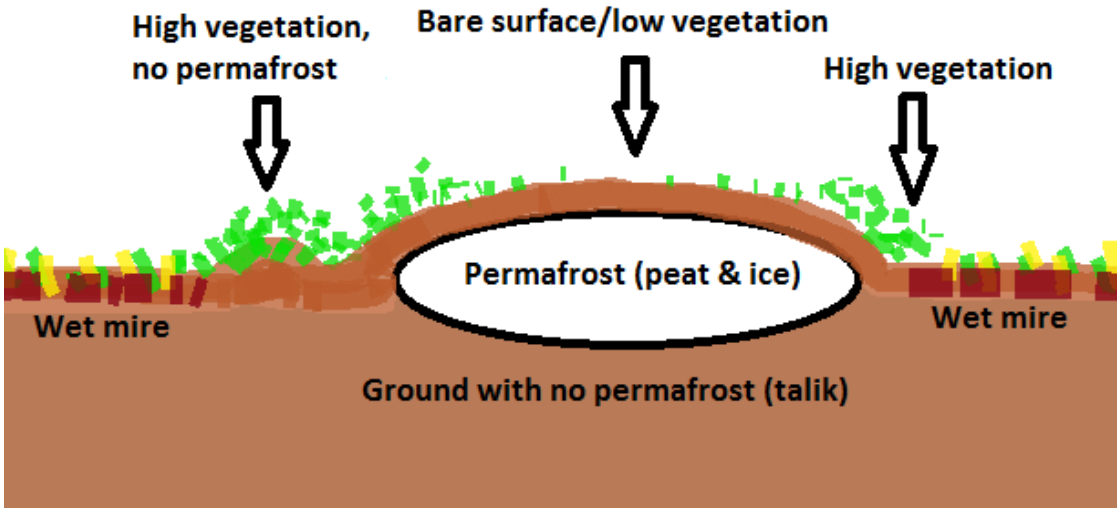

Figure 16: Illustrates a situation where high "buffer vegetation" is on both sides of a palsa. To the left, a rim ridge with elevated peat and high vegetation is situated between the real palsa edge and the wet mire. No permafrost is evident here. On the right side, high vegetation is present on the real palsa edge, where permafrost is evident.

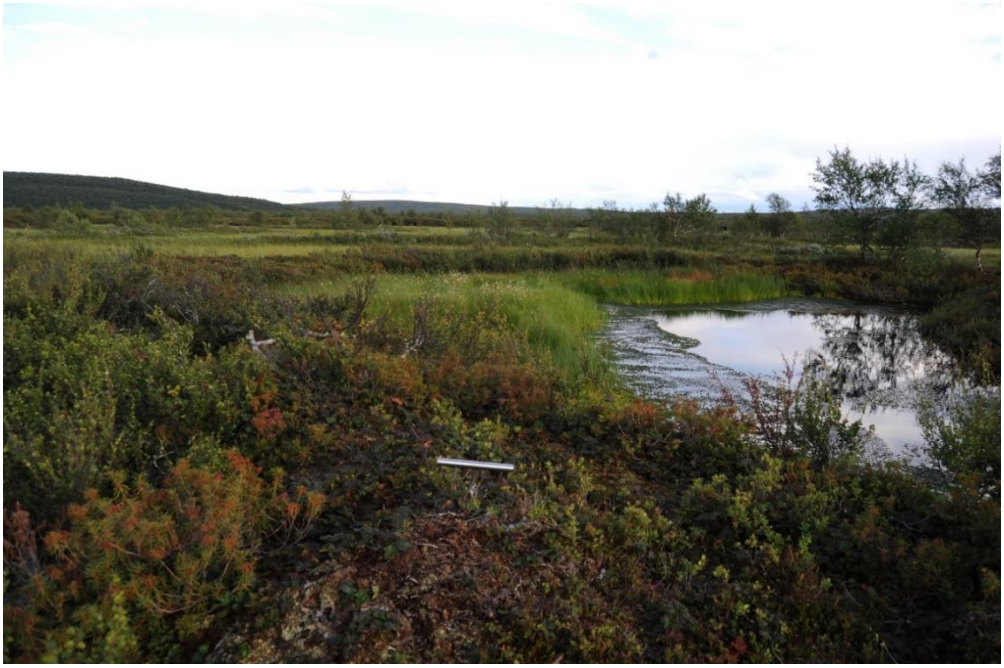

Figure 17: A rim ridge of peat and high vegetation, similar with the vegetation present at the palsa edges. The rim ridge is situated around a small degrading palsa in Suossjavri. No permafrost (AL < 1.1 m) was found in this rim ridge. Photo from August 2014, by Amund F. Borge.

Palsas with proximity to moraines

From observations in the field and of aerial images, there are apparently many palsas situated next to moraines, as a boundary between the wet mire and the moraines. Such palsas are usually difficult to delineate and to notice on aerial images if they are small. This is due to a gradual transition between moraines and palsas observed on aerial images. Thus, flickering is sometimes necessary to detect palsas next to moraines. The gradual transition is probably a result of relatively similar vegetation between the start of moraines and the edge of palsas, as observed during the fieldwork. Figure 19 illustrates an example of a palsa (69.3819 N, 24.103 E) with close connection to a moraine/till. This palsa are approximately 1-1.5 m above the mire and decrease in height (with no sharp elevation changes) to 0.2-0.5 m above the mire when it meets the moraine/till. In the transition zone from mire to moraine/till, a thin peat cover (10-50 cm) over the till (in this example larger rocks) is present, making a very similar vegetation as the vegetation of the palsa edge. A generalization of the challenges related to palsas next to moraines are sketched in Figure 18.

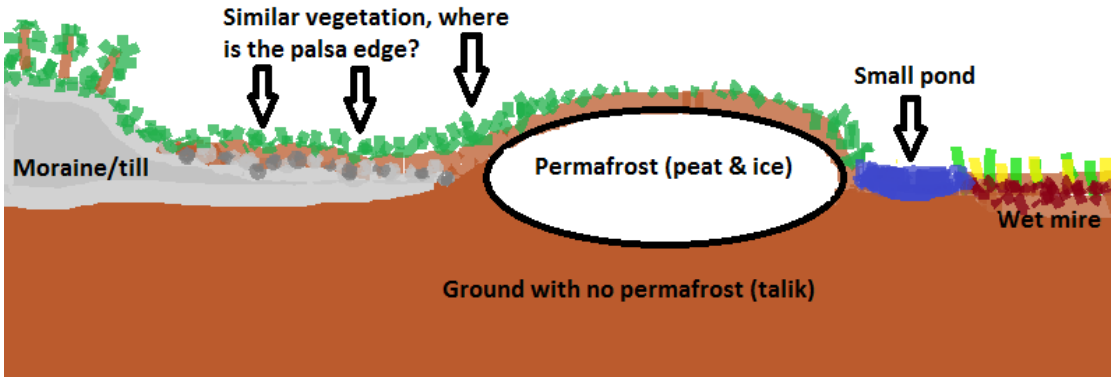

Figure 18: Sketch of a "confined" palsa: situated beside a moraine. It is a slow transition of different vegetation between the moraine and the palsa, making delineation of the edge difficult. The palsa edge on the right side is easily delineated, as a sharp border between the vegetation on the palsa and the wet mire is visible.

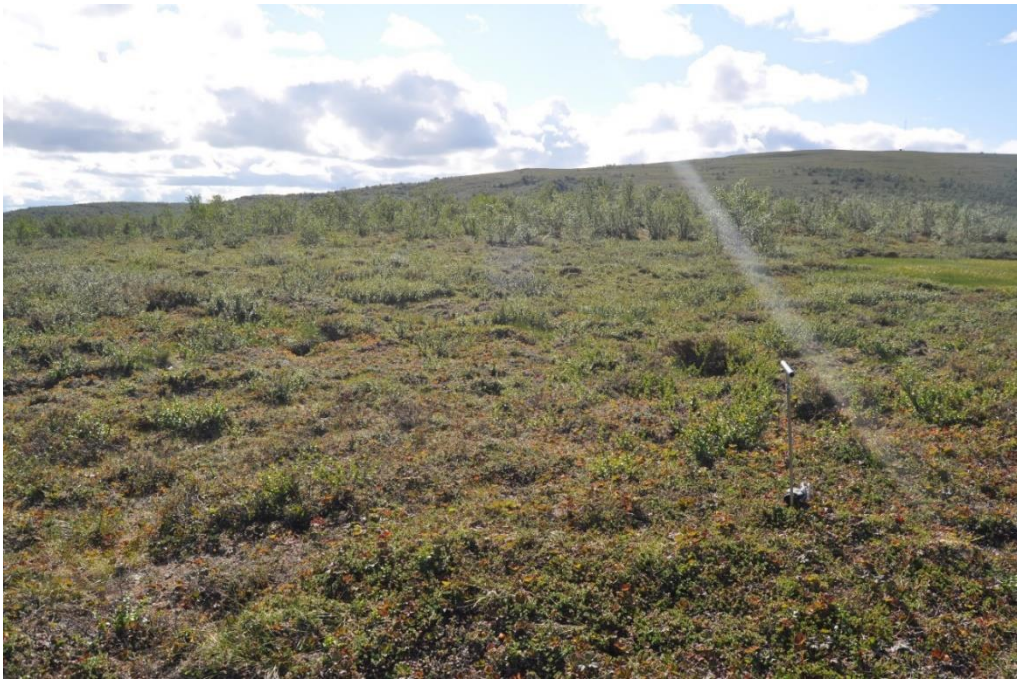

Figure 19: A palsa with a gradual transition into a moraine, with no sharp visible edge. The stick marks the approximate limit of where permafrost was found (AL < 1.1 m). The direction of the photo is towards the moraine/till. Photo from August 2014, by Amund F. Borge.

5.2.2 Observations of continued degradation 2011-2014

There were several examples of degrading palsas in Suossjavri. Presented here are several observations of small palsas that degraded markedly from 2011 (aerial images from Norgeibilder.no) until the fieldwork was conducted. Aerial images from 2003 and 2009 (Norgeibilder.no) further show the fine-scale development of the palsas in the last decade.

Observation 1

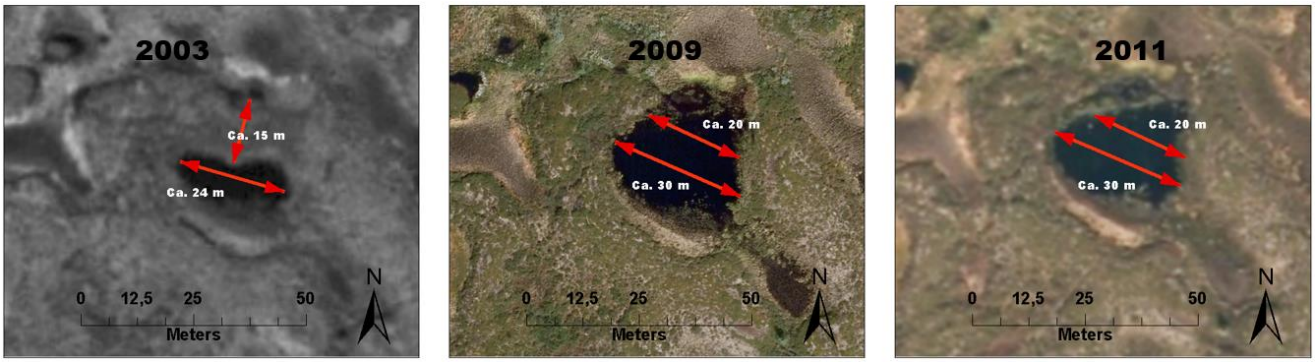

Figure 20: Aerial images from 2003, 2009 and 2011 of a degrading palsa (69.3826 N, 24.2494 E) situated in Suossjavri, where the centre has collapsed and turned into a thermokarst lake. All images from Norgeibilder.no.

Figure 21: 2014 – Image of the same palsa as in Figure 20. Photo from August 2014, by Amund F. Borge.

The centre of a palsa (69.3826 N, 24.2494 E, palsa mire 6 in Figure 36) has collapsed and turned into a thermokarst lake from between 2003 and 2014 (Figure 20 and 21). The longest diameter in both 2009 and 2011 from edge to edge over the thermokarst lake was approximately 30 m. In 2014, the diameter was measured to approximately 42 m. The height above the wet mire for the palsa was in 2014 approximately 1 m.

Observation 2

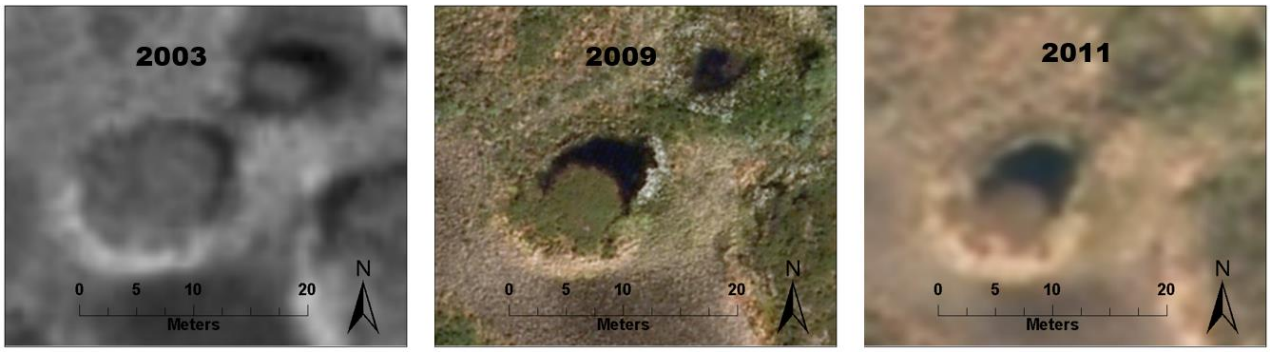

Figure 22: Aerial mages from 2003, 2009 and 2011 of a small degrading palsa (69.3827 N, 24.2487 E) situated in Suossjavri. In 2011, only a small remnant is still above the water. All images from Norgeibilder.no.

Figure 23: 2014 – The palsa from Figure 22 has been totally degraded. Notice the dead vegetation, a sign of recently degraded palsa where the vegetation from the surface of a palsa dies as it sinks into the water. Photo from August 2014, by Amund F. Borge.

A small palsa (69.3827 N, 24.2487 E, palsa mire 6 in Figure 36) from 2003 steadily degraded up to 2014 (Figure 22 and 23). In 2014, the palsa vanished and no permafrost (AL > 1.1 m) was detected in the nearby vegetation. Notice the grey vegetation (Figure 23): dead vegetation originated from the surface of the palsa and a sign of a recently degraded palsa as the vegetation dies when it sinks into the thermokarst lake. Later, new vegetation that prefers a wet environment will probably fill the thermokarst lake and remove most of the signs of the former palsa (Pissart, 2013).

Observation 3

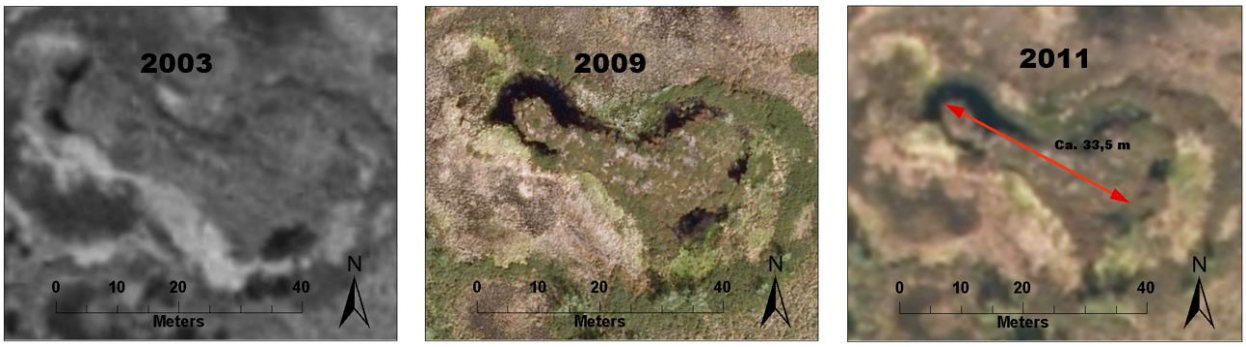

Figure 24: Aerial mages from 2003, 2009 and 2011 of a degrading palsa (69.3875 N, 24.256 E) situated in Suossjavri. All images from Norgeibilder.no.

Figure 25: 2014: Continued degradation of the palsa in Figure 24. Photo from August 2014, by Amund F. Borge.

A palsa (69.3875 N, 24.256 E, palsa mire 6 in Figure 36) degraded from 2003 to 2014 (Figure 24 and Figure 25). Degradation from 2011 to 2014 was particularly significant. The palsa had a maximum length of approximately 33.5 m in 2011, but in August 2014, the size of the remnants was roughly 6x5 m and with a height of only about 0–40 cm above the water. Surprisingly, there was some permafrost evident in the remnants, with an AL of 45 cm at the centre.

Observation 4

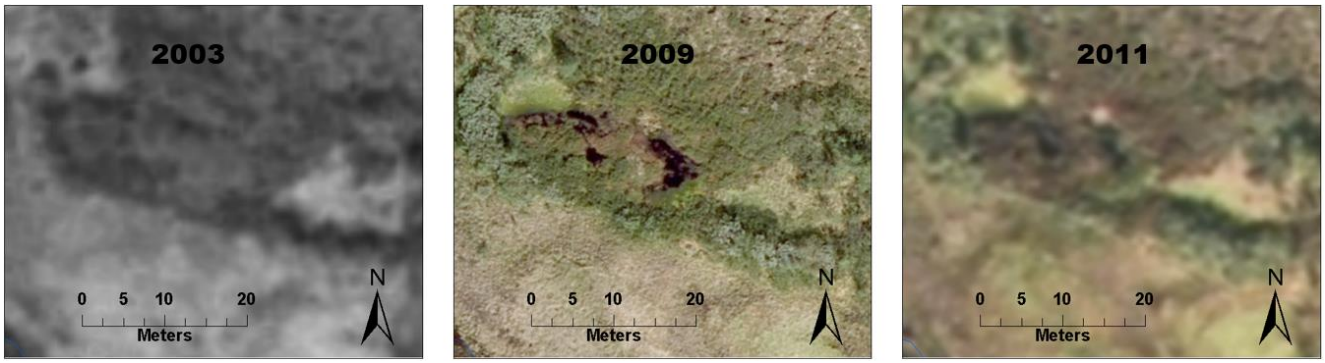

Figure 26: Aerial mages from 2003, 2009 and 2011 of a small degrading palsa (69.3829 N, 24.1027 E) situated in Suossjavri. All images from Norgeibilder.no.

Figure 27: 2014 – Only small remnants of vegetation are remaining from the degradation of the palsa in Figure 26. Photo from August 2014, by Amund F. Borge.

A palsa (69.3829 N, 24.1027 E, palsa mire 3 in Figure 36) degraded from 2003 to 2014 (Figure 26 and 27). In 2014, only small remnants of vegetation are remaining just above the water and no permafrost (AL > 1.1 m) is evident.

5.3 Delineation of palsas

5.3.1 Georeferencing

The accuracy in form of RMSE from the process of georeferencing is presented in Table 6 for all images used in this thesis. Several images have been georeferenced several times for different palsa mires. The RMSE values were generally within 0.6-2 m. One exception was an RMSE of 4.2 m for palsa mire 1 in Lakselv (Figure 28) in image W-21, coverage number WF-2120 from 1959 (Table 6). This is probably due to a mix of the palsa mire situated unfavourable in the corner of the image, and the relative high relief around the mire in comparison with other areas.

Table 6: Present the accuracy of the georeferencing process for all images and all palsa mires for Lakselv, Suossjavri and Goatheluoppal. Several images have been georeferenced several times for different palsa mires. CPs are abbreviation for Control Points. The RMSE values are in meters. ND = No Data

Study sites	Palsa mire	Image 1950s	No. of CPs 1950s	RMS 1950s	Image 1980s	No. of CPs 1980s	RMS 1980s
Lakselv	1	WF-2120_W-21	5*	4.2**	-	-	-
	2	WF-2120_W-21	7	0.78	-	-	-
	3	WF-2120_W-19	8	1.60	-	-	-
	4	WF-2120_X-17	8	1.94	-	-	-
	5 and 6	WF-2120_X-15	5***	1.10	-	-	-
	7	WF-2120_X-15	7	1.67	-	-	-
	8	WF-2120_Y-14	6	1.88	-	-	-
Suossjavri	1, 2 and 3	WF-2121_J-50	8	1.23	NLF-7523_K-3	11	0.68
	4	WF-2121_K-47	8	0.76	NLF-7523_K-4	9	1.39
	5	WF-2121_K-47	7	0.75	NLF-7523_K-4	9	1.39
	6	WF-819_M-1	8	0.74	NLF-7523_K-6	8	0.68
	7 - upper part	WF-819_K-3	8	0.93	NLF-7523_J-4	9	1.52
	7 - lower part	WF-819_K-2	7	1.05	NLF-7523_J-5	9	1.52
Goatheluoppal	1, 2 and 3	WF-2033_C-16	7	1.82	NLF-6442_P-6	8	1.51
	4 and 5	WF-2033_C-16	ND	ND	NLF-6442_Q-4	8	0.73
	6	WF-2033_C-14	8	0.80	NLF-6442_Q-4	10	0.92

Comments
* Difficult to find good control points
** Large RMS, possibly because of the mire situated in the image corner and with a larger relief in the landscape
*** Difficult to find good control points, because of large landscape changes.

5.3.2 Lakselv

The total area in 1959 for all palsas delineated in Lakselv was 945067 m^2, while the total area in 2008 was 491791 m^2 (Table 7). Thereby, the area in 2008 is 52 % of the total area in 1959,

where the remaining 48 % of the area of palsas has degraded. Figure 28 is a map of all palsas delineated in Lakselv, divided in 8 palsa mires. Figure 29 shows individual maps of all 8 palsa mires. Palsa mire 1, which include mostly small palsas, has the highest difference between 1959 and 2008 (-94 %), with almost no palsas left in 2008. Palsa mire 3, which include several large peat plateaus, has the lowest difference with -31 %. Figure 30, 31, 32 and 33 demonstrates examples of large thermokarst lakes that have disappeared in favor of cornfields, a palsa which has been replaced by a cornfield in an unnatural way, examples of disintegration of larger peat plateaus, and some more examples of thermokarst lakes and degrading palsas, respectively.

Table 7: Area of all palsa mires in Lakselv for 1959 and 2008, divided in 8 different palsa mires, and with the difference between these years in both m^2 and %.

	1959 [m^2]	**2008 [m^2]**	**Difference [m^2]**	**Difference [%]**
Palsa mire 1	28252	1610	-26642	-94
Palsa mire 2	102316	55020	-47296	-46
Palsa mire 3	125125	80995	-44130	-35
Palsa mire 4	78327	19114	-59213	-76
Palsa mire 5 and 6	184832	51475	-133357	-72
Palsa mire 7	376769	259424	-117345	-31
Palsa mire 8	49446	24153	-25293	-51
Total all palsas	**945067**	**491791**	**-453277**	**-48**

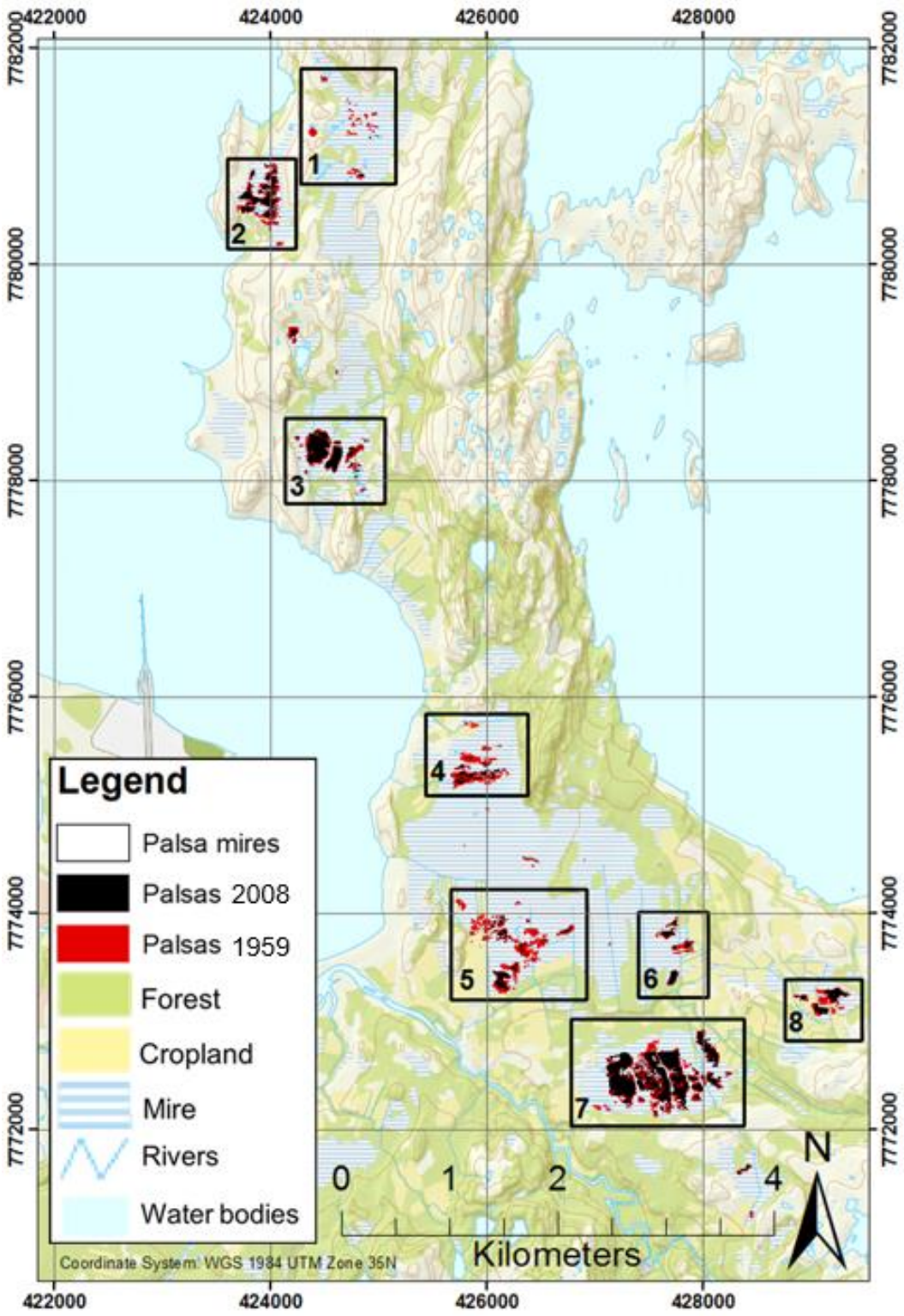

Figure 28: All palsas delineated in Lakselv, Finnmark, divided in 8 different palsa mires. Some smaller palsas are outside these 8 palsa mires. Background map from the Norwegian Mapping Authority (Kartverket, 2015b).


1)
2)
3)
4)
N
0
100
200
Meters
Palsas 2009
Palsas 1959

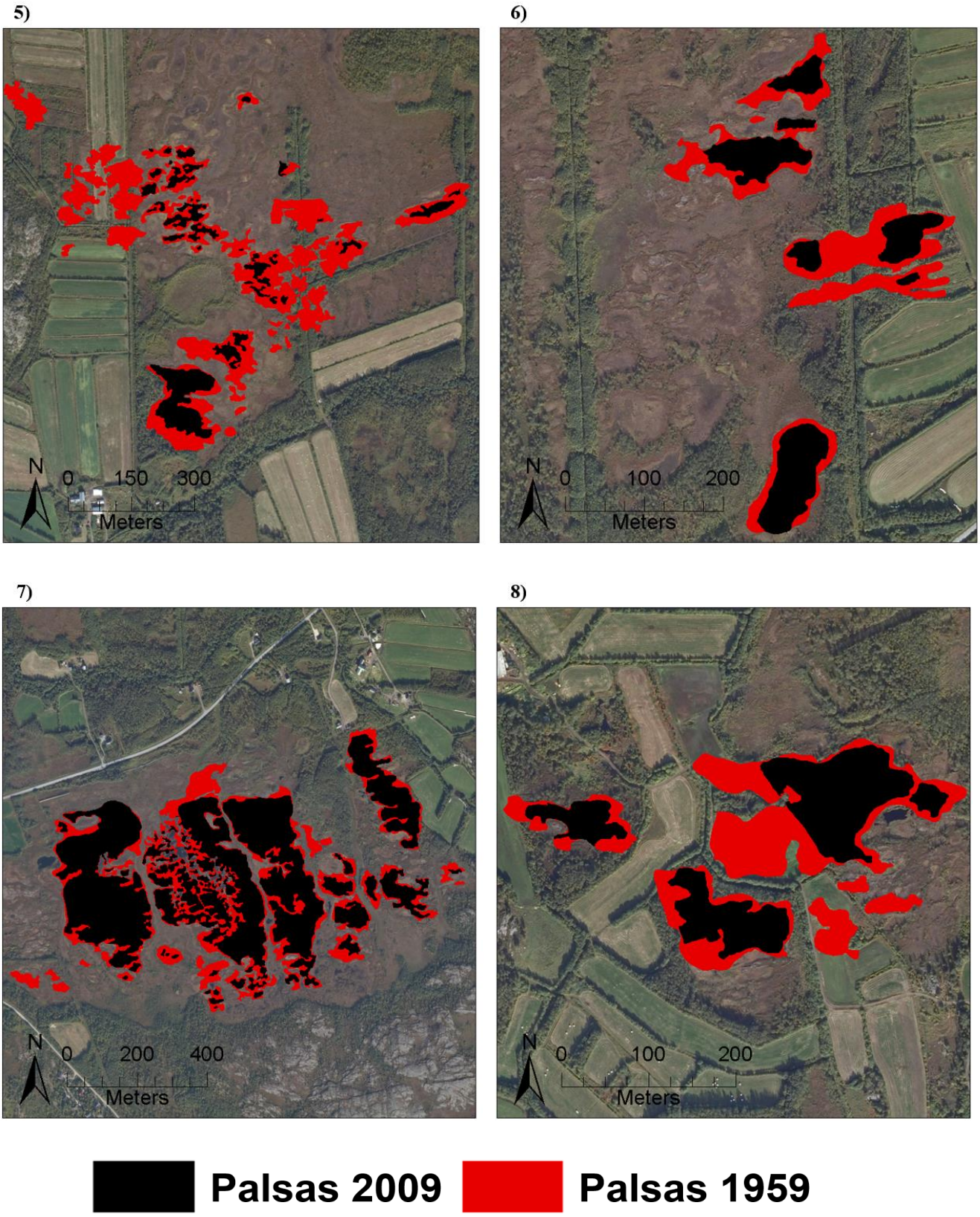

Figure 29: Individual maps of all 8 palsa mires delineated in Lakselv. All background images are from 2008 from Norgeibilder (2015).

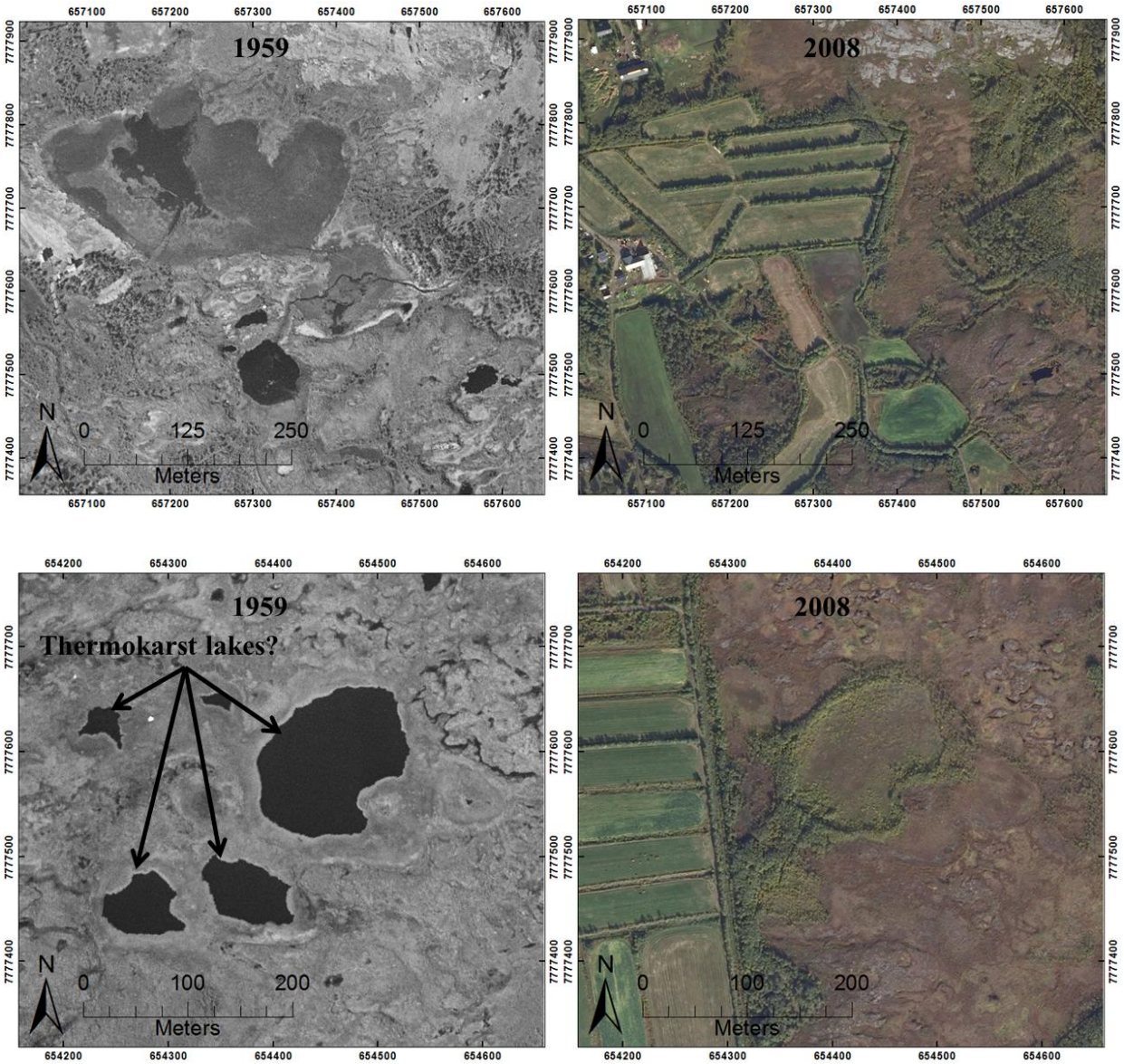

Figure 30: Examples of large thermokars lakes that have disappeared and partly replaced by cornfields between 1959 and 2008 (Norgeibilder, 2015). Upper images from palsa mire 5, and lowermost images from palsa mire 8 (Figure 28).

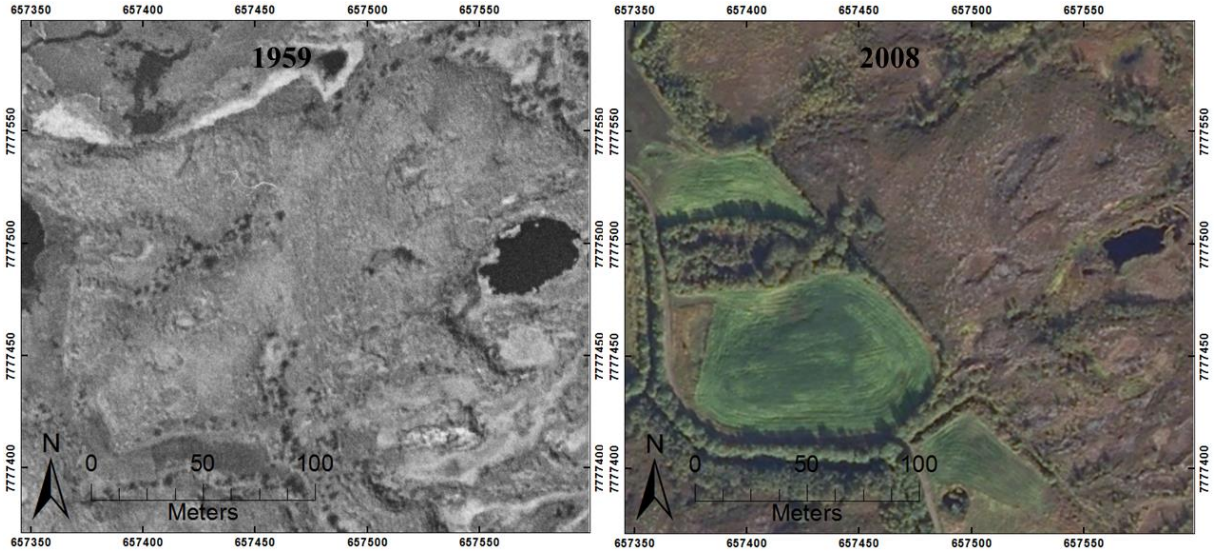

Figure 31: A larger palsa in palsa mire 8 (Figure 28) has partly been replaced by cornfields between 1959 and 2008 (Norgeibilder, 2015). Notice the unnaturally sharp divide between the cornfield and the palsa in the aerial image from 2008.

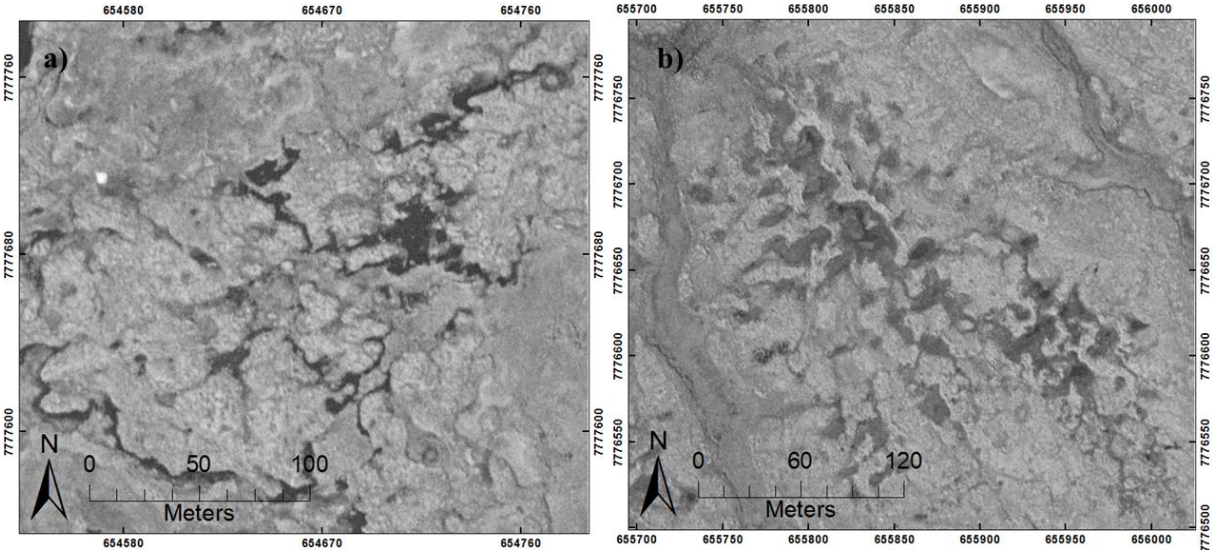

Figure 32: Examples of disintegration of larger peat plateaus in 1959. Image a) are from palsa mire 5, while image c) from palsa mire 7 (Figure 28).

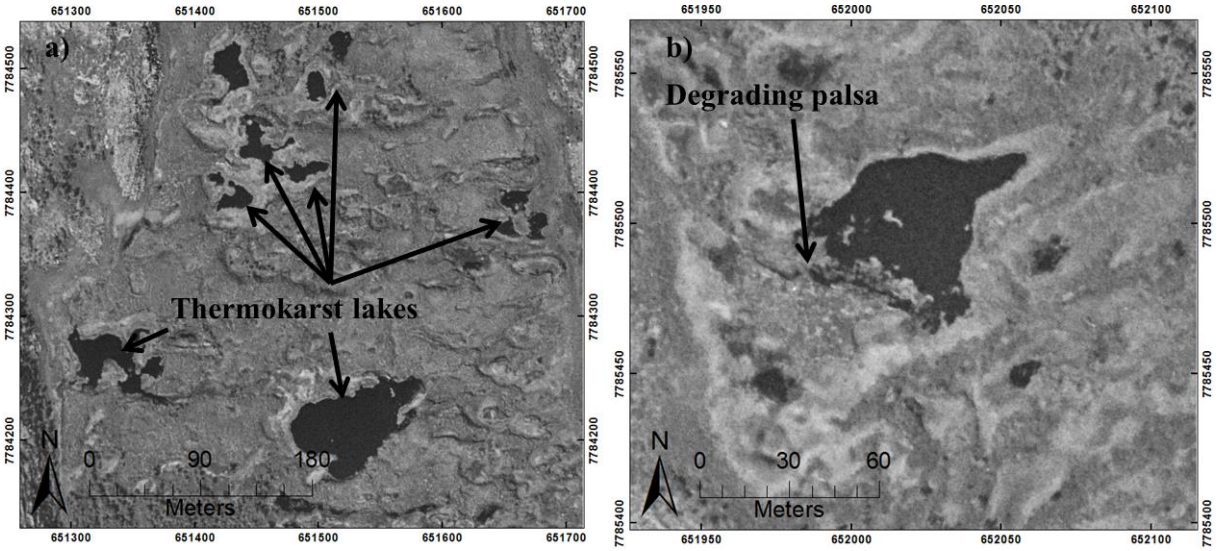

Figure 33: Examples of thermokarst lakes and degrading palsas. Image a) from palsa mire 1 and image b) from palsa mire 2 (Figure 28).

5.3.3 Suossjavri

The total area of all palsas delineated in Suossjavri was 739817 m^2 in 1956/1959, 648695 m^2 in 1982, 553342 m^2 in 2003 and 494507 m^2 in 2011 (Table 8). A total area of 245310 m^2 (-33 % of the original area of palsas in 1956/1959) has thereby degraded in the time span from 1956/1959 to 2012. Figure 36 is a map of all palsas delineated in Suossjavri, where the palsas have been divided in 7 different palsa mires. Suossjavri has several large peat plateaus, and Table 8 illustrates the difference between the changes for the smaller palsas compared with the large peat plateaus. For several of the palsa mires in Suossjavri (e.g. palsa mire 2, 3 and 6, excluding the large peat plateau in palsa mire 6), the difference from 1959 to 2011 are about 50-60 %. In comparison, the difference for the large peat plateaus are only between 10-28 %. Figure 34 and Figure 35 demonstrate the mean annual degradation between 1956/1959-1982, 1982-2003, and 2003-2011. An acceleration in the rate of degradation is observed from these figures. Figure 37 are individually maps of all 7 palsa mires. Finally, some examples of degrading palsas and thermokarst lakes in 1956/1959 are presented (Figure 38).

Table 8: Area of all palsa mires in Suossjavri for 1956/1959, 1982, 2003 and 2011, divided in 7 different palsa mires. Four of the largest peat plateaus are excluded from these mires, and are listed individually. The total differences between these years are listed as both m^2 and %. PM is an abbreviation for Palsa Mire, PP for Peat Plateau and MPP for Mega Peat Plateau.

	1956/1959 [m^2]	1982 [m^2]	2003 [m^2]	2011 [m^2]	2011 - 1956/1959 [m^2]	2011 - 1956/1959 [%]
PM 1	18785	16919	14073	10894	-7890	-42
PM 2	42014	32147	21913	16224	-25790	-61
PM 3	39817	30859	21254	15276	-24541	-62
PM 4 (excl. PP)	11341	9024	6912	4708	-6633	-58
PP in PM 4	29205	27127	23616	20984	-8221	-28
PM 5 (excl. PP)	74885	64118	55095	44358	-30527	-41
PP in PM 5	90426	86654	83216	77614	-12812	-14
PM 6 (excl. PP)	31256	23446	16095	12727	-18529	-59
PP in PM 6	90306	84655	78686	73562	-16744	-19
PM 7 (excl. MPP)	185063	152651	125596	103834	-81229	-44
MPP in PM 7	126720	121095	106885	114326	-12394	-10
Total all palsas	**739817**	**648695**	**553342**	**494507**	**-245310**	**-33**

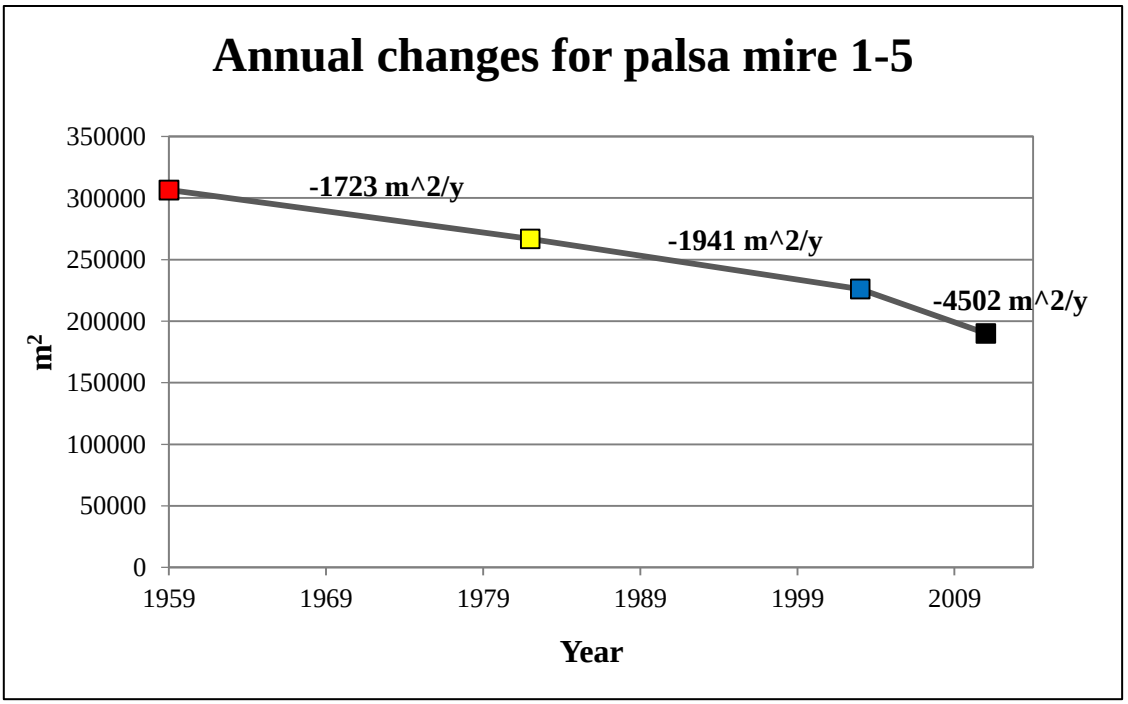

Figure 34: The total area of palsas for palsa mire 1-5 (Figure 36) in Suossjavri in 1959, 1982, 2003 and 2011, with mean annual changes in area of palsas between 1959 to 1982, 1982 to 2003 and 2003 to 2011.

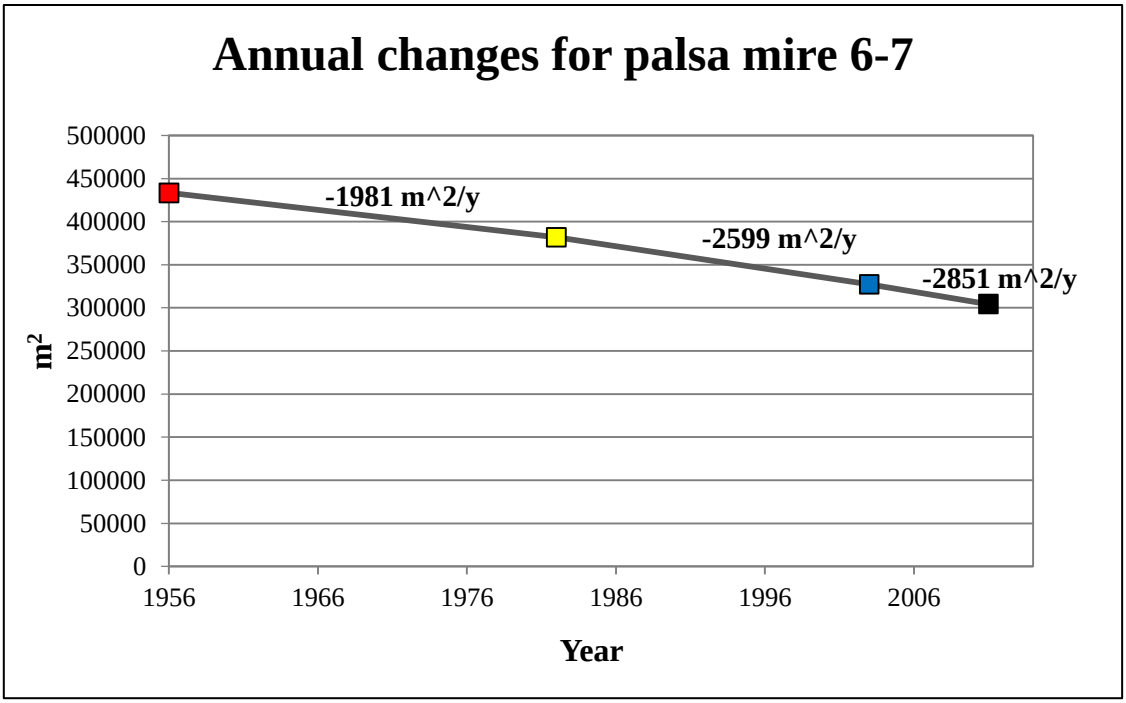

Figure 35: The total area of palsas for palsa mire 6 and 7 (Figure 36) in Suossjavri in 1956, 1982, 2003 and 2011, with mean annual changes in area of palsas between 1956 to 1982, 1982 to 2003 and 2003 to 2011.

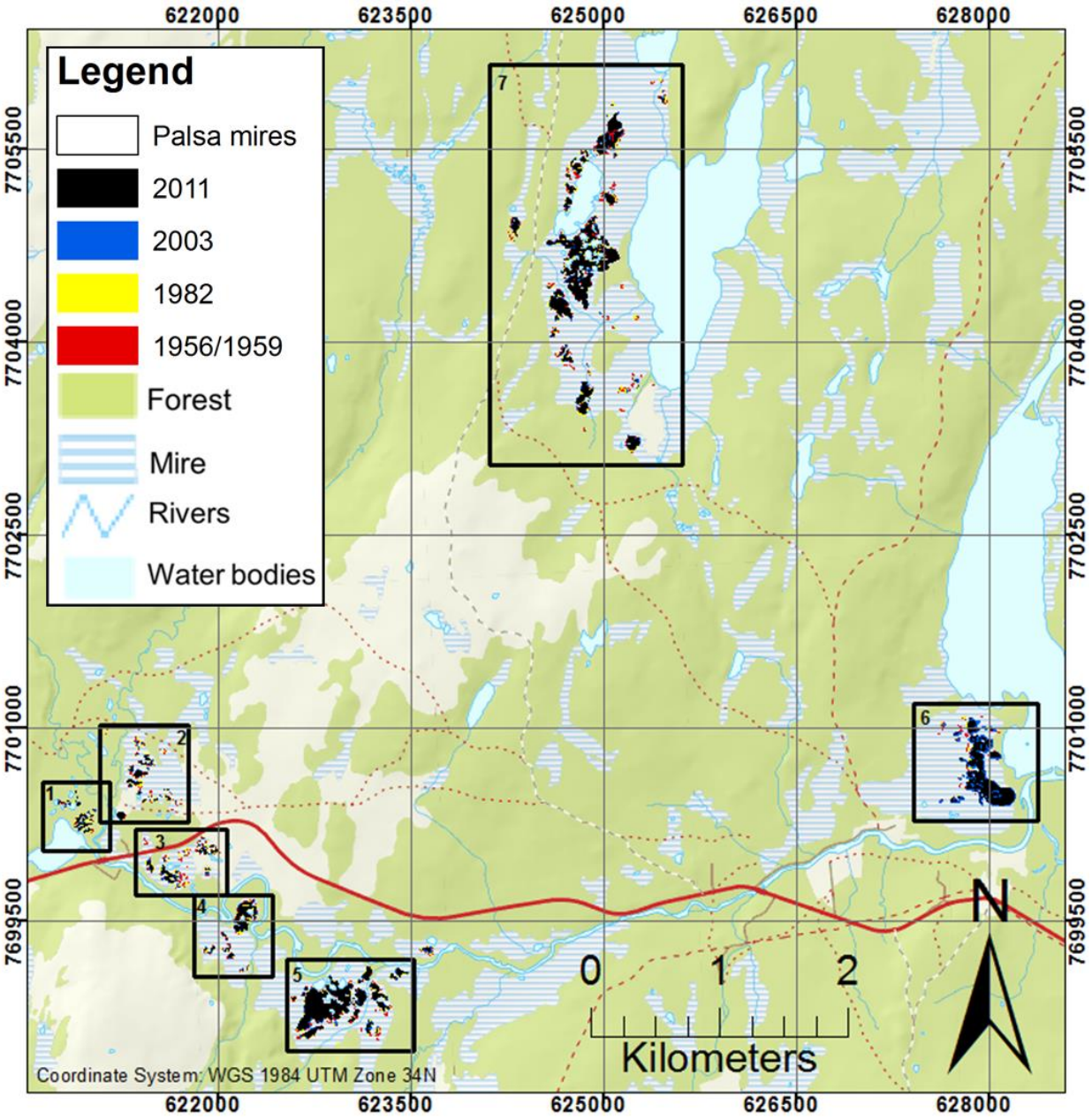

Figure 36: All palsas delineated in Suossjavri, Finnmark, divided in 7 palsa mires. Background map from the Norwegian Mapping Authority (Kartverket, 2015b).

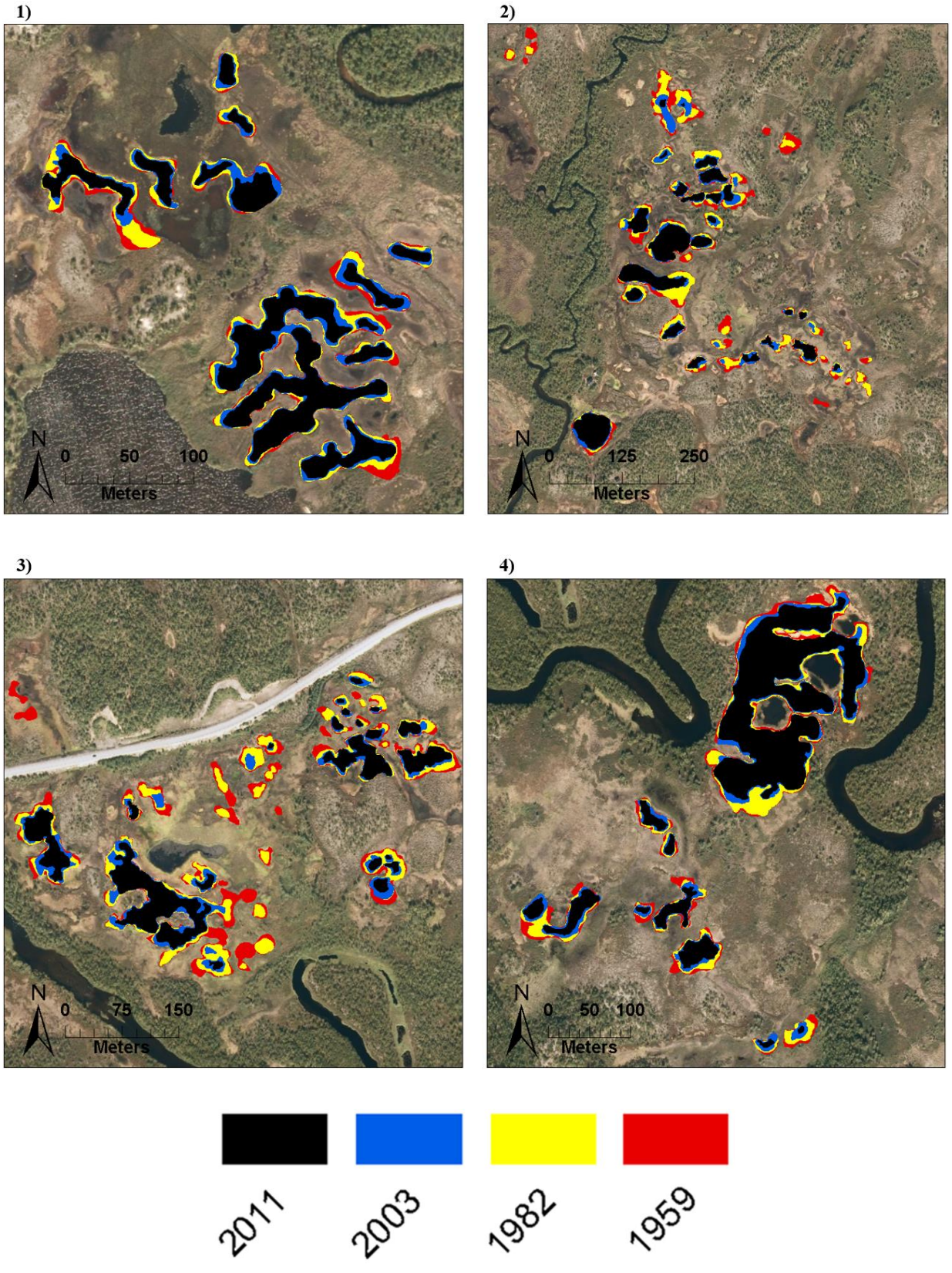
1)
N
0 50 100
Meters
2)
N
0 125 250
Meters
3)
N
0 75 150
Meters
4)
N
0 50 100
Meters
2011
2003
1982
1959

5)

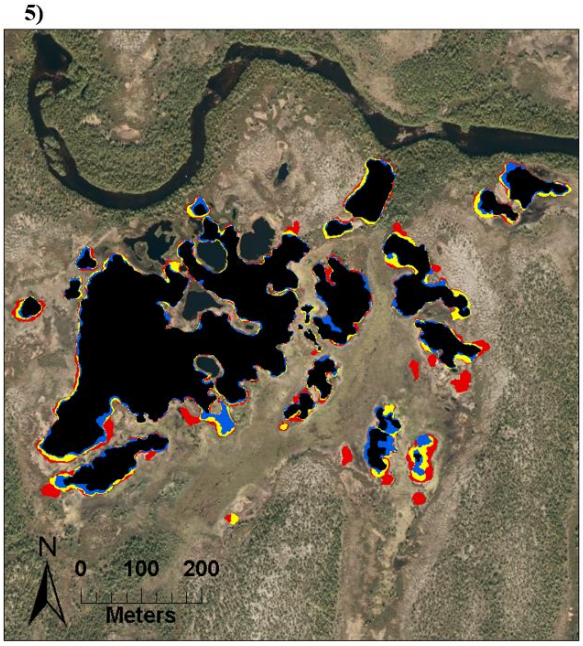

6)

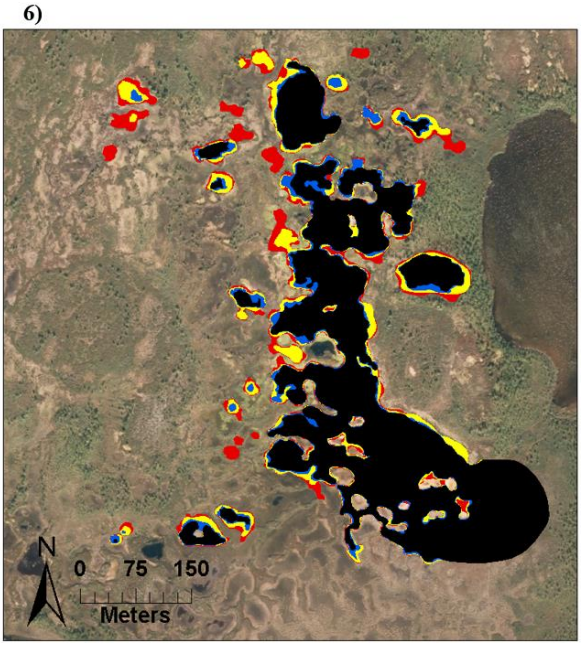

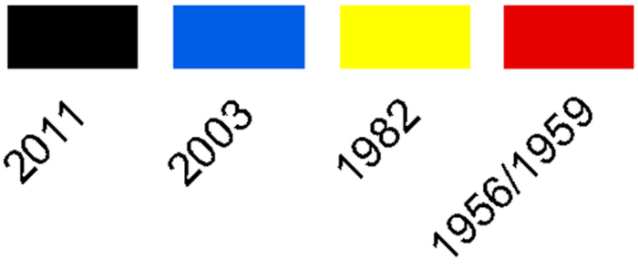

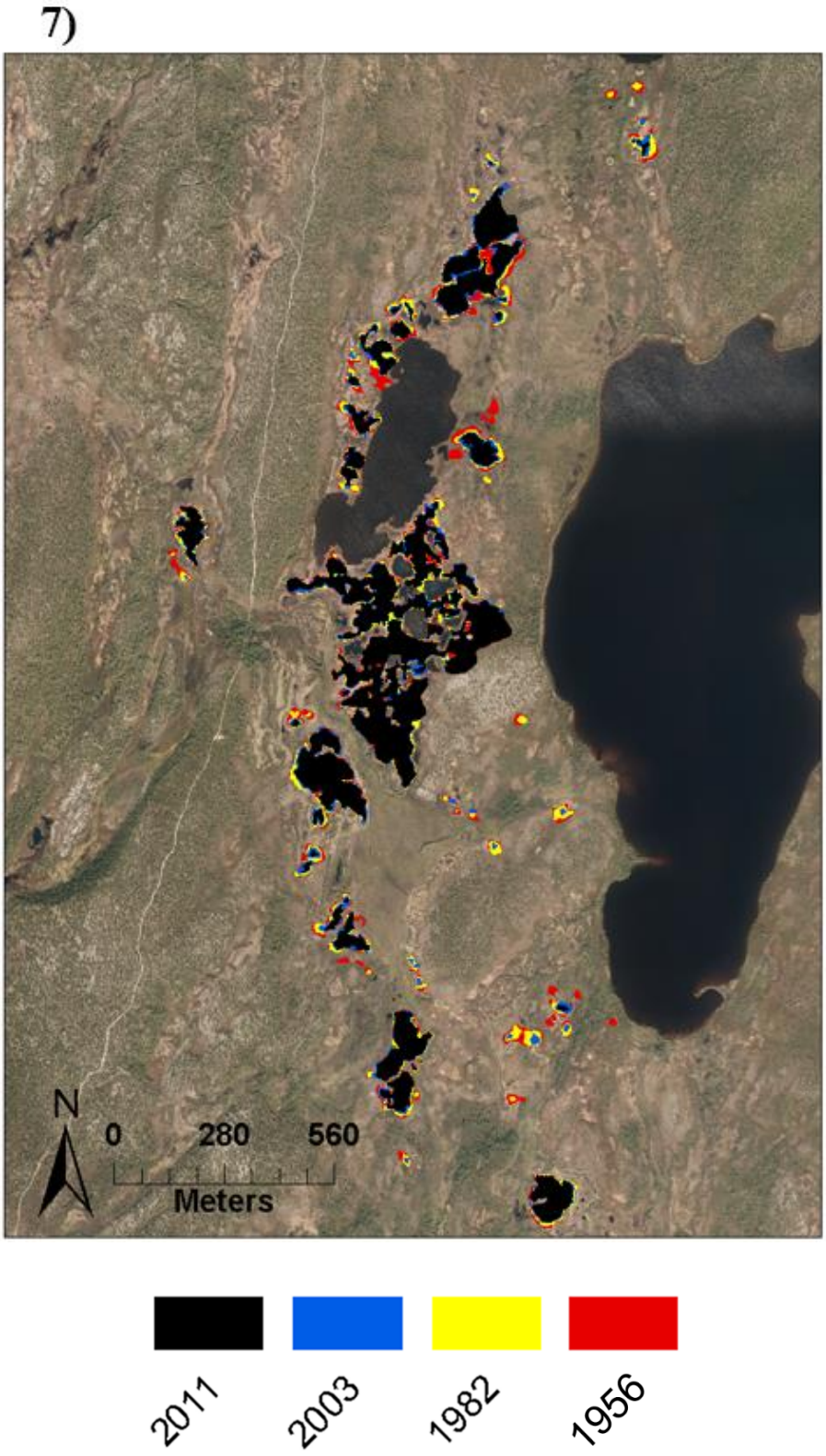

Figure 37: Individually maps of palsa mires 1-7 (Figure 36) in Suossjavri study site. All background images from 2011 are from Norgeibilder (2015).

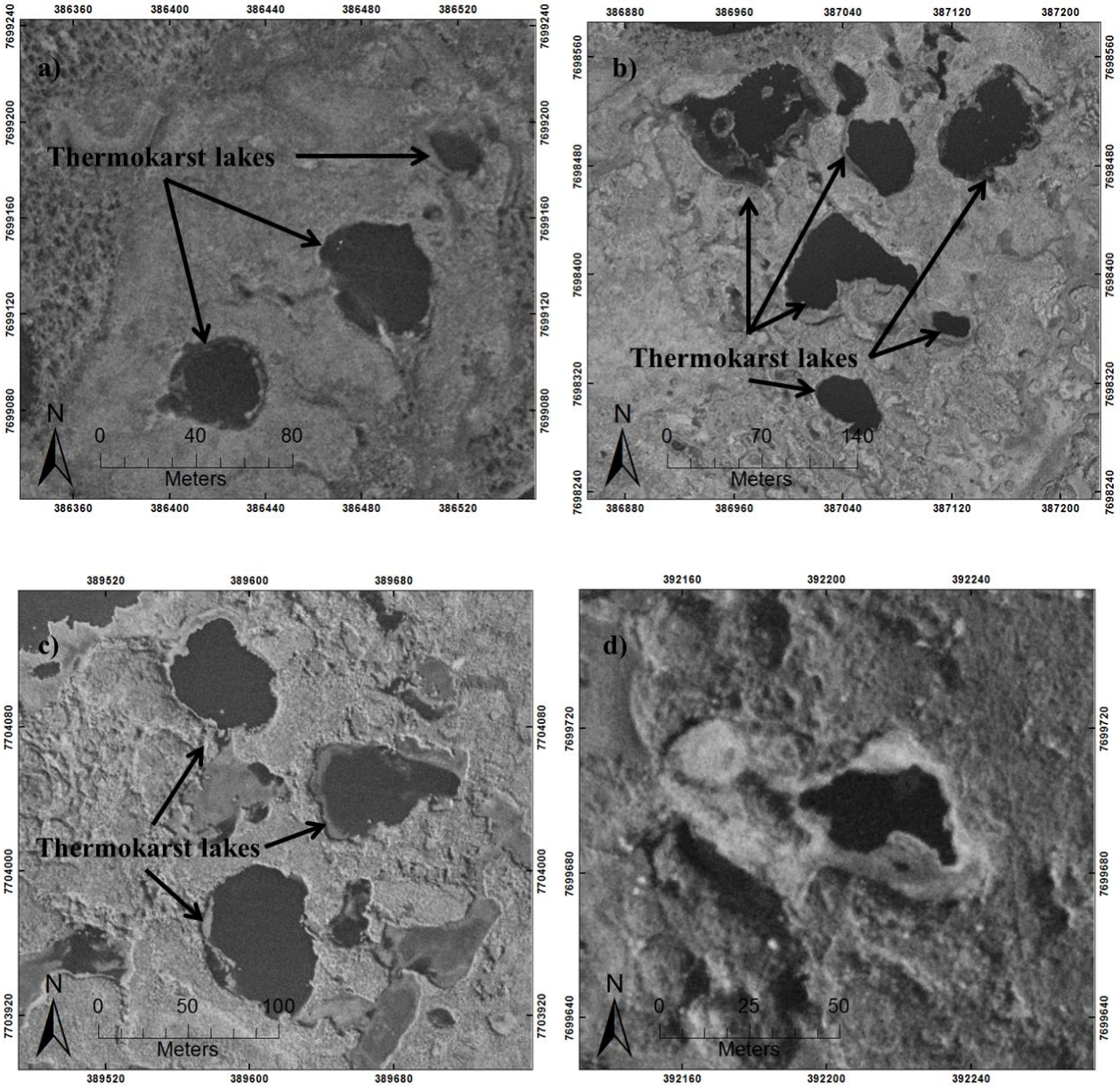

Figure 38: Examples of degrading palsas and thermokarst lakes in Goatheluoppal in aerial images from 1956/1959. Image a) are from palsa mire 3, b) from palsa mire 4, c) from palsa mire 7 and d) from palsa mire 8 (Figure 36).

4.2.1 Goatheluoppal

The total area for all palsas delineated in Goatheluoppal was 501659 m^2 in 1958, 348973 m^2 in 1980, 212879 m^2 in 2003 and 146834 m^2 in 2012 (Table 9). A total area of 354825 m^2 (-71 % of the original area of palsas in 1958) has thereby degraded in the time span from 1958 to

2012. Figure 40 is a map of all palsas delineated in Goatheluoppal. The palsa mires in Goatheluoppal are not so distinctly divided like in Lakselv and Suossjavri. For convenience when presenting the figures of the results, the palsa mires have still been divided in 6 smaller regions (Figure 41). Nevertheless, the change in area of palsas is not divided in several palsa mires for Goatheluoppal (Table 9). Figure 39 illustrates the mean annual degradation between 1958-1980, 1980-2003, and 2003-2012. Finally, some examples of indications of former palsas, degrading palsas and thermokarst lakes in 1958 are presented (Figure 42).

Table 9: Area of all palsa mires in Goatheluoppal for 1958, 1980, 2003 and 2012, with total changes and mean annual changes between the years.

	Total all palsas	Annual changes [m^2/y]	Comments
1958 [m^2]	501659		
1980 [m^2]	348973	-6940*	* Between 1958-1980
2003 [m^2]	212879	-5917*	* Between 1980-2003
2012 [m^2]	146834	-7338*	* Between 2003-2012
Mean annual changes [m^2/y]		-6571*	* Between 1958-2012
Total diff [m^2]	**-354825**		
Total diff [%]	**-71**		

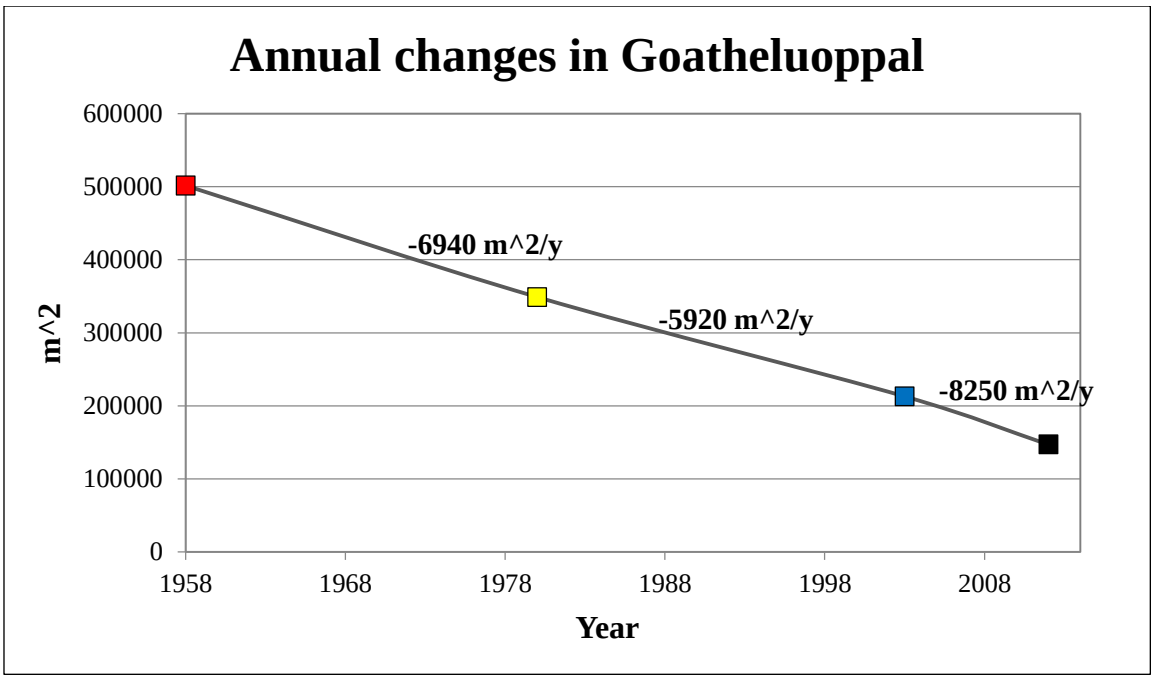

Figure 39: The total area of palsas in Goatheluoppal in 1958, 1980, 2003 and 2012, with mean annual changes in area of palsas between 1958 to 1980, 1980 to 2003 and 2003 to 2011.

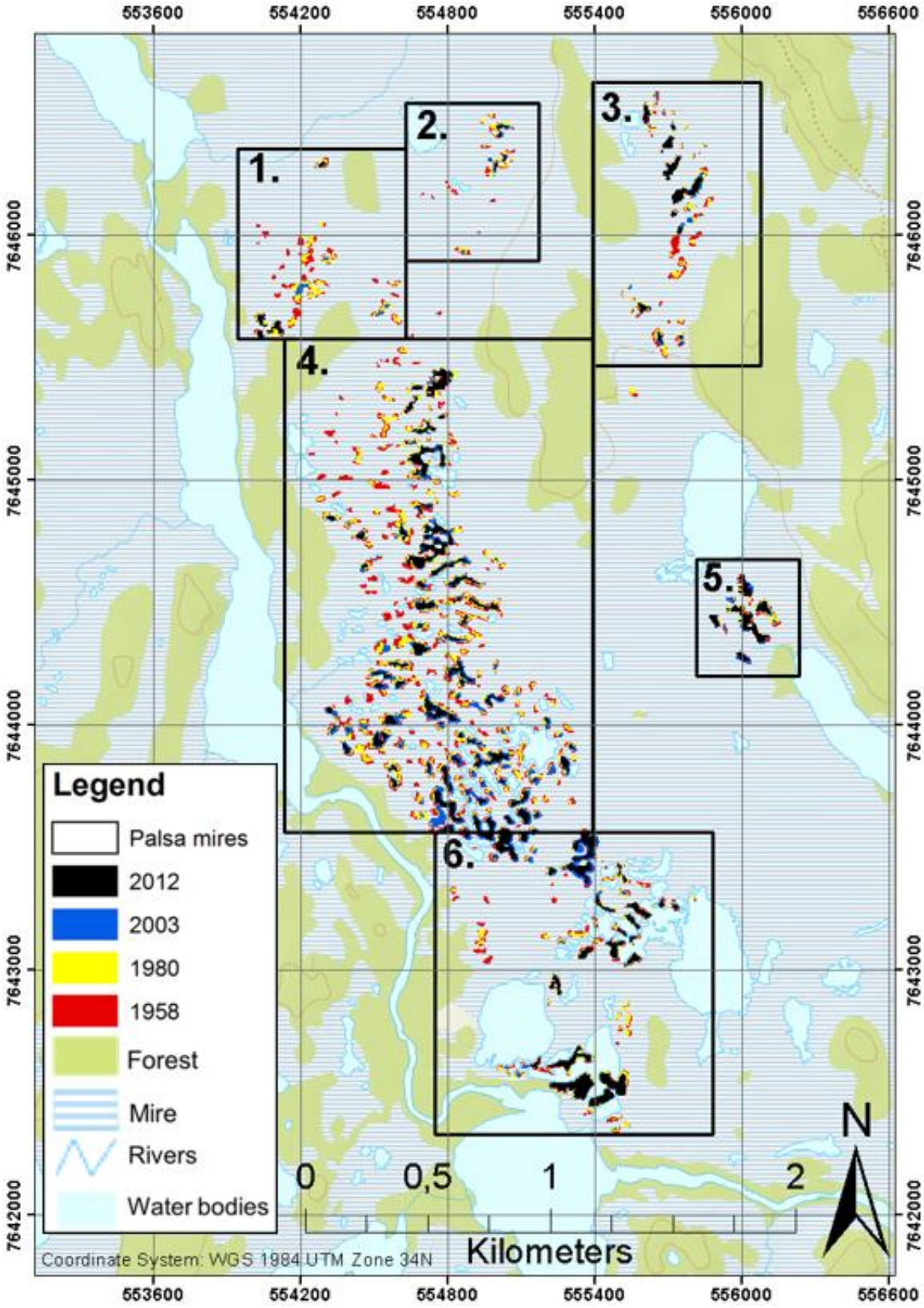

Figure 40: All palsas delineated in Goatheluoppal, Finnmark. Six black frames represent the outline of the individual maps in Figure 41. Background map from the Norwegian Mapping Authority (Kartverket, 2015b).

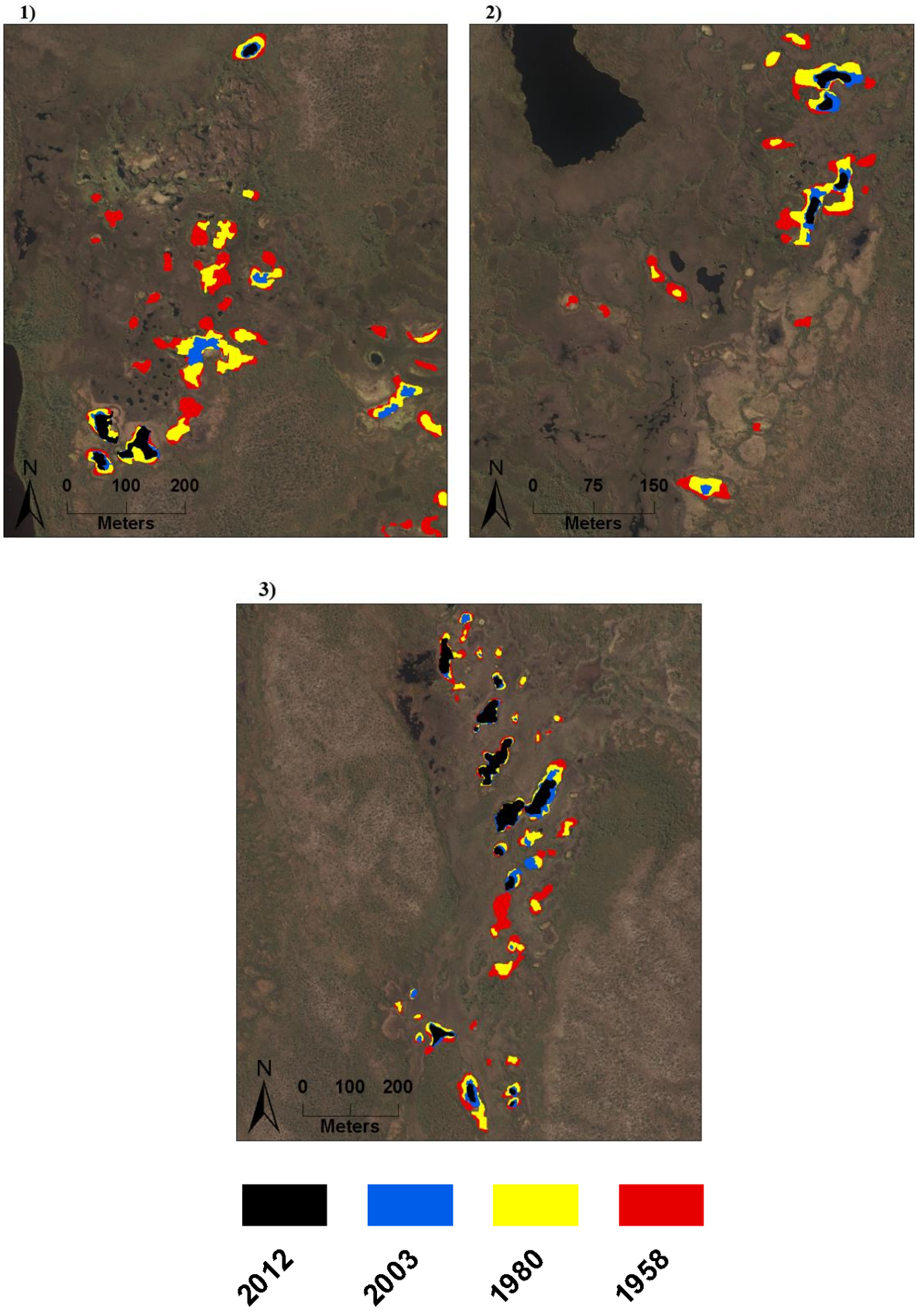
1)
2)
3)
N
0 100 200
Meters
N
0 75 150
Meters
N
0 100 200
Meters
2012
2003
1980
1958

4)

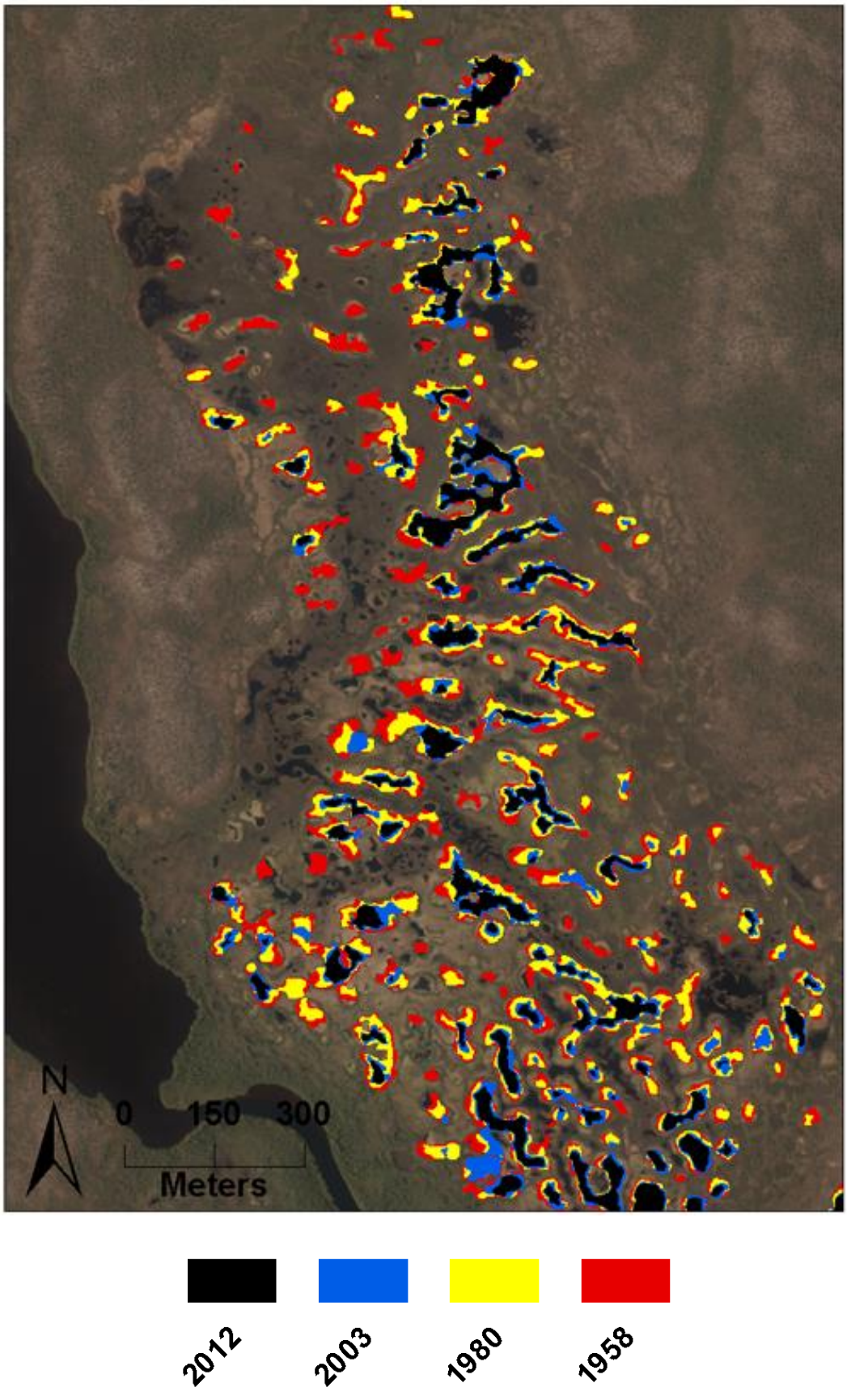

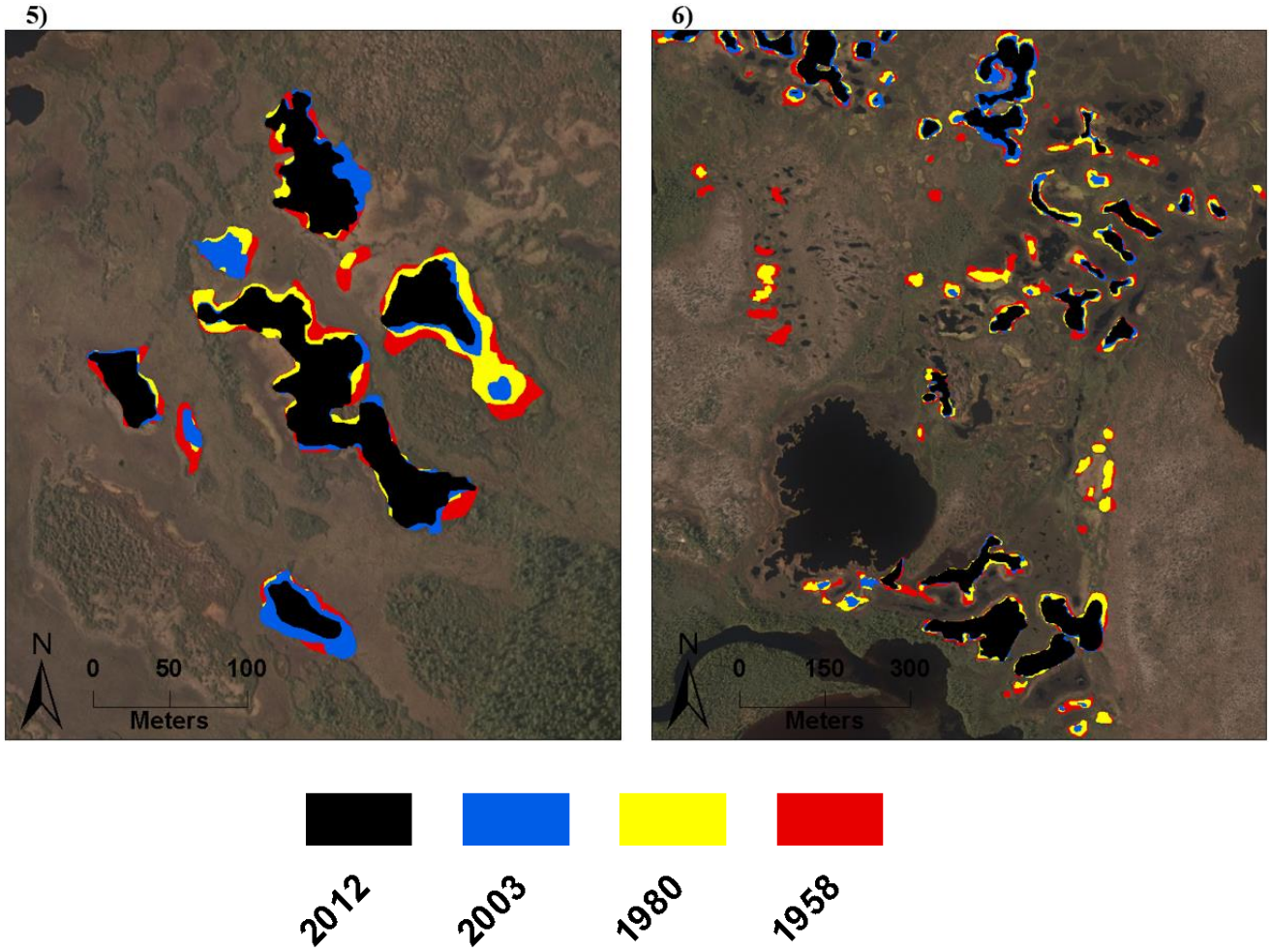

Figure 41: Maps of all palsas in Goatheluoppal divided in 6 areas (Figure 40). All background images from 2012 from Norgeibilder (2015).

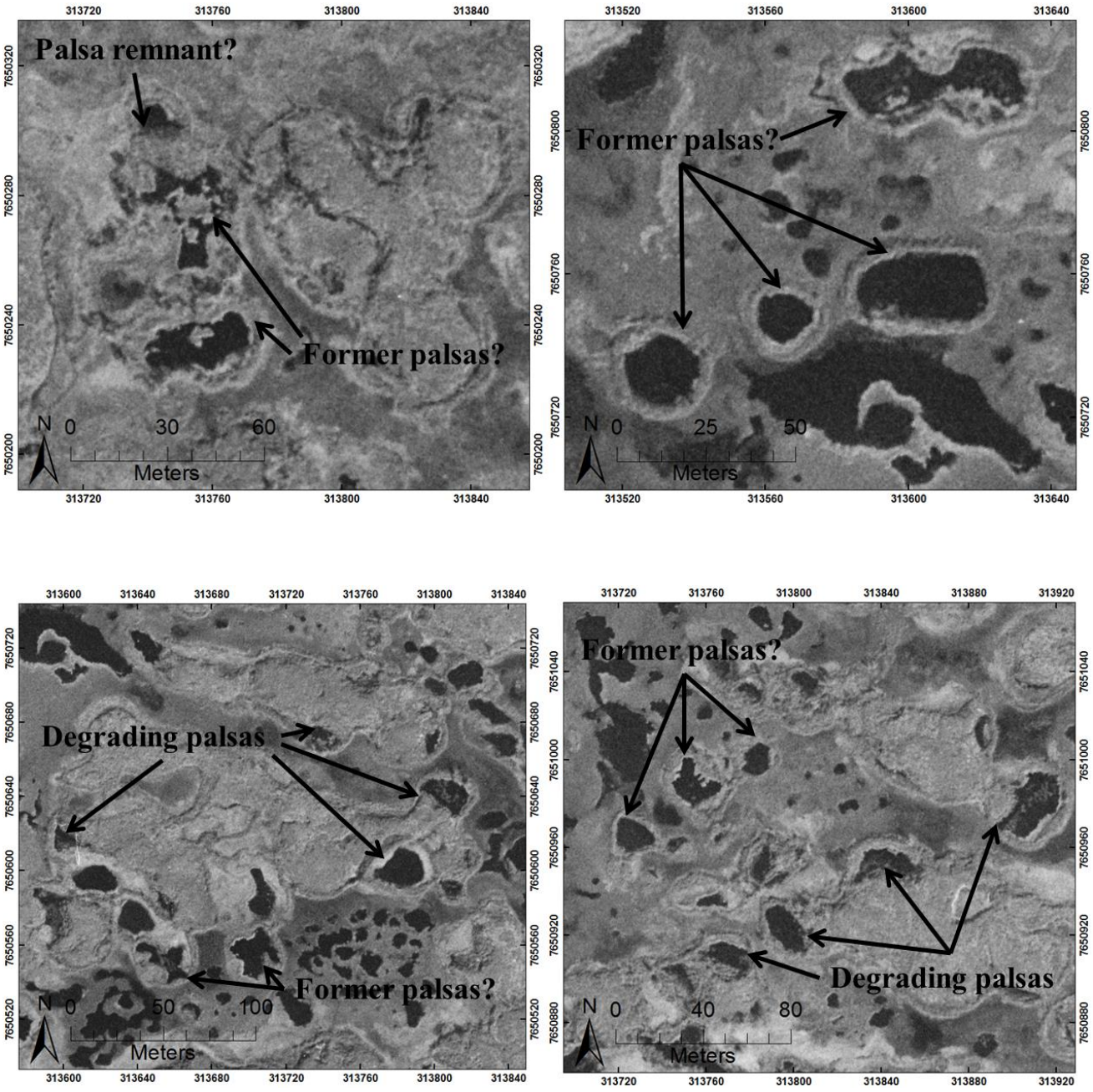

Figure 42: Examples of thermokarst lakes, degrading palsas and most likely the extent of some former palsas visible by ridges of peat/vegetation in rings around thermokarst lakes. Aerial images from 1958. All examples from palsa mire 4 (Figure 40).

5.4 Results of GDM

5.4.1 Hierarchical partitioning

Table 10 presents the independent effect from the HP of the topography and land cover variables (HP 1). The four most important variables according to the results, in ascending order, are *Water*, *MinElevation*, and *Flat* and *Mire* (which are equally important). *TWI* has by far the lowest independent effect with 4.7 %.

Table 11 presents the independent effect from the HP of the climate variables (HP 2). The four most important climate variables, in ascending order, are *FDD*, *TDD*, *MAP* and *MaxSD*. The lowest independent effect has *MSP*, with only 4.5 %.

HP of the four most important topography/land cover variables together with the four most important climate variables (HP 3) are presented in Figure 43. The figure shows that the climate variables are dominating, with all four variables as the four variables with the highest independent effect. Further, precipitation as *MAP* and *MaxSD* have the highest independent effect, in front of the temperature variables *TDD* and *FDD*. Of topography and land cover variables, *Mire* has the highest independent effect.

Table 10: HP 1 – demonstrating the independent effect (I) in percentage of the topography and land cover variables to explain the distribution of palsas for the calibration area. The four highest independent effects are marked in bold.

		I [%]
Topograhy variables:	*MinElevation*	**21.8**
	TWI	4.7
	Slope	9.7
	Flat	**25.8**
Land cover variables:	*Mire*	**25.8**
	Water	**12.2**

Table 11: HP 2 – demonstrating the independent effect (I) in percentage of the climate variables to explain the distribution of palsas for the calibration area. The four highest independent effects are marked in bold.

		I [%]
Climate variables:	*MAAT*	8.2
	FDD	**18.2**
	TDD	**21.4**
	MAP	**22**
	MSP	4.5
	MaxSD	**25.8**

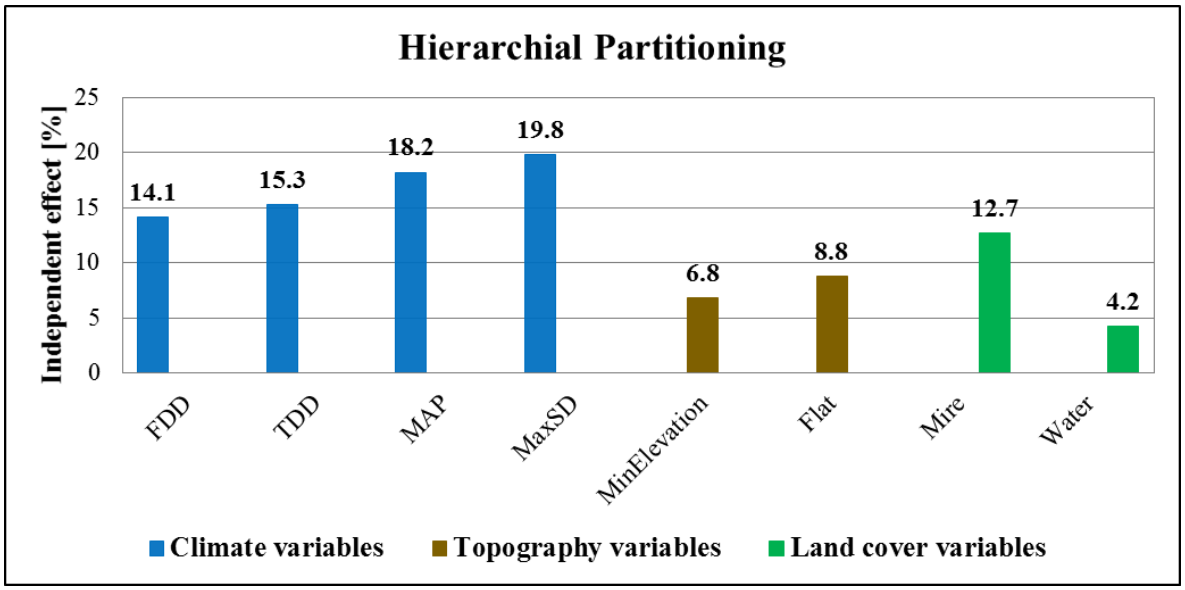

Figure 43: HP 3 – demonstrating the independent effect (in percentage) of the four most important topography/land cover variables and the four most important climate variables to explain the distribution of palsas for the calibration area.

5.4.2 Contemporary results

Figure 44 includes boxplots of all the environmental explanatory variables, grouped in presence/absence of palsas for the calibration area. Table 12 contains a correlation matrix using Spearman`s rank order. From the table, four correlations are above the threshold of 0.7: the correlation between *MAP* and *MaxSD*, *MaxSD* and *TDD*, *MAAT* and *FDD*, and *MinElevation* and *TDD*. By using the results from the HP, and by experimenting using backward and forward selection based on AIC and *p*-values ($p < 0.01$), I decided to remove

MaxSD, *MAAT* and *MinElevation* in the further analysis towards the final GLM. Furthermore, *TDD* was preferred over *MinElevation*, as *MinElevation* is a non-causal variable, a surrogate of climate, which will only be valid for the calibration area. The most important variable in HP, *MaxSD*, was removed because *MAP* was more important in the model when it was together with other variables. Thus, *MAP* explained a variety not explained by *MaxSD*.

Table 12: Correlation matrix using Spearson`s rank order. Correlations between explanatory variables above 0.7 are marked in bold.

Variables	1	2	3	4	5	6	7	8	9	10	11	12
1. MAP	1											
2. MSP	-0.48	1										
3. MaxSnow	**0.89**	-0.47	1									
4. MAAT	0.27	0.16	0.12	1								
5. TDD	-0.54	0.28	**-0.75**	0.23	1							
6. FDD	-0.59	0.08	-0.49	**-0.86**	0.17	1						
7. MinElevation	0.41	-0.25	0.65	-0.38	**-0.91**	0.00	1					
8. Slope	0.36	-0.25	0.37	0.03	-0.31	-0.22	0.18	1				
9. Flat	-0.50	0.29	-0.50	-0.10	0.37	0.34	-0.22	-0.56	1			
10. TWI	-0.31	0.14	-0.29	-0.10	0.18	0.25	-0.07	-0.51	0.68	1		
11. Water	-0.25	0.30	-0.36	0.13	0.39	0.05	-0.30	-0.40	0.28	0.15	1	
12. Mire	-0.32	0.15	-0.34	-0.07	0.29	0.24	-0.18	-0.32	0.60	0.52	0.13	1

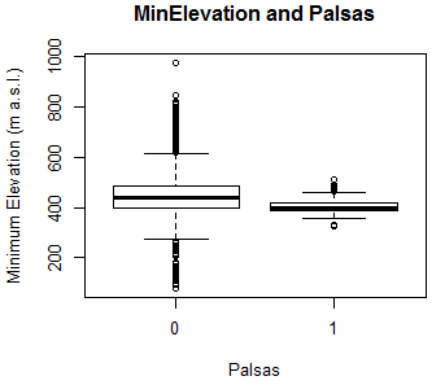
MinElevation and Palsas
Minimum Elevation (m a.s.l.)
200
400
600
800
1000
0
1
Palsas

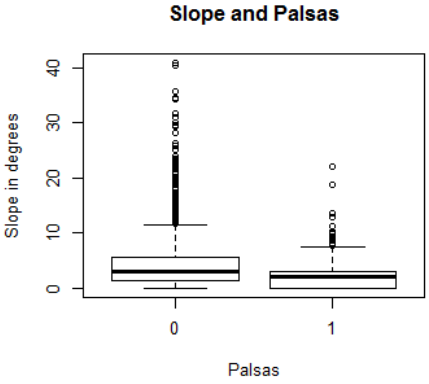
Slope and Palsas
Slope in degrees
0
10
20
30
40
0
1
Palsas

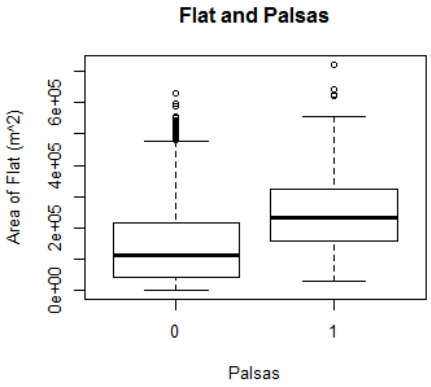
Flat and Palsas
Area of Flat (m^2)
0e+00
2e+05
4e+05
6e+05
0
1
Palsas

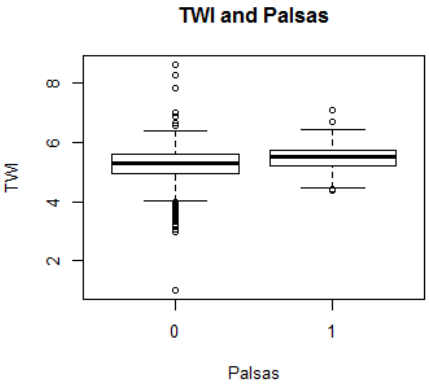
TWI and Palsas
TWI
2
4
6
8
0
1
Palsas

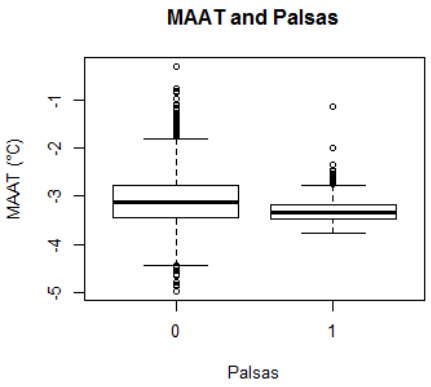
MAAT and Palsas
MAAT (°C)
-5
-4
-3
-2
-1
0
1
Palsas

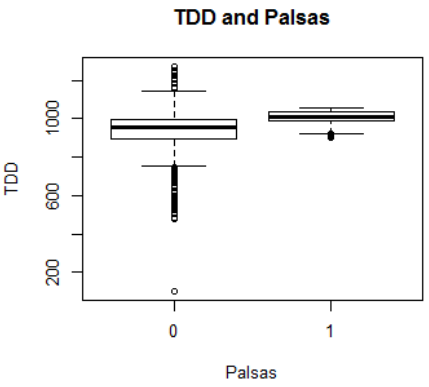
TDD and Palsas
TDD
200
600
1000
0
1
Palsas

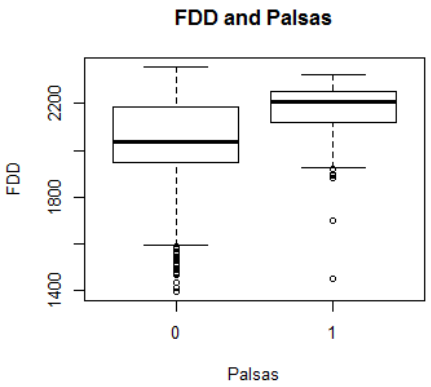
FDD and Palsas
FDD
1400
1800
2200
0
1
Palsas

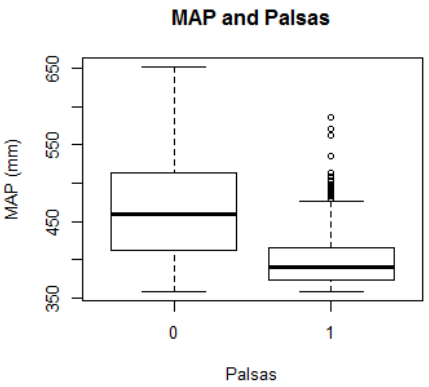
MAP and Palsas
MAP (mm)
350
450
550
650
0
1
Palsas

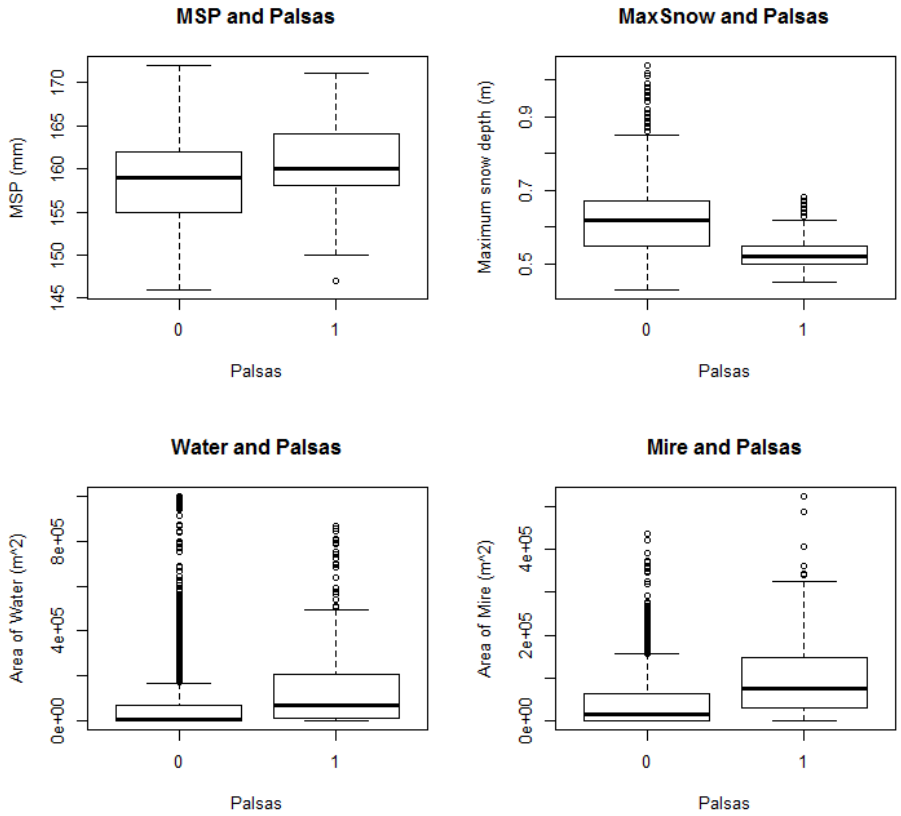

Figure 44: Boxplots of all the environmental explanatory variables grouped in presence (0) and absence (1) of palsas for the calibration area. The whiskers in the boxplots extends to the most extreme data points which is no more than 1,5 times the interquartile range from the box.

5.4.3 Final model

The variables utilized in the final GLM are *FDD*, *TDD*, *MAP*, *MSP*, *Water* and *Mire*. All variables were originally significant ($p < 0.01$). After investigating the response curves and the boxplots of the final variables, I decided to use a nonlinear (quadratic) response of both *Water* and *TDD*. Both changes gave a notably lower AIC for the GLM, but with two variables (TDD^2 and *MSP*) just above the significance level of $p < 0.01$. Table 13 contains the final GLM with estimates of the regression coefficients. From the table, the presence of palsas has a positive response with increasing *MSP*. This result partly conflict the theory that summer precipitation and moisture have a negative effect on palsas (Matti Seppälä, 2006). Therefore, the model was tested again without *MSP* and checked against the evaluation areas. Without

MSP in the GLM, the AUC-value for *Varanger* decreased significantly, while the AUC-value for Southwest remained the same. Thus, the *MSP* remained in the final GLM.

The AUC-value of the final GLM is 0.878 (Table 13). The value of the AUC is thus inside the range (0.81-0.90) of being considered as good (Swets, 1998). The response curves in a univariate setting for the final explanatory variables are presented in Figure 45.

Table 13: The final GLM. Includes the explanatory variables of the final GLM, deviance residuals, the estimates of the regression coefficient, standard errors, z-values and the significance level of these variables for the model. The AUC-value for the final model for the calibration area is also listed.

Final GLM:

Palsas = FDD + TDD + TDD^2 + MAP + MSP + Water + $Water^2$ + Mire

Deviance residuals:

Min	1Q	Median	3Q	Max
-1.935	-0.538	-0.204	-0.011	3.162

Coefficients:

	Estimate	Std. Error	z-value	Pr(>|z|)	
Intercept	-8.997E+01	2.51E+01	-3.592	3.28E-04	***
FDD	3.476E-03	7.93E-04	4.382	1.17E-05	***
TDD	1.373E-01	5.05E-02	2.718	0.0066	**
TDD^2	-6.111E-05	2.52E-05	-2.421	0.0155	*
MAP	-9.081E-03	2.12E-03	-4.280	1.87E-05	***
MSP	5.090E-02	1.99E-02	2.553	0.0107	*
Water	6.203E-06	1.03E-06	6.002	1.95E-09	***
$Water^2$	-6.997E-12	1.42E-12	-4.943	7.68E-07	***
Mire	7.783E-06	9.45E-07	8.237	< 2E-16	***

Significance codes: 0 '***' 0.001 '**' 0.01 '*' 0.05 '.' 0.1 ' ' 1

Null deviance: 1861.8 on 1993 degrees of freedom

Residual deviance: 1242.0 on 1985 degrees of freedom

AUC-value: **0.878**

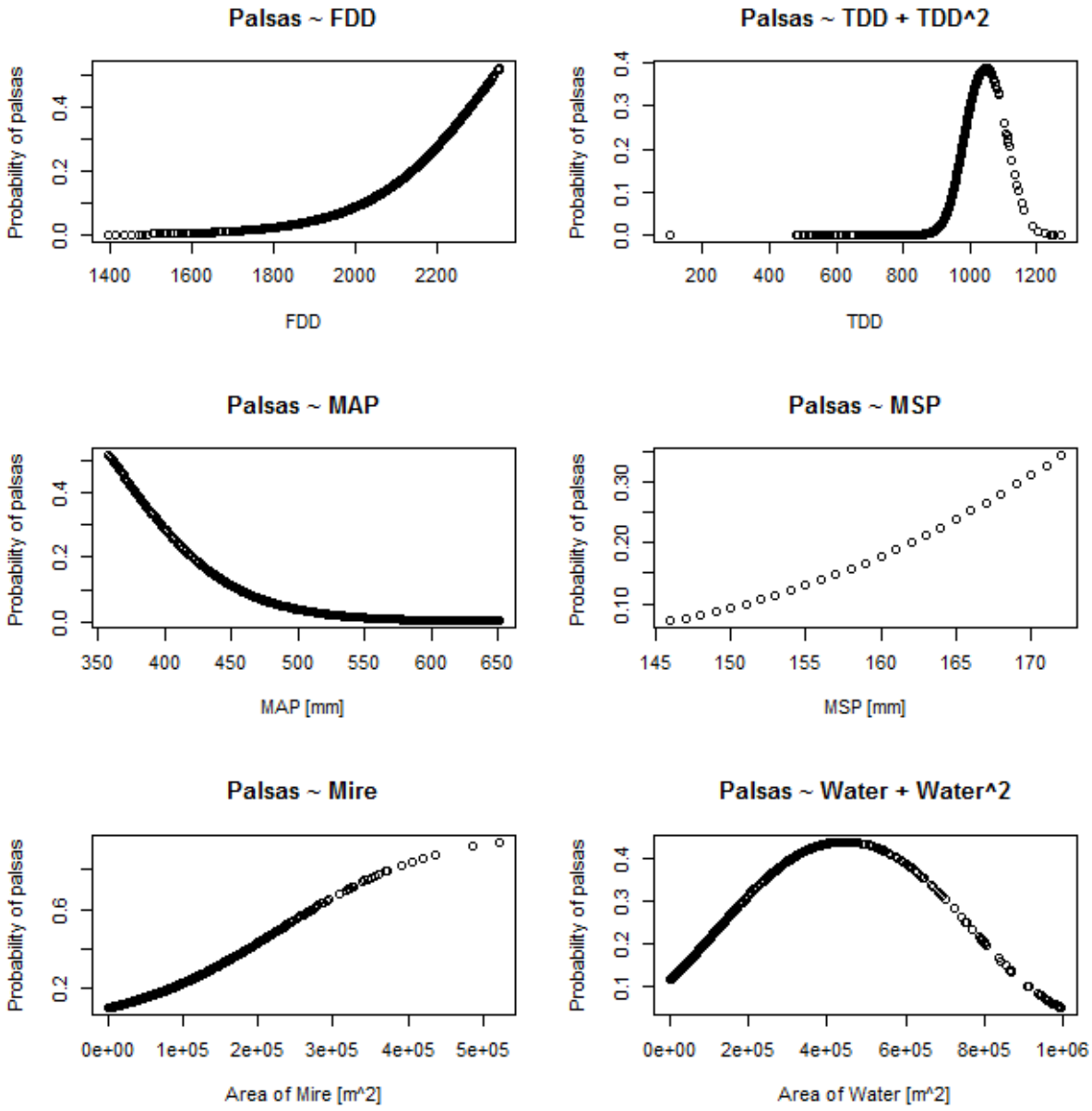

Figure 45: Response curves in a univariate setting for the final explanatory variables utilized in the final GLM. The response curves for TDD and water are nonlinear (quadratic) with a humped curve.

5.4.4 Final probability map of palsas in Finnmark

The final probability map of palsas in Finnmark, based on the final GLM, is presented in Figure 46. The logit link function in eq. 3.3 was used to achieve a probability surface.

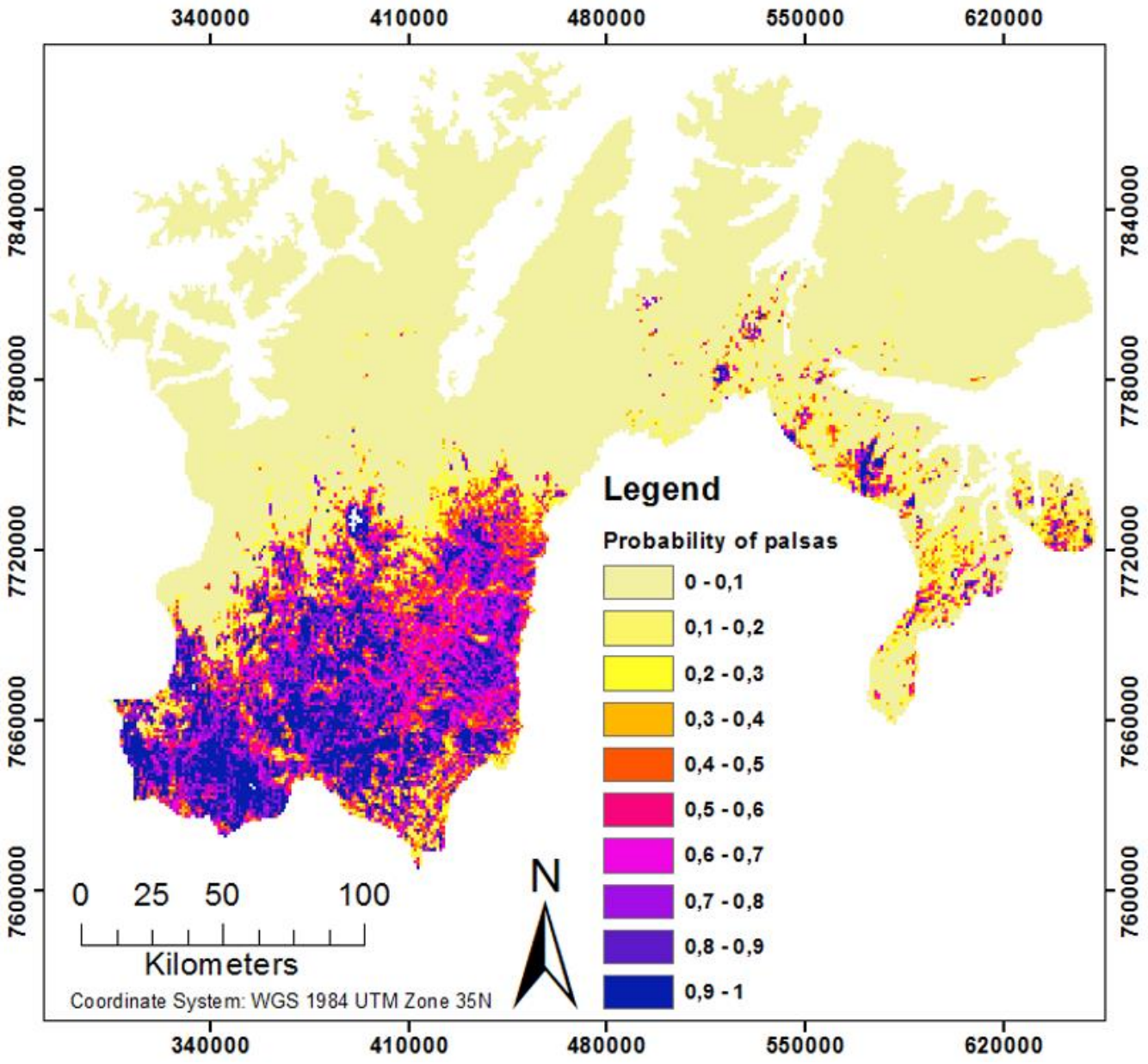

Figure 46: Probability map of presence of palsas in 1x1 km grid cells in Finnmark based on the final GLM.

5.4.5 Evaluation of the final GLM

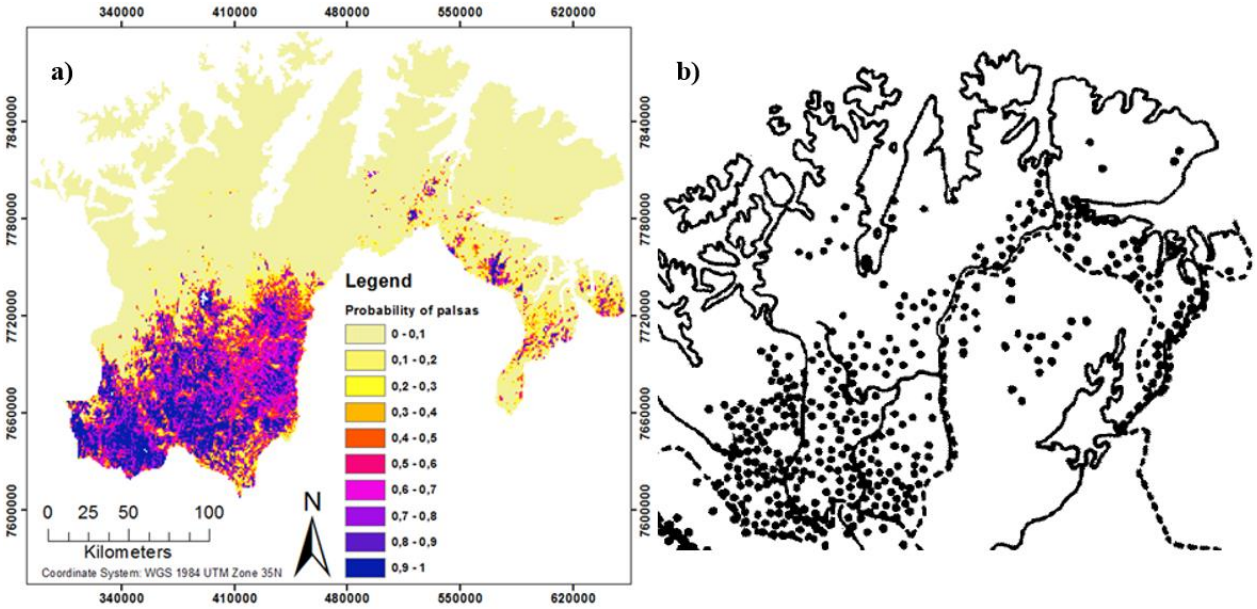

Figure 47: Comparison between the probability map (a) and a part of the map of the distribution of palsas by Sollid and Sørbel (1998) (b), which is revised from Sollid and Sørbel (1974). Black dots in map b indicate palsa mires.

Visual inspection of the probability map compared to a map of distribution of palsas by Sollid and Sørbel (1998) in Figure 47 reveal that in a coarse scale (i.e. the overall extent of regions with high probability) the probability map fits well. At smaller scale, the density of high probabilities are very high in the centre of the distribution (centre of Finnmarksvidda) compared to the density of dots (palsa mires) in the map by Sollid and Sørbel (1998). This is especially evident in western part of Finnmarksvidda, close to the border of Finland. In contrast, the probabilities are low in many outskirt areas where palsas are present. Actually, some palsa "outliers" in the map by Sollid and Sørbel (1998) are not visible at all (in form of higher probabilities than the surrounding area) in the probability map.

Table 14 present the AUC-value and the AUC-stability (eq. 4.2) for the evaluation areas *Southwest* and *Varanger* using the final GLM (Table 13). The maps in Figure 48 and 49 show the probability of palsas for the evaluation areas *Southwest* and *Varanger*, respectively, together with the observations of the presence of palsas.

Table 14: AUC-values and AUC-stability (eq.4.2) for the two evaluation areas Southwest and Varanger.

	Value
AUC calibration area	0.878
AUC evaluation area *Southwest*	0.764
AUC evaluation area *Varanger*	0.822
AUC-stability (*Southwest*/calibration)	0.936
AUC-stability (*Varanger*/calibration)	0.870

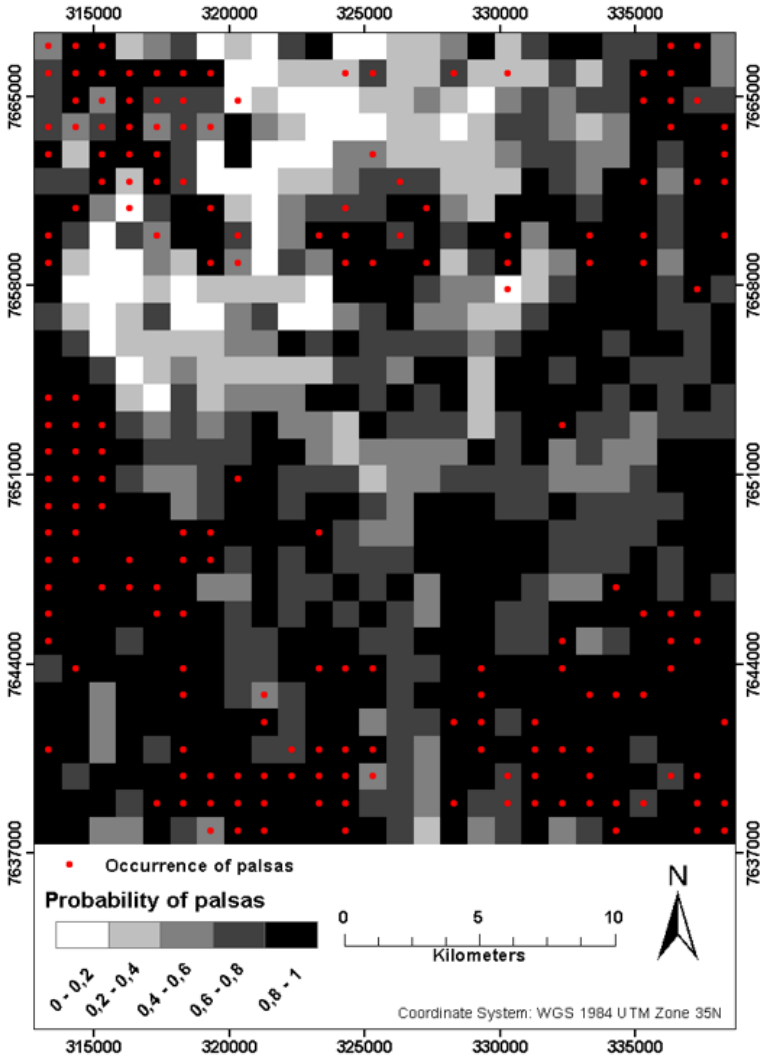

Figure 48: Map of the probability of palsas for the evaluation area Southwest. Occurrences of palsas in the 1x1 km grid cells are represented by red dots.

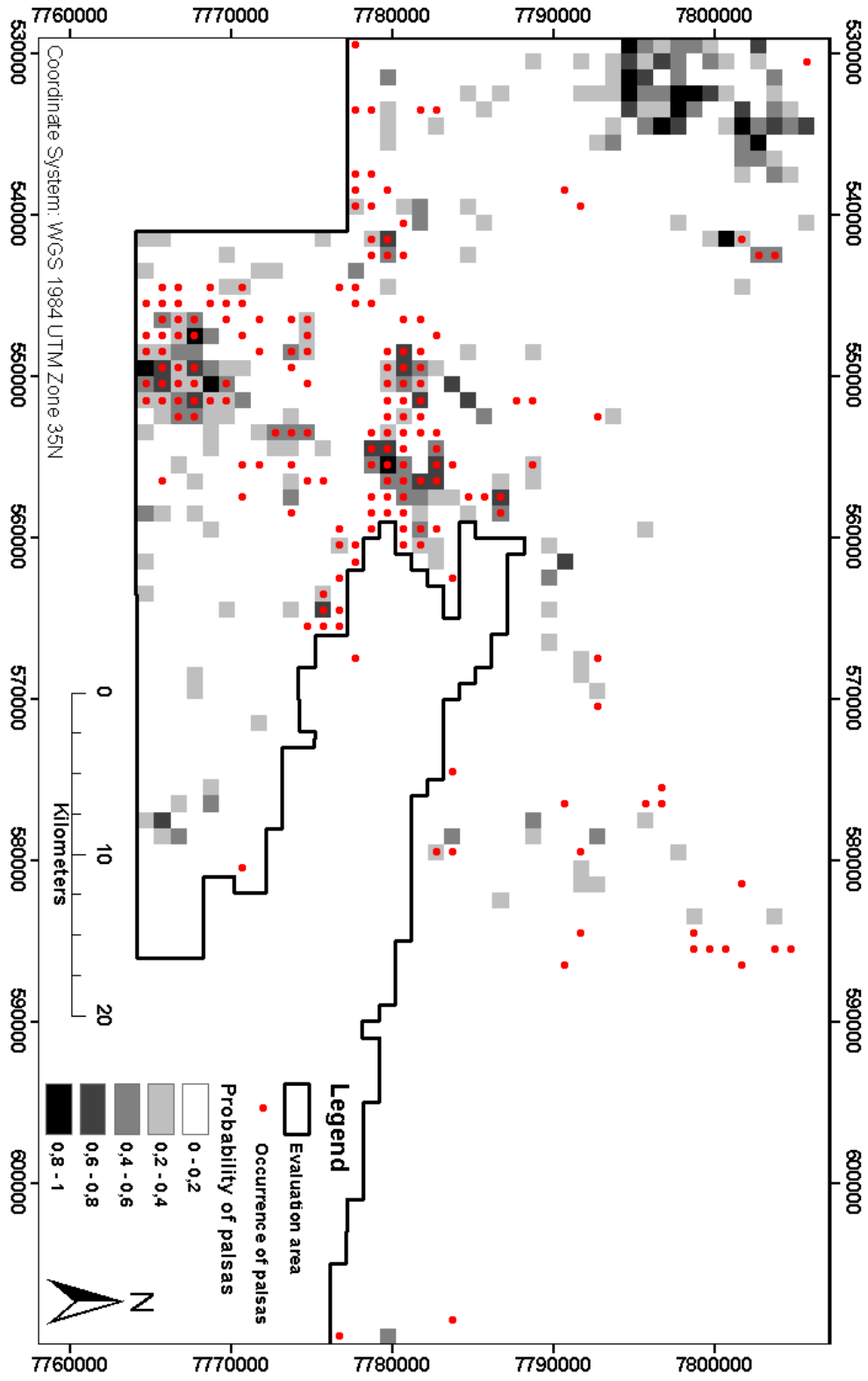

Figure 49: Map of the probability of palsas for the evaluation area Varanger. Occurrences of palsas in the 1x1 km grid cells are represented by red dots.

5.4.6 Estimating the total area of palsas

Table 15: Results of how well the final GLM fits the evaluation areas with different threshold of probability. It includes the sensitivity (eq. 2.1), specificity (eq. 2.2) and the correct classification rate (overall) (eq. 2.3) of the model for the evaluation areas based on different thresholds of probability.

Southwest			***Varanger***		
Threshold: 0,6:			Threshold: 0,2:		
	True positive	165		True positive	68
	False positive	410		False positive	171
	False negative	17		False negative	108
	True negative	188		True negative	2358
	Sensitivity [%]	90.7		Sensitivity [%]	38.6
	Specificity [%]	31.4		Specificity [%]	93.2
	Overall [%]	**45.3**		Overall [%]	**89.7**
Threshold: 0,8:			Threshold: 0,4:		
	True positive	146		True positive	40
	False positive	243		False positive	66
	False negative	36		False negative	136
	True negative	355		True negative	2463
	Sensitivity [%]	80.2		Sensitivity [%]	22.7
	Specificity [%]	59.4		Specificity [%]	97.4
	Overall [%]	**64.2**		Overall [%]	**92.5**
Threshold: 0,9:			Threshold: 0,6:		
	True positive	123		True positive	17
	False positive	149		False positive	26
	False negative	59		False negative	159
	True negative	449		True negative	2503
	Sensitivity [%]	67.6		Sensitivity [%]	9.7
	Specificity [%]	75.1		Specificity [%]	98.97
	Overall [%]	**73.3**		Overall [%]	**97.59**

To estimate the total area of palsas in Finnmark, the procedure explained in Chapther 4.2.5 has been followed. Table 15 includes results of how well the final GLM fits the evaluation areas with different thresholds of probability. From the table, it is clear that the probability of palsas is generally too high in *Southwest*, while it is generally too low in *Varanger* (because of the low sensitivity with increasing thresholds). When selecting a suitable threshold, the

results from the evaluation area *Southwest* are weighted the most. This is because a larger amount of palsas is situated in *Southwest* than in *Varanger*, and because palsas in Finnmark mostly are situated in continental areas in Finnmarksvidda. Thus, a threshold of 0.8 is selected as the threshold to find the total area of palsas in Finnmark.

In the final GLM model, 2848 grid cells in Finnmark have a probability of occurrence of palsas at or above 0.8. The total area of mire in these 2848 grid cells is 1469,861 km^2.

Table 16 contains information about the proportion of palsas by mires in Lakselv, Suossjavri and Goatheluoppal for 2008, 2011 and 2012, respectively. Following the procedure, the palsa mires have been divided into grid cells. Not all grid cells with palsas from these three study sites have been utilized, since some grid cells included large peat plateaus or several palsas that were not delineated. In total, at least 8.5 % of the area of mires was covered with palsas in 2008/2011/2012 (Table 16). This is an underestimation of the proportion of palsas by mire for these three areas, and I therefore choose to use 10 % as the proportion of palsas by mire in 2010 in the final calculations.

Thereby, the estimate of total area of palsas in Finnmark for around year 2010 is:

$$\mathbf{1469.861}\ \boldsymbol{km^2}\ *\ \mathbf{0.1}\ =\ \mathbf{146,986}\ \boldsymbol{km^2} \approx\ \mathbf{147}\ \boldsymbol{km^2} \qquad (5.1)$$

147 km^2 is approximately 0.3 % of the total area of Finnmark.

Table 16: The proportion of palsas by area of mire for the three study sites Lakselv, Suossjavri and Goatheluoppal for 2008, 2011 and 2012, respectively. The table also contains information about the number of grid cells used for the computation of the proportion of palsas following the procedure explained in 4.2.5.

	Lakselv 2008	**Suossjavri 2011**	**Goatheluoppal 2012**	**Total**
Number of grid cells	12	8	6	26
Area of palsas [m^2]	481200	389095	140436	1010731
Area of mire [m^2]	4625678	2977900	4353600	11957178
Palsas/mire	0,104	0,131	0,032	0,085

5.5 A simple carbon gas release model

This section presents the results of the simple model of carbon gas release from thawing palsas in Finnmark, as explained in Section 4.3 (flowchart in Figure 12). The model uses inputs from the results of both total degradation of palsas and the total area of palsas in Finnmark. Table 17 presents the total degradation of the area of palsas for all of the three study sites. Based on these numbers, an estimate of 40 % degradation in 50 years (1960-2010) for whole Finnmark is used in the model. From Section 5.4.6 (eq. 5.1), the total area of palsas in 2010 was estimated to be 147 km^2.

By using 2 m as mean height for the permafrost core, a peat content of 15 % and a bulk density of dry OM of 0,11 g/cm3 in the calculations give a mass of dry OM in 2010 of 48510 tonnes. This mass is in 1960 of 80 850 tonnes assuming 40 % degradation. Thus, the mass of peat thawed is 32 340 tonnes. Using 50 % as carbon content of peat results in 16170 tonnes of carbon available to microbial decomposition.

How much CO_2 or CH_4 could potentially this amount of carbon be a constituent of? The atomic mass of C is 12*u*, while the atomic mass of CO_2 and CH_4 are 44*u* and 16*u*, respectively (Table 18). The proportion of mass of carbon for CO_2 is then 27.27 %, while the proportion for CH_4 is 75 %. Using these proportions, the potential mass of all CO_2 or CH_4 molecules are easily calculated by simply divide the mass of carbon by the proportions, which gives 59 296 tonnes of CO_2 or 21 560 tonnes of CH_4. This gives a potential mean annual flux (when divided by 50 years) of 1186 tonnes of CO_2 or 431 tonnes of CH_4 from thawing of organic-rich permafrost in palsa mires in Finnmark, assuming that the rate of decomposition is similar to the rate of degradation.

The organisation Statistics Norway has the overall responsibility for official statistics in Norway, including information about gas emissions from different sources and counties in Norway. According to Statistics Norway (2015), the total gas emissions of CO_2 and CH_4 from Finnmark in 2010 was 1 304 000 tonnes and 7752 tonnes, respectively. Thus, the total human emissions of CH_4 for one year (2010) is less than 1/3 of the total estimated potential release of CH_4 from the degradation of palsas over 50 years (1960-2010).

Table 17: The total degradation of the area of palsas in percent for Lakselv, Suossjavri and Goatheluoppal from 1950s to 2010s, with number of years between the degradation.

Study site:	Total degradation [%]	Number of years
Lakselv 1959 - 2009	-48	50
Suossjavri 1956/1959 - 2011	-33	52-55
Goatheluoppal 1958 - 2012	-71	54

Table 18: The atomic mass (u) of CO_2 and CH_4, and the proportion of mass of carbon for CO_2 and CH_4.

	Atomic mass [u]
CO_2	
1 x C	1 x 12
2 x O	2 x16
Total [u]	**44**
Proportion of carbon [%]	**27.27**
CH_4	
1 x C	1 x12
4 x H	4 x 1
Total [u]	**16**
Proportion of carbon [%]	**75.00**

6. Discussion

This chapter contains a discussion of the delineation process (6.1), of the GDM-process (6.2) and of the carbon gas release model (6.3). Furthermore, the delineation process and the GDM-process are split into discussion of the methodological aspect and the results.

6.1 The delineation process

6.1.1 Methodological aspect

It is impossible to quantify the accuracy of the methodology used in the delineation process. Nonetheless, it is my opinion that the accuracy is sufficient for the purposes of this thesis. The high amount of palsas delineated and the large observed changes are the main reasons for this opinion. The largest uncertainty by this method is possibly the use of different types of images (e.g. by image type, spatial and radiometric resolution), which may make the method prone to systematic errors (see Appendix A.1, A.2 and A.3). With respect to georeferencing of the aerial images, the RMSE is considered to be mostly within acceptable levels (one exception, see Table 6).

The use of climate data from the meteorological stations is related to two issues: (a) The existence of larger data gaps, and (b) an unknown correlation between the weather at the study sites and the stations. The last issue applies especially for the palsa mires in Goatheluoppal, where the nearest met-station, Kautokeino, is situated 30 km away and with a 133 m lower elevation. Furthermore, Goatheluoppal is situated closer to the coast, thus are probably more affected by maritime air masses than Kautokeino met-station. Thus, Kautokeino met-station is possibly not very representative for short time weather variations, but as the weather in Finnmarksvidda is relatively homogenous (see Figure 4), the main longterm trends over decades in Kautokeino are probably also representative for Goatheluoppal. Banak and Cuovddatmohkki meteorological stations are situated very close to the study sites. Thus climate data from these stations should represent the climate at the study sites satisfactorily.

The results from the delineation process may not be representative for the entire Finnmark. Most likely, the results from Suossjavri are most representative for the largest share of palsas in Finnmark, since the largest share are in the centre of Finnmarksvidda. The existence of palsas in maritime Lakselv probably depend on other factors than the existence of palsas in more continental areas, and may thus be representative for coastal and periphery palsa mires like the large peat plateaus in inner parts of Varangerfjorden. The rate of degradation of palsas in Goatheluoppal is most likely at the upper end of the scale.

6.1.2 Results

The results show that there has been a steady decrease in area of palsas between 1950s and 2010s. Thus, the formation and degradation of palsas are not in balance. Actually, no new palsas were found and no palsas increased notably in area between 1950s and 2010s. However, detection of new small embryo palsas can be difficult, and small palsas may have formed and disappeared within the periods. Furthermore, the results from both Suossjavri and Goatheluoppal show that there has been a tendency towards an acceleration in degradation (except between 1982-2003 in Goatheluoppal) (Figure 34, 35 and 36). This is especially evident for the last period (2003-2011/2012). The annual rate of degradation for palsa mire 1-5 in Suossjavri has more than doubled from 1982-2003 to 2003-2011 (Figure 34). Observations from the field (see 5.3.2) indicate that the degradation of palsas has continued at least at the same rate for the period 2011-2014 in palsa mires around Suossjavri. The observations also reveal the dynamic environment of palsas, where small palsas can thaw completely in a couple of years.

The results in Suossjavri show that there is a clear difference between the rate of degradation for large peat plateaus and smaller palsas, whereas smaller palsas degrade much faster (in means of percentage of degradation by former extent) than large peat plateaus (Table 8). This is also, to a lesser extent, evident in Lakselv, where the palsa mires with the largest peat plateaus have the slowest rate of degradation (Table 7). A possible explanation for the difference in degradation rate between palsas and larger peat plateaus is that they degrade by different mechanisms (Sollid and Sørbel, 1998). Dome palsas are known to be higher than peat plateaus, resulting in more block erosion, while low peat plateaus are mostly eroded by thermal erosion from water (Sollid and Sørbel, 1998). However, many of the palsas delineated

are probably “residual” palsas from the fractioning of larger peat plateaus and are therefore not originally single dome palsas. These “residual” palsas have also had a large degradation rate. Another explanation may thus simply be the following: If the lateral rate of degradation (by e.g. block erosion) is the same for smaller and larger palsas with the same form, the percentage of degradation (compared to former extent) is largest for smaller palsas.

Is it possible to explain the observed degradation by climate data from the nearby meteorological stations? For all three meteorological stations, an increase in mean wind speed is evident (Figure 15, 19 and 23). An increase in mean wind speed promotes a lower maximum depth of snow in convex topography like the top of palsas (Seppälä, 1982). Thus, the observed increase in wind speed cannot explain the lateral degradation. Nonetheless, wind has the potential of being an important agent in eroding palsas vertically by surface abrasion (Seppälä, 2003).

The met-station Banak has a weak positive trend of both increasing temperatures and precipitation throughout the last 50 years (Figure 13 and 14). The mean temperature registered at Banak for 1966-2014 of 0.96 °C (Table 3) is much higher than the preferable range in MAAT of -2 °C to -5 °C (Seppälä, 2006). Furthermore, the mean temperature for 1998-2014 of 1.57 °C is even higher. With these temperatures, a low conductivity ratio and a negligible snow cover are necessary in order to have possibilities of negative temperatures in the ground. The high mean wind speed of 4.81 m/s for 1966-2014 (Table 3) is probably important for the survival of palsas, as it prevents the formation of a thick snow cover during winter (Seppälä, 1982). The high temperatures and the further increase observed at Banak have most likely been a major driver of the documented degradation of palsas in Lakselv. The increase in MAP observed in the last 15 years has probably further accelerated the degradation rate (Table 3). According to Hanssen-Bauer (2005), the outer parts of Finnmark (including Lakselv) have experienced significant increasing summer precipitation during 1895 to 2004. Increase in summer precipitation most likely has a negative effect on the existence of palsas in Lakselv, as it decreases the insulation properties of peat (Seppälä, 2006). Altogether, the climate observed at Banak today is not in favor of the existence of palsas.

Cuovddatmohkki also has experienced a weak positive trend of both temperature and precipitation throughout the last 50 years (Figure 16 and 17). In Cuovddatmohkki, the mean

temperature for the whole period was -1.97 °C, while the mean temperature from 1995-2014 (-1.51 °C) was 1 °C higher than the mean MAAT for 1967-1980 (-2.59 °C) (Table 4). The increase in precipitation in Cuovddatmohkki between the period 1967-1980 and 1995-2014 of more than 60 mm (Table 4) had also most likely a negative effect on the palsa mires in Suossjavri. Although MAP has increased, no increase in the maximum depth of snow is observed in Cuovddatmohkki (Figure 17, table 4). Further, there are large variations in the maximum snow depth. Thus, the data of maximum snow depth does not imply any change in impact from this climate variable for 1967-2014. Altogether, the increase in both temperature and precipitation are probably explaining the accelerated rate of degradation at Suossjavri.

A large variability in temperature has been observed in Kautokeino, with a MAAT ranging from approximately -5.5 °C to 0.2 °C (mean of -2 °C) in the period 1922 to 2013 (Figure 16 and 17). The temperature is probably slightly lower for the palsa mires in Goatheluoppal, as it is situated at a higher elevation. Table 4 shows that the mean temperature in 1997-2013 is almost 1 °C warmer than the period 1939 to 1970. The well-known warming trend from the early 1900s to the 1930s (Hanssen-Bauer, 2005) is clearly visible in the figure. Actually, the temperature in 1922-1938 is nearly as warm as in 1997-2013.

The precipitation in Kautokeino from 1998 to 2013 was 434 mm, increasing from 327 mm for the period 1922 to 1969. Since Goatheluoppal is located further west and at higher elevation, the precipitation is probably higher than in Kautokeino (also suggested by the map of normal precipitation in Figure 4). Therefor, the increase in precipitation has most likely had a negative effect on the survival of palsas in this area. No trend in maximum snow depth is observed (Figure 22). Overall, the increase in rate of degradation observed at Goatheluoppal is best explained by the increase in both precipitation and temperature during the last two decades.

Although no increase in maximum snow depth in Cuovddatmohkki nor Kautokeino has been observed, the largest increase in precipitation in inner Finnmark has occurred during winter and spring according to Hanssen-Bauer (2005). As maximum snow depth apparently is a local and very variable climatic factor when comparing single years, other measures of snow cover (like the mean snow cover) may have been more convenient for the investigation of the relationship between snow cover and degradation of palsas. MAAT at all the three

meteorological stations are outside the range of being favorable for palsas, which has been proposed to be within -2 °C to -5 °C (Luoto et al., 2004).

There are few other studies of changes in area of palsas in Fennoscandia. There are some studies of degradation of palsas, but these studies are often qualitative and limited to a few palsas (e.g. Zuidhoff, 2002; Hofgaard and Myklebust. 2012, 2014), or they are of palsa mires situated at marginal areas (e.g. Sollid and Sørbel, 1998; Zuidhoff and Kolstrup, 2000). Zuidhoff and Kolstrup (2000) studied lateral changes for some palsas in Sweden's most southerly major palsa mire by mapping palsas using aerial images. Their results showed a 50 % decrease in the area of palsas between 1960 and 1997 – consistent with the results from this thesis. They suggest that the decay of palsas are the result of the 1-1.5 °C increase in mean annual temperature in northern Sweden during the last 100 years, and probably in combination with increased snowfall since ca. 1930. Also Sollid and Sørbel (1998), investigating palsas in Dovrefjell, concluded that the tendency of the degradation in that area was a result of the warming trend, which started in the 1930s.

NINA (Hofgaard and Myklebust, 2012, 2014) performed surveillance of palsa mires in Goatheluoppal in 2004 and 2011 and in Ferdesmyra in 2008 and 2014. Their research focused on both change in palsa form and in vegetation by inspecting transects. Hofgaard and Myklebust (2014) concluded that the size and height of the observed palsas in Ferdesmyra, which is located in Sør-Varanger, east in Finnmark, decreased significantly between 2008 and 2014. By observing aerial images, they concluded that most of the palsas in Ferdesmyra which existed in the 1970s, today have completely disappeared. Furthermore, they believe that the process of degradation has been going on for a long time (Hofgaard and Myklebust, 2014). They relate the fast decay of palsas with an increase in temperature of almost 1.5 °C since the 1970s.

In Goatheluoppal, NINA investigated the southernmost part of the palsas investigated in this thesis, and two areas further south/west. From 2004 to 2011, they surpringly found no overall change in the distribution and size of palsas (Hofgaard and Myklebust, 2014). Still, by observation from helicopter in both 2004 and 2011, they observed a fast reduction in the extent of palsas slightly further north of their study site, where palsas investigated in this thesis are located. They relate this reduction with increasing temperatures and especially the

increase in precipitation since the beginning of the 20th century (Hofgaard and Myklebust, 2014).

As the studies of Zuidhoff and Kolstrup (2000), Hofgaard and Myklebust (2014) and Sollid and Sørbel (1998) are at the margin of the distribution of palsas, a tendency of degradation during the second half of the 20th century is not surprising due to a more unfavourable climate for the existence of palsas. The results of this thesis further demonstrate the ongoing degradation of palsas in marginal areas (Lakselv), but it also shows quantitatively that widespread degradation is ongoing closer to the centre of the distribution of palsas (Suossjavri and Goatheluoppal). This has also indirectly been observed by Luoto and Seppälä (2003), who used GLM and observation of thermokarst lakes originating from palsas to estimate that the former distribution of palsas was about three times larger than the present distribution in a 3370 km^2 area in northern part of Finnish Lapland.

The palsa mires were likely not in equilibrium even as early as the 1950s, as many thermokarst lakes and other indications of degradation of palsas were observed in all the three study sites on the aerial images from the 1950s (see e.g. Figure 30, 38 and 42). According to Hanssen-Bauer (2005), there was a period in almost all off Norway known as "the early 20th century warming" which followed a rather cold period around 1900 and culminated in the 1930s. This warming period is clearly visible on the temperature record for Kautokeino (Figure). Thus, there is a possibility that the degradation already started during this period, as the temperature in the 1920s-1930s was as high or almost as high as the temperatures in the last decade (Table 5; Hanssen-Bauer, 2005). This is especially plausible for the palsa mires in Lakselv: the temperature in Lakselv during the last 50 years is not sustainable for the preservation of palsas. Furthermore, the palsa mires in Lakselv had several large lakes on the aerial images from 1959 that had mostly dried out in 2009 (see Figure 30 and Figure 33). Most likely was these lakes thermokarst lakes, thus indicating extensive permafrost thaw before 1959. Direct human influence by agriculture and farming cannot be ruled out in Lakselv, as parts of the palsa mires had turned into croplands with some examples of sharp unnatural boundaries (Figure 31).

According to Oksanen (2005), most of the palsas in northern Europe and northwestern Russia were formed during LIA. Of 38 palsas with relatively reliable dating, 18 were formed during

LIA and 15 were formed before – and thus survived – the Medieval warm period (Oksanen, 2005). It is likely that the palsa mires that were formed during LIA and situated at the margins of the palsa distribution, probably started to decay already when the temperature started to increase at the end of LIA. The equilibrium spatial model Cryogrid 1.0 by Gisnås et al. (2013) supports this, where permafrost in LIA underlaid ca. 14 % of Norway, compared to 6.1-6.4 % at present. Furthermore, their results indicate that the permafrost degradation during the past 50 years has been at the same magnitude as that between LIA and 1960-1990. Moreover, Lilleøren et al. (2011) further state that the permafrost extent in northern Norway is more sensitive to climate changes than in southern Norway, due to its lower relief in areas of permafrost aggradation during LIA. In the study by Farbrot et al. (2013), utilizing the same model (Cryogrid 1.0) specifically for Finnmark, they found that most of the permafrost areas in Finnmark has been warming in between 1961-1990 to 1981-2010. In addition, the model shows possible degradation mainly along the margin of the permafrost areas (Farbrot et al., 2013). The area with the largest decay of palsas, Goatheluoppal, is situated in an area of permafrost warming, but not of permafrost degradation according to the model (Farbrot et al., 2013). Thus, the results suggests a more widespread degradation of permafrost in Finnmarksvidda than what the model indicates.

Although modelling studies indicates widespread decay of permafrost since the LIA (Gisnås et al., 2013; Lilleøren et al., 2011; Farbrot et al., 2013), their results cannot be validated directly in means of e.g. boreholes, as most of the boreholes in Norway first were installed in the beginning of 1990s (Christiansen et al., 2010). However, the presence of relict permafrost landforms in northern Norway indicates a degradation (Lilleøren et al., 2011). Furthermore, this direct study of permafrost degradation reinforce the results of the modelling studies. Altogether, modelling studies and studies of permafrost landforms gives strong indications of widespread permafrost decay in the isolated and sporadic permafrost zone in Finnmark. Thus, even if some cold and dry years in succession may be in favor of permafrost aggradation in palsa mires (Zuidhoff and Kolstrup, 2000; Seppälä, 1982, 1990), many palsa mires in Finnmark have probably not been in equilibrium with the climate during more or less the entire 20th century.

Although the rate of degradation observed in this thesis appears to be high, the rate is consistent (i.e. at the same magnitude) with rates observed in other places of degradation of

palsas, for example in northern Sweden (Zuidhoff and Kolstrup, 2000) and the discontinuous permafrost zone in Canada (e.g Kershaw, 2003; Payette et al., 2004; Vallee and Payette, 2007). That does not imply that this degradation rate is common for most palsa mires, due to the tendency to investigate palsa mires in marginal permafrost areas (e.g. Sollid and Sørbel, 1998; Zuidhoff and Kolstrup, 2000). Thus, it would be interesting to investigate the development of palsas in places that are (apparently) more favored for the existence of palsas in northern Fennoscandia, for example in more continental areas in inner Finnmark.

6.2 GDM

6.2.1 Methodological aspect

Since the quality of the model is a result of the input data, the quality and accuracy of the input data are of great importance. A major drawback related to the response variable is that there has been no validation of the accuracy of the mapping of presence/absence of palsas. Therefore, inaccuracy of the response variable, the presence or absence of palsas within each grid cell, is a potential source of error. Errors can be that small palsas are not detected when interpreting aerial images, or that features other than permafrost mounds have been misinterpreted as palsas. Validation requires direct observations in the field for a fraction of the presence of palsas. This kind of validation is a time consuming process and outside the scope for this master thesis.

Climate data was earlier not incorporated in GDM due to the quality of the data. Still, Aalto and Luoto (2014) emphasized the need for accurate climate data. The gridded climate data from the Norwegian Meteorological Institute (MET, 2015a, 2015b) is based on interpolation between meteorological stations. The distribution of these stations in Norway is biased such that most stations are situated in populated lowlands, i.e. mostly near the coast or in valleys (Tveito et al., 2000). The result of this bias is that the climate characteristics in mountains and unpopulated areas are poorly described (Tveito et al., 2000). Inner parts of Finnmark have few meteorological stations, which results in higher uncertainties in the gridded climate data compared with densely populated areas in south of Norway. In addition, the appearance of strong winter inversions in mire areas in northern Fennoscandia hampers interpolating climate data (see e.g. Nordli, 1990; Pike et al., 2013). Thus, the unnatural pattern of winter

temperatures (*FDD*) in Figure 8 reflects this. Generally, climate has been recognized as important to explain the distribution of palsas at a broad spatial scale (from 10 km^2 to 1000 km^2), establishing more general distribution patterns (e.g. Luoto et al., 2004; Fronzek et al., 2006). Due to this relationship between climate and surface processes, and exaggerated by the uncertainties and the accuracy of the gridded climate data, the climate variables are probably not optimal at explaining local variations in the distribution of palsas.

Because map layers of much higher resolution have produced the topography and land cover variables, these variables are most likely of sufficient accuracy for the purposes of this thesis.

More explanatory variables can always be gathered, and the choice of variables is in the end subjective, preferably based on existing knowledge and results of former studies. In this thesis, some commonly used variables such as frost index (often referred to as frost number, see e.g. Luoto et al., 2004a) and different land cover of forests have not been used. Frost index is determining the net cooling effect of low atmospheric temperatures using *FDD* and *TDD* (Anisimov and Nelson, 1997). Luoto et al. (2004a) found that the frost index had a higher modelling performance in statistical modelling than *FDD* and *TDD* to determine the connection of climate to palsas. As the distribution of palsas in northern Fennoscandia coincide with the distribution of fell birch, and the northern limit of scots pine forest is close to the southern limit of the palsa region in northern Fennoscandia (Ruuhijarvi, 1960, references therein Luoto et al., 2004b), variables of different tree covers could have been of importance. In the study by Aalto and Luoto (2014), cover of both coniferous and deciduous forest was of significance for the spatial modelling of palsas. Nevertheless, the importance of these variables was small. As the gathering of different explanatory variables always could have been more comprehensive, the performance of the final model could have been improved.

According to Hjort et al. (2014), a model with explanatory variables that cover a wider range of environmental conditions in the calibration area than the evaluation area is more likely to give better predictions in the evaluation area than the reverse. The calibration area has, compared with more inner parts of Finnmark, a relatively heterogenic climate and a wider range of climatic conditions than the evaluation area *Southwest* (see Figure 4), with temperature and precipitation gradients, some mountains, plateaus and the lake Ieshjoka (see

e.g. shaded relief (hillshade) of the topography in Figure 7). Still, the evaluation area *Varanger* has both areas of warmer and wetter climate than what occur in the calibration area (see Figure 4). When extrapolating the area to whole Finnmark, values of the explanatory variables (except *Water* where the whole possible range is covered) will fall outside the range covered by the calibration area. Thus, the statistical relationship do not necessarily hold true (Fronzek et al., 2006).

An important finding in the results to Hjort et al. (2014) was that good performance in model calibration and within-area evaluation does not necessary imply a good extrapolation potential. Because this thesis has independent evaluation areas with greater spatial distance than most other studies, the evaluation in form of AUC is most likely more representative for extrapolation potential than studies using a split-data or within area approach (see e.g. Aalto and Luoto, 2014; Fronzek et al., 2006; Hjort et al., 2010; Luoto and Seppälä, 2002; Marmion et al., 2008). This could explain the lower performance of the final GLM in the evaluation areas than many other comparable studies that use within-area evaluation or split-data approach (Aalto and Luoto, 2014; Fronzek et al., 2006; Luoto and Seppälä, 2002).

A drawback of using the marginal palsa region *Varanger* as evaluation area is the much lower prevalence (i.e. the ratio between present and absence) of palsas compared to the calibration area, which affect the statistical performance (Hjort et al., 201). Thus, as Table 15 clearly demonstrates, the overall classification rate in *Varanger* increases when using higher threshold probabilities. However, sensitivity (true positive rate) decrease substantially with higher thresholds. The reason for the increase in the overall classification rate is that it weights the amount of true positives and true negatives equally (eq. 2.4). Consequently, the amount of true positives can be zero and the overall classification rate will still be higher than the overall classification rate for *Southwest* because of the low prevalence of palsas. Nonetheless, using *Varanger* as evaluation area gives a better understanding in how the model tackles marginal palsa areas.

The size of palsas is much smaller than the spatial resolution used in this thesis, but the question is whether a finer resolution is appropriate when also utilizing climate data. If only land cover and topographic variables were used in the model, a much finer resolution had been possible due to the resolution of the DEM (10x10 m) and the vector data in the land

cover maps. Hjort and Luoto (2006) found substantially variating results at different spatial resolution in the importance of different groups of variables by using variation partitioning. These results reflect the consensus that different group of variables are of importance at different scales (e.g. Aalto and Luoto, 2014; C. Harris et al., 2009), and thus the results of the importance of variables in the statistical modelling have to be interpreted in light of that knowledge.

During the calibration of the model, it was clear that the most important variable from the HP, *MaxSD*, had to be removed from the model and replaced by *MAP* in order to achieve the best GLM. This effect demonstrates the problem of multicollinearity in GLM: the significance of explanatory variables can be depressed when used together with other highly correlated variables (Hjort and Luoto, 2013).

6.2.2 Results

Most of the results regarding the direction and form of the response curves are consistent with the available literature and theory on the relationships between the explanatory variables and the presence of palsas (see Table 13 and Figure 45). *Mire* was obviously, positively correlated with the presence of palsas. As a linear variable, *Water* was positively correlated, consistent with the study of Luoto and Seppälä (2002). As a nonlinear quadratic variable, which further enhanced the model, the variable was correlated to the presence of palsas with a humped response curve (Figure 45). Hjort and Luoto (2008) using logistic regression have also observed this relationship. Furthermore, it is logical: when the proportion of water in a grid cell increases, less space is available for palsas.

FDD was positively correlated with the presence of palsas. Thus, cold winter temperatures is needed to produce an ice core during winter (Seppälä, 1986). As a linear variable, *TDD* was negatively correlated with the presence of palsas. This is obvious because high temperatures during summer thaws the permafrost in the ice core. However, *TDD* as a nonlinear quadratic variable further enhanced the model. The boxplot (Figure 44) and the humped response curve (Figure 45) of *TDD* indicates that palsas are not situated in places with too cold summers, but rather in a narrow temperature range. These results are supported by the literature, as several studies state that the upper limit of palsas are restricted by the thickness of peat (Luoto and Seppälä, 2002; Sollid and Sørbel, 1998). Production of peat is dependent on summer

temperatures, as too low temperatures restrict the production. Further, it needs to be high enough temperatures during the summers to ensure the availability of liquid water to feed the ice core in palsas (Kujala et al., 2008). Also, MAAT seems to have a potential as a quadratic variable, as the boxplot of *MAAT* indicates that palsas are located in a preferred range (Figure 44). A quadratic relathionship between MAAT and the occurrence of palsas has been observed by Luoto et al. (2004a). However, *MAAT* was not further investigated, as the variable was of less explanatory importance compared to the other variables.

MSP was surprisingly positive correlated with the presence of palsas. Other statistical modelling studies have found the opposite: negative correlation between summer precipitation and the presence of palsas (e.g. Luoto et al., 2004; Parviainen and Luoto, 2007). Studies that show a negative correlation between *MSP* and the presence of palsas are in agreement with the general theory: summer precipitation and moisture have a negative effect on palsas because it decreases the insulation properties of the peat (Seppälä, 2006). Furthermore, thermal erosion by water in connection with palsas is the most common form of erosion for peat plateaus, according to Sollid and Sørbel (1998). A presence of water is on the other hand necessary to develop palsas, since palsas grow from sucking extra water from the mire during its formation (Kujala et al., 2008). Consequently, a complex (nonlinear) relationship between summer precipitation and palsas is most likely present. However, a nonlinear component of *MSP* was not indicated by the boxplot (Figure 44) and it did not increase the predictive power of the GLM. For this variable, the range of 146-172 mm (Table 2) in the calibration area is most likely too narrow. However, the AUC-value of the GLM model in the evaluation area *Varanger* was surprisingly better when including *MSP* with positive correlation, than when excluding the variable. Thus, the complex relationship between *MSP* and the presence of palsas remains unexplained.

The climate and land cover variables were dominating in the final GLM (Table 13), while the climate variables were the dominating group of explanatory variables when using HP (Figure 43). As discussed above, the choice of area for calibration is a key to determine the importance of the explanatory variables. The calibration area is situated in the transition from the periphery towards inner parts of the distribution of palsas. Thus, climate is probably decisive in this region for the general pattern. The climate may be (or was) favourable for the

existence of palsas almost everywhere in more inner parts of the palsa distribution, and local factors are thus probably more important here for the presence or absence of palsas.

The results of HP was generally consistent with the results of the GLM, with the exceptions of *MaxSD*, *Water* and *MSP* (Figure 43, Table 10 and 11). *MaxSD* was in HP the variable with the highest independent effect to explain the variation in presence/absence of palsas. This indicate that the low significance of *MaxSD* when calibrating the GLM was due to high correlations with other variables. *Water* had a surprisingly low independent effect compared to the significance in the GLM. This may partly be explained by the drawback of HP not handling nonlinear explanatory variables. Thus, as *Water* improved the GLM significantly when adding a quadratic term, these improvements are not possible to detect by HP. Furthermore, HP indicates that precipitation (*MAP* and *MaxSD*) is more important than temperature (*FDD* and *TDD*) to explain the variation of palsas in the calibration area.

The results from HP show that *MSP* has by far the lowest independent effect of the climate variables (Table 11). Still, this variable is significant in the GLM (Table 13). This can be due to MSP explaining variations in the distribution of palsas that the other variables cannot explain – even if *MSP* in a univariate modelling setting explains the distribution poorly. Furthermore, the short range in *MSP* (Figure 44) may suggest that this variable has too small variations in the calibration area to have a large independent effect on the variation of palsas.

The AUC-values for the evaluation areas were inside the range of fair and good, indicating that the final GLM can be transferred to other regions (Table 14). As discussed above, the low prevalence of palsas in *Varanger* may affect the statistical importance of this evaluation area.

When comparing the probability map with the map of distribution of palsa mires by Sollid and Sørbel (1998), it appears to be an overestimation of probability in the centre of the distribution area (inner Finnmark). This is especially evident in the southeastern part of Finnmarksvidda, roughly between Karasjok and the Finnish border. An overestimation of palsas in the centre of the palsa distribution is also indicated by the overestimation of probabilities in the evaluation area *Southwest* (Figure 48), with very low sensitivity values (Table 15). The map by Sollid and Sørbel (1998) is based on observations by several researchers and had most likely strongly underestimates palsa mires that existed in the 1970s. Thus, the map is probably closer to a presence-only map than an absence-presence map.

However, the high probabilities in inner parts of Finnmarksvidda seems to be unrealistic. On the other hand, in the periphery there seem to be underestimations of the probabilities of palsas. In particular are clusters of outliers of palsas, like in Lakselv, greatly underestimated in terms of probabilities.

Overall, the general pattern of the probability map fits quite well with the extent of the region of palsas in the map by Sollid and Sørbel (1998). The main problem with the final map is that local variability appears to be low (see e.g. Figure 48). For example, almost all grid cells in some larger areas in the centre of the distribution have a very high probability (>0.9) of presence of palsas (Figure 46). This low variation of probabilities can be a result of the large dominance the climate variables have on the final model, whereas the occurrence of palsas follows climatic gradients.

It is difficult to know whether the estimate of the total area of palsas is an over- or underestimate, as there are many uncertaintites and rough estimates. Furthermore, there exist few qualitative studies for comparison about palsas and permafrost in Finnmark. According to Farbrot et al. (2013), approximately 19 % of the land area of Troms and Fnnmark are underlain with permafrost. Assuming that these numbers are correct, the proportion of palsas by total permafrost area in Finnmark is only 1.5 %. Since permafrost in palsa mires is believed to dominate in Finnmark (Christiansen et al., 2010; Farbrot et al., 2013), this number seems to be a conservative estimate. However, a palsa s a very visible permafrost form, and no estimate of palsa area for Finnmark has been made before. Thus, the assumption that permafrost in palsas dominates are probably biased by the visible nature of palsas which often are situated close to roads and easily visible on aerial images. The total area of permafrost in palsas in Finnmark is probably a very small fraction when compared to more discontinous/continous permafrost higher up in the mountains, invisible to the naked eye. Even in the palsa-rich sites of Lakselv, Suossjavri and Goatheluoppal, the proportion of palsas by mire was in total only around 10 % (Table 16). Furthermore, the proportion of mire in the gridcells was below 50 % (Table 16), and an estimate below 1 % as the area of palsas is thus more realistic than an estimate of several percent. Thus, it is probably most correct to state that palsas in Northern Norway are in the isolated (and not in the sporadic or discontinous) permafrost zone, following the general classification of isolated permafrost areas as areas underlain by less than 10 % permafrost.

6.3 Carbon model

First, it is important to emphasise that the simple carbon model only estimates one side of the carbon budget: the increase in flux of carbon out of the terrestrial reservoir as newly thawed organic matter is available for microbial decomposition. The possible increase in flux of carbon from the atmosphere to the terrestrial reservoir due to higher temperatures is however not considered and out of scope for this thesis.

Since the method utilized in the detection of palsas does not rule out lithalsas, the average dry OM bulk density is probably higher than what is reality for the mapped palsas. Furthermore, as it is known that the ice-rich inner core in palsas also usually contains silt and other mineral substances (Pissart, 2013), the density is further exaggerated.

According to E. A. Schuur et al. (2008), a key question regarding the permafrost carbon-climate relationship is the amount of organic-rich permafrost vulnerable to release into the atmosphere. In several modelling studies of potential release of greenhouse gases from thawing permafrost, both the amount of organic rich permafrost and the rate of thawing have been very roughly estimated or based on assumptions (see e.g. Koven et al., 2011; Schneider von Deimling et al., 2012). This thesis has tried to estimate these two factors by combining statistical modelling and direct observations. However, more information about common height of palsas and the depth of the permafrost core in Finnmark is needed to more accurately quantify the permafrost volume of palsas.

Two main limitations of the model are: a) it does not take into account the rate of carbon release to the atmosphere, and b) it does not investigate which form carbon will be released as. This model assume that all of the thawed organic matter are available for microbial decomposition, which globally are the dominant pathway of carbon from the terrestrial reservoir to the atmosphere (E. A. Schuur et al., 2008). There are studies showing that permafrost carbon rapidly can be decomposed and released in a time span of only a few years (Zimov et al., 2006); however, the majority of thawed permafrost carbon is likely to be released slowly over decades (Schuur et al., 2013). Furthermore, microbial decomposition rates are much slower in an anaerobic (without oxygen) than aerobic (with oxygen) environment, influencing the feedback to warming (Schuur et al., 2008).

Whether the release of carbon is in the form of CO_2 or CH_4 is substantial. CH_4 is known to have a much larger global warming potential (GWP) than CO_2 (33 times the GWP of CO_2 over a century long time scale according to Shindell et al. (2009)). The main factor determining the form in which carbon is released, is whether oxygen is available (CO_2) or not (CH_4 and other components) during the microbial decomposition (E. Schuur et al., 2013). Microbial decomposition at upland environments are often aerobic and in lowland environments (for example wetlands) anaerobic at higher latitudes (Schuur et al., 2013). Due to the high ice content of palsas, degradation of palsas usually involves thermokarst development. Thus, the deposition of carbon ends in an oxygen limited aquatic environment, and the release of methane is favourable (Schuur et al., 2013). Therefore, a larger bulk of the available carbon for microbial decomposition from thawing palsas will probably be released as CH_4. The microbial decomposition of the organic matter will consequently be slow, where the rate of permafrost thawing most likely exceeds the rate of decomposition. Hence, the estimates of the annual emissions of gas release from the model are probably optimistic, as the amount of carbon released needs to be stretched over more than 50 years.

The rough estimates in Section 5.4 indicate that the release of CH_4 and CO_2 from thawing palsas are, when compared with human emissions of CO_2 and CH_4 in Finnmark, rather insignificant in the global carbon cycle. If all the carbon through microbial decomposition are released as CH_4 in the timespan of 50 years (worst-case estimate), the emission is still only less than 3/50 of the total human emissions of CH_4 in Finnmark for 2010. However, if the degradation in Finnmark is representative for vast areas of organic-rich discontinuous, sporadic and isolated permafrost zones like in Siberia, the potential release of carbon is worth studying.

7. Conclusions

From the work of this thesis, the following conclusions are drawn:

- The area of palsas have steadily decreased in all three study sites over the period 1950s to 2008/2011/2012, with a total decrease in area of 48 %, 33 % and 71 % for the delineated palsa mires in Lakselv, Suossjavri and Goatheluoppal, respectively Furthermore, the rate of degradation was highest during the period 2003 to 2011/2012 in Suossjavri and Goatheluoppal. Observations from fieldwork in palsa mires in Suossjavri indicate a continued degradation in this area between 2011 and 2014.
- Signs of degradation (for example many thermokarst lakes) on aerial images from the 1950s suggest that the degradation started at the latest in the 1950s. Probably, the tendency of decay already started during the warming period in the 1920s-1930s. The palsa mires in Lakselv have probably not been in equilibrium with the climate during most of the 20th century due to high temperatures.
- The most important factors for the increase in rate of degradation of palsas are most likely the increase in both temperature and precipitation observed in the last few decades.
- The extent of the degradation of permafrost, both in space and time, have probably been underestimated in earlier studies of permafrost in Finnmark (Christiansen et al., 2010; Farbrot et al., 2013). Furthermore, the predicted and ongoing climate change with higher temperatures and increasing precipitation at higher latitudes (IPCC, 2014), are fatal news for the existence of palsas in large parts of Finnmark which already are at their brink of survival.
- The probability of presence of palsas increase with 1) decreasing freezing degree days (*FDD*), 2) a humped curve of thawing degree days (*TDD*), 3) decreasing normal annual precipitation (*MAP*), 4) increasing normal annual summer precipitation (*MSP*), 5) increasing area of mire (*Mire*) and 6) a humped curve of area of Water (*Water*). The variables *TDD* and *Water* were found to be nonlinear (quadratic) predictors of the presence/absence of palsas.
- At the scale/resolution utilized in the statistical modelling, hierarchical partitioning indicates that the climate variables dominates the importance of the explanatory

variables to independently explain the variation in palsas. Of these, *MaxSD* has the highest independent effect to explain the variation. *Mire* is the most important topography/land cover variable.

- The probability map of palsas seems to explain the general extent of palsas quite well when compared to the map of palsas by Sollid and Sørbel (1998). Still, the map has difficulties of explaining local variations. Furthermore, the evaluation areas indicate that the model overestimates probabilities near the centre of the distribution area, while it underestimates the probabilities in the outskirts of the distribution area. Some areas with "outliers" of palsas are not visible on the map.
- The total area of palsas in Finnmark in 2010 is estimated to be roughly 0.3 % of the total area of Finnmark.
- The total amount of potential carbon gas released in the form of CH_4 from decay of palsas from 1960 to 2010 in Finnmark is less than 3/50 of the human emissions of CH_4 in Finnmark for the year 2010. Thus, compared to human emissions, the potential amount of carbon gas release from decay of palsas in Finnmark is rather insignificant.

I encourage further research on palsa mires in core areas of the distribution to increase the knowledge about the extent of the ongoing degradation. Today's models of carbon fluxes in areas underlain by some degrees of permafrost are hampered by uncertainties in the amount of thawed organic material. Thus, accurate permafrost models (i.e. transient models) with emphasis on soil, vegetation and land cover are needed.

References

Aalto, J., and Luoto, M. (2014). Integrating climate and local factors for geomorphological distribution models. *Earth Surface Processes and Landforms, 39*(13), 1729-1740.

Aalto, J., Venäläinen, A., Heikkinen, R. K., and Luoto, M. (2014). Potential for extreme loss in high-latitude Earth surface processes due to climate change. *Geophysical Research Letters, 41*(11), 3914-3924.

Akaike, H. (1998). Information theory and an extension of the maximum likelihood principle *Selected Papers of Hirotugu Akaike* (pp. 199-213): Springer.

Anderson, D. R., and Burnham, K. P. (2002). Avoiding pitfalls when using information-theoretic methods. *The Journal of Wildlife Management*, 912-918.

Anisimov, O. A., and Nelson, F. E. (1997). Permafrost zonation and climate change in the northern hemisphere: results from transient general circulation models. *Climatic Change, 35*(2), 241-258.

Askheim, S., (2013). *Finnmarksviddas Grunnfjellsområde*. Store Norske Leksikon (SNL). Downloaded 20.04.15 from https://snl.no/Finnmarksviddas_grunnfjellsomr%C3%A5de.

Askheim, S., Thorsnæs, G. and Dalfest, T (2015). *Finnmarks Natur*. Store norske leksikon (SNL). Downloaded 21.04.15 from https://snl.no/Finnmarks_natur.

Bense, V. F., Kooi, H., Ferguson, G., and Read, T. (2012). Permafrost degradation as a control on hydrogeological regime shifts in a warming climate. *Journal of Geophysical Research-Earth Surface, 117*. doi: 10.1029/2011jf002143

Chevan, A., and Sutherland, M. (1991). Hierarchical partitioning. *The American Statistician, 45*(2), 90-96.

Christiansen, H. H., Etzelmüller, B., Isaksen, K., Juliussen, H., Farbrot, H., Humlum, O., Johansson, M., Ingeman-Nielsen, T., Kristensen, L., Hjort, J., Holmlund, P., Sannel, A. B. K., Sigsgaard, C., Akerman, H. J., Foged, N., Blikra, L. H., Pernosky, M. A., and Odegard, R. S. (2010). The Thermal State of Permafrost in the Nordic Area during the International Polar Year 2007-2009. *Permafrost and Periglacial Processes, 21*(2), 156-181. doi: 10.1002/ppp.687

Dannevig, P. (2009). *Finnmark: klima*. Store norske leksikon (SNL). Downloaded 22.04.15 from https://snl.no/Finnmark%2Fklima.

DeLeo, J. M. (1993). *Receiver operating characteristic laboratory (ROCLAB): software for developing decision strategies that account for uncertainty.* Paper presented at the Uncertainty Modeling and Analysis, 1993. Proceedings., Second International Symposium on.

Etzelmüller, B., Berthling, I., and Sollid, J. L. (2003). Aspects and concepts on the geomorphological significance of Holocene permafrost in southern Norway. *Geomorphology, 52*(1-2), 87-104. doi: 10.1016/s0169-555x(02)00250-7

Farbrot, H., Isaksen, K., and Etzelmüller, B. (2008). Present and past distribution of mountain permafrost in the Gaissane Mountains, northern Norway. *International Conference on Permafrost ICOP Proceedings, 9*, 427-432.

Farbrot, H., Isaksen, K., Etzelmüller, B., and Gisnås, K. (2013). Ground Thermal Regime and Permafrost Distribution under a Changing Climate in Northern Norway. *Permafrost and Periglacial Processes, 24*(1), 20-38. doi: Doi 10.1002/Ppp.1763

Fielding, A. H., and Bell, J. F. (1997). A review of methods for the assessment of prediction errors in conservation presence/absence models. *Environmental Conservation, 24*(01), 38-49.

Fox, J. (2005). The R Commander: A Basic Statistics Graphical User Interface to R. *Journal of Statistical Software, 14*(9): 1--42.

Fronzek, S., Luoto, M., and Carter, T. R. (2006). Potential effect of climate change on the distribution of palsa mires in subarctic Fennoscandia. *Climate Research, 32*(1), 1-12. doi: 10.3354/cr032001

Gisnås, K., Etzelmüller, B., Farbrot, H., Schuler, T. V., and Westermann, S. (2013). CryoGRID 1.0: Permafrost Distribution in Norway estimated by a Spatial Numerical Model. *Permafrost and Periglacial Processes, 24*(1), 2-19. doi: 10.1002/ppp.1765

Gruber, S., and Hoelzle, M. (2001). Statistical modelling of mountain permafrost distribution: local calibration and incorporation of remotely sensed data. *Permafrost and Periglacial Processes, 12*(1), 69-77.

Hanssen-Bauer, I. (2005). Regional temperature and precipitation series for Norway: Analyses of time-series updated to 2004. *Met. no report, 15*(2005), 1-34.

Harris, C., Arenson, L. U., Christiansen, H. H., Etzelmüller, B., Frauenfelder, R., Gruber, S., Haeberli, W., Hauck, C., Hoelzle, M., and Humlum, O. (2009). Permafrost and climate in Europe: Monitoring and modelling thermal, geomorphological and geotechnical responses. *Earth-Science Reviews, 92*(3), 117-171.

Harris, S. (1993). *Palsa-like mounds developed in a mineral substrate, Fox Lake, Yukon Territory.* Paper presented at the Proceedings of the 6th International Conference on Permafrost.

Hjort, J. (2014). Which Environmental Factors Determine Recent Cryoturbation and Solifluction Activity in a Subarctic Landscape? A Comparison between Active and Inactive Features. *Permafrost and Periglacial Processes, 25*(2), 136-143. doi: 10.1002/ppp.1808

Hjort, J., Etzelmüller, B., and Tolgensbakk, J. (2010). Effects of Scale and Data Source in Periglacial Distribution Modelling in a High Arctic Environment, western Svalbard. *Permafrost and Periglacial Processes, 21*(4), 345-354. doi: 10.1002/ppp.705

Hjort, J., and Luoto, M. (2006). Modelling patterned ground distribution in Finnish Lapland: An integration of topographical, ground and remote sensing information. *Geografiska Annaler Series a-Physical Geography, 88A*(1), 19-29. doi: 10.1111/j.0435-3676.2006.00280.x

Hjort, J., and Luoto, M. (2008). Can abundance of geomorphological features be predicted using presence-absence data? *Earth Surface Processes and Landforms, 33*(5), 741-750. doi: 10.1002/esp.1572

Hjort, J., and Luoto, M. (2009). Interaction of geomorphic and ecologic features across altitudinal zones in a subarctic landscape. *Geomorphology, 112*(3-4), 324-333. doi: 10.1016/j.geomorph.2009.06.019

Hjort, J., and Luoto, M. (2011). Novel theoretical insights into geomorphic process–environment relationships using simulated response curves. *Earth Surface Processes and Landforms, 36*(3), 363-371.

Hjort, J., and Luoto, M. (2013). 2.6 Statistical Methods for Geomorphic Distribution Modeling. In J. F. Shroder (Ed.), *Treatise on Geomorphology* (pp. 59-73). San Diego: Academic Press.

Hjort, J., Ujanen, J., Parviainen, M., Tolgensbakk, J., and Etzelmüller, B. (2014). Transferability of geomorphological distribution models: Evaluation using solifluction

features in subarctic and Arctic regions. *Geomorphology, 204*, 165-176. doi: 10.1016/j.geomorph.2013.08.002
Hofgaard, A. (2004). Etablering av overvåkingsprosjekt på palsmyrer. *NINA Oppdragsmelding 841: 32 pp., 841*.
Hofgaard, A. and Myklebost, H.E. (2012). Overvåking av palsmyr. Første gjenanalyse i Goahteluoppal, Vest-Finnmark. Endringer fra 2006 til 2011. *NINA Rapport 841:* 44 pp., 841
Hofgaard, A. and Myklebost, H.E. (2014). Overvåking av palsmyr. Første gjenanalyse i Ferdesmyra, Øst-Finnmark. Endringer fra 2008 til 2013. *NINA Rapport 1035:* 49 pp., 1035
IPA (2014). *What is Permafrost?* International Permafrost Association. Downloaded 20.05.15 from http://ipa.arcticportal.org/resources/what-is-permafrost.
IPCC (2014). Climate Change 2014: Synthesis Report. Contribution of Working Groups I, II and III to the Fifth Assessment Report of the Intergovernmental Panel on Climate Change [Core Writing Team, R.K. Pachauri and L.A. Meyer (eds.)]. IPCC, Geneva, Switzerland, 151 pp.
Isaksen, K., Farbrot, H., Blikra, L. H., Johansen, B., Sollid, J. L., and Eiken, T. (2008). Five year ground surface temperature measurements in Finnmark, northern Norway. *International Conference on Permafrost ICOP Proceedings, 9*, 789-794.
Kartverket. (2015a). *Flybildearkiv for Norge*. The Norwegian Mapping Authority (©Kartverket). Downloaded 20.05.15 from http://159.162.103.4/geovekst/Flybildearkiv/
Kartverket. (2015b). *Velkommen.* The Norwegian Mapping Authority (©Kartverket). Downloaded September 2014 from http://data.kartverket.no/download/
Kershaw, G. (2003). *Permafrost landform degradation over more than half a century, Macmillan/Caribou Pass region, NWT/Yukon, Canada.* Paper presented at the Proceedings of 8th International Conference on Permafrost, Zurich. Permafrost [1], M. Phillips, S. Springman i L. Arenson (red.).
Koven, C. D., Ringeval, B., Friedlingstein, P., Ciais, P., Cadule, P., Khvorostyanov, D., Krinner, G., and Tarnocai, C. (2011). Permafrost carbon-climate feedbacks accelerate global warming. *Proceedings of the National Academy of Sciences, 108*(36), 14769-14774.
Kujala, K., Seppälä, M., and Holappa, T. (2008). Physical properties of peat and palsa formation. *Cold Regions Science and Technology, 52*(3), 408-414. doi: 10.1016/j.coldregions.2007.08.002
Lewkowicz, A. G., and Ednie, M. (2004). Probability mapping of mountain permafrost using the BTS method, Wolf Creek, Yukon Territory, Canada. *Permafrost and Periglacial Processes, 15*(1), 67-80.
Lilleøren, K. S., and Etzelmüller, B. (2011). A regional inventory of rock glaciers and ice-cored moraines in Norway. *Geografiska Annaler, 93*(3), 175-191. doi: DOI: 10.1111/j.1468-0459.2011.00430.x
Lilleøren, K. S., Etzelmüller, B., Schuler, T. V., Gisnås, K., and Humlum, O. (2012). The relative age of mountain permafrost—estimation of Holocene permafrost limits in Norway. *Global and Planetary Change, 92*, 209-223.
Loisel, J., Yu, Z., Beilman, D. W., Camill, P., Alm, J., Amesbury, M. J., Anderson, D., Andersson, S., Bochicchio, C., and Barber, K. (2014). A database and synthesis of northern peatland soil properties and Holocene carbon and nitrogen accumulation. *The Holocene*, 0959683614538073.

Lundqvist, G. (1951). En palsmyr sydost om Kebnekaise. *GFF, 73*(2), 209-225.
Lundqvist, G. (1953). Tillägg till palsfrågan. *GFF, 75*(2), 149-154.
Lundqvist, J. (1962). *Patterned ground and related frost phenomena in Sweden*: [Generalstabens Litogr. Anst. Förl.[i] distr.].
Luoto, M., Fronzek, S., and Zuidhoff, F. S. (2004a). Spatial modelling of palsa mires in relation to climate in northern Europe. *Earth Surface Processes and Landforms, 29*(11), 1373-1387. doi: 10.1002/esp.1099
Luoto, M., Heikkinen, R. K., and Carter, T. R. (2004b). Loss of palsa mires in Europe and biological consequences. *Environmental Conservation, 31*(1), 30-37. doi: 10.1017/s0376892904001018
Luoto, M., and Hjort, J. (2005). Evaluation of current statistical approaches for predictive geomorphological mapping. *Geomorphology, 67*(3-4), 299-315. doi: 10.1016/j.geomorph.2004.10.006
Luoto, M., and Seppälä, M. (2002). Modelling the distribution of palsas in Finnish lapland with logistic regression and GIS. *Permafrost and Periglacial Processes, 13*(1), 17-28.
Luoto, M., and Seppälä, M. (2003). Thermokarst ponds as indicators of the former distribution of palsas in Finnish lapland. *Permafrost and Periglacial Processes, 14*(1), 19-27. doi: 10.1002/ppp.441
Mac Nally, R. (2000). Regression and model-building in conservation biology, biogeography and ecology: the distinction between–and reconciliation of–'predictive'and 'explanatory'models. *Biodiversity and Conservation, 9*(5), 655-671.
Marmion, M., Hjort, J., Thuiller, W., and Luoto, M. (2008). A comparison of predictive methods in modelling the distribution of periglacial landforms in Finnish Lapland. *Earth Surface Processes and Landforms, 33*(14), 2241-2254.
Marmion, M., Hjort, J., Thuiller, W., and Luoto, M. (2009). Statistical consensus methods for improving predictive geomorphology maps. *Computers and Geosciences, 35*(3), 615-625.
Matthews, J. A., Dahl, S. O., Berrisford, M. S., and Nesje, A. (1997). Cyclic development and thermokarstic degradation of palsas in the mid-Alpine zone at Leirpullan, Dovrefjell, southern Norway. *Permafrost and Periglacial Processes, 8*(1), 107-122. doi: 10.1002/(sici)1099-1530(199701)8:1<107::aid-ppp237>3.0.co;2-z
McCullagh, P., Nelder, J. A., and McCullagh, P. (1989). *Generalized linear models* (Vol. 2): Chapman and Hall London.
MET (2015a). Kart med temperaturnormal for Norge. Norwegian Meteorological Institute (MET). Downloaded 20.04.15 from http://met.no/Klima/Klimastatistikk/Klimanormaler/Temperatur/.
MET (2015b). Kart med nedbørnormal for Norge. Norwegian Meteorological Institute (MET). Downloaded 20.04.15 from http://met.no/Klima/Klimastatistikk/Klimanormaler/Temperatur/.
MET (2015c). *Nord-Norge siden 1900.* Norwegian Meteorological Institute (MET) Downloaded 22.04.15 from http://met.no/Klima/Klimautvikling/Klima_siste_150_ar/Regioner/Nord_-_Norge/.
MET (2015d). *What is eKlima?* Norwegian Meteorological Institute (MET). Downloaded 25.04.15 from http://sharki.oslo.dnmi.no/portal/page?_pageid=73,39035,73_39049and_dad=portal&_schema=PORTAL.

Nordli, P. Ø. (1990). Inversion Characteristics in a Valley. Data from Máze (Masi) on Finnmarksvidda, Northern Norway. *Geografiska Annaler. Series A, Physical Geography, 72*(2), 157-166. doi: 10.2307/521111

Norgeibilder. (2015). *Norge i bilder.* The Norwegian Mapping Authority, the Norwegian Public Roads Administration and the Norwegian Forest and Landscape Institute. Downloaded during the period January 2014 to April 2015 from norgeibilder.no.

Oksanen, P. O. (2005). *Development of palsa mires on the northern European continent in relation to Holocene climatic and environmental changes*: University of Oulu.

Olea, P. P., Mateo-Tomás, P., and De Frutos, Á. (2010). Estimating and modelling bias of the hierarchical partitioning public-domain software: implications in environmental management and conservation. *Plos One, 5*(7), e11698.

Parviainen, M., and Luoto, M. (2007). Climate envelopes of mire complex types in Fennoscandia. *Geografiska Annaler Series a-Physical Geography, 89A*(2), 137-151. doi: 10.1111/j.1468-0459.2007.00314.x

Payette, S., Delwaide, A., Caccianiga, M., and Beauchemin, M. (2004). Accelerated thawing of subarctic peatland permafrost over the last 50 years. *Geophysical Research Letters, 31*(18). doi: 10.1029/2004gl020358

Pike, G., Pepin, N. C., and Schaefer, M. (2013). High latitude local scale temperature complexity: the example of Kevo Valley, Finnish Lapland. *International Journal of Climatology, 33*(8), 2050-2067. doi: 10.1002/joc.3573

Pissart, A. (2013). 8.16 Palsas and Lithalsas. In J. F. Shroder (Ed.), *Treatise on Geomorphology* (pp. 223-237). San Diego: Academic Press.

R Core Team (2014). R: A language and environment for statistical computing. Foundation for Statistical Computing, Vienna, Austria. URL http://www.R-project.org/.

Ridefelt, H., Etzelmüller, B., and Boelhouwers, J. (2010). Spatial Analysis of Solifluction Landforms and Process Rates in the Abisko Mountains, Northern Sweden. *Permafrost and Periglacial Processes, 21*(3), 241-255.

Riseborough, D., Shiklomanov, N., Etzelmüller, B., Gruber, S., and Marchenko, S. (2008). Recent advances in permafrost modelling. *Permafrost and Periglacial Processes, 19*(2), 137-156. doi: 10.1002/ppp.615

Robin, X., Turck, N., Hainard, A., Tiberti, N., Lisacek, F., Sanchez J. C. and Müller, M. (2011). pROC: an open-source package for R and S+ to analyze and compare ROC curves. *BMC Bioinformatics*, 12, pp. 77.

Romanovsky, V., Drozdov, D., Oberman, N., Malkova, G., Kholodov, A., Marchenko, S., Moskalenko, N., Sergeev, D., Ukraintseva, N., and Abramov, A. (2010). Thermal state of permafrost in Russia. *Permafrost and Periglacial Processes, 21*(2), 136-155.

Schaefer, K., Zhang, T., Bruhwiler, L., and Barrett, A. P. (2011). Amount and timing of permafrost carbon release in response to climate warming. *Tellus B, 63*(2), 165-180.

Schneider von Deimling, T., Meinshausen, M., Levermann, A., Huber, V., Frieler, K., Lawrence, D., and Brovkin, V. (2012). Estimating the near-surface permafrost-carbon feedback on global warming. *Biogeosciences, 9*, 649-665.

Schuur, E., Abbott, B., Bowden, W., Brovkin, V., Camill, P., Canadell, J., Chanton, J., Chapin III, F., Christensen, T., and Ciais, P. (2013). Expert assessment of vulnerability of permafrost carbon to climate change. *Climatic Change, 119*(2), 359-374.

Schuur, E. A., Bockheim, J., Canadell, J. G., Euskirchen, E., Field, C. B., Goryachkin, S. V., Hagemann, S., Kuhry, P., Lafleur, P. M., and Lee, H. (2008). Vulnerability of

permafrost carbon to climate change: Implications for the global carbon cycle. *BioScience, 58*(8), 701-714.
Seppälä, M. (1982). *An experimental study of the formation of palsas.* Paper presented at the Proc. 4th Can. Permafrost Conf.
Seppälä, M. (1986). The origin of palsas. *Geografiska annaler. Series A. Physical geography, 68*(3), 141-147.
Seppälä, M. (1988). Palsas and related forms. *Advances in periglacial geomorphology*, 247-278.
Seppälä, M. (1990). Depth of snow and frost on a palsa mire, Finnish Lapland. *Geografiska annaler. Series A. Physical geography*, 191-201.
Seppälä, M. (1994). SNOW DEPTH CONTROLS PALSA GROWTH. *Permafrost and Periglacial Processes, 5*(4), 283-288. doi: 10.1002/ppp.3430050407
Seppälä, M. (2003). Surface abrasion of palsas by wind action in Finnish Lapland. *Geomorphology, 52*(1-2), 141-148. doi: 10.1016/s0169-555x(02)00254-4
Seppälä, M. (2005). Dating of palsas. *Quaternary studies in the northern and Arctic regions of Finland. Geological Survey of Finland, Special Paper, 40*, 79-84.
Seppälä, M. (2006). Palsa mires in Finland. *The Finnish environment, 23*, 155-162.
Seppälä, M. (2011). Synthesis of studies of palsa formation underlining the importance of local environmental and physical characteristics. *Quaternary Research, 75*(2), 366-370. doi: 10.1016/j.yqres.2010.09.007
Seppälä, M., and Kujala, K. (2009). The role of buoyancy in palsa formation. In J. Knight and S. Harrison (Eds.), *Periglacial and Paraglacial Processes and Environments* (Vol. 320, pp. 51-56).
Shindell, D. T., Faluvegi, G., Koch, D. M., Schmidt, G. A., Unger, N., and Bauer, S. E. (2009). Improved attribution of climate forcing to emissions. *Science, 326*(5953), 716-718.
Sjöberg, Y., Frampton, A., and Lyon, S. W. (2013). Using streamflow characteristics to explore permafrost thawing in northern Swedish catchments. *Hydrogeology Journal, 21*(1), 121-131. doi: 10.1007/s10040-012-0932-5
Skog og landskap. (2015). Nedlastning av kartdata – AR5. The Norwegian Forest and Landscape Institute. Downloaded in September 2015 from http://www.skogoglandskap.no/kart/ar5/artikler/2008/nedlasting_ar5.
Smith, M. W., and Riseborough, D. W. (2002). Climate and the limits of permafrost: A zonal analysis. *Permafrost and Periglacial Processes, 13*(1), 1-15. doi: 10.1002/ppp.410
Smith, S., Romanovsky, V., Lewkowicz, A., Burn, C., Allard, M., Clow, G., Yoshikawa, K., and Throop, J. (2010). Thermal state of permafrost in North America: a contribution to the international polar year. *Permafrost and Periglacial Processes, 21*(2), 117-135.
SNL (2009). *Gáisene.* Store norske leksikon (SNL). Downloaded 21.04.15 from https://snl.no/G%C3%A1isene.
SNL (2014). *Finnmarksvidda.* Store Norske Leksikon (SNL). Downloaded 20.04.15 from https://snl.no/Finnmarksvidda.
SNL (2015). *Finnmark.* Store Norske Leksikon (SNL). Downloaded 20.04.15 from https://snl.no/Finnmark.
Sollid, J., and Sørbel, L. (1974). Palsa bogs at Haugtjørnin, Dovrefjell, South Norway.
Sollid, J. L., and Sørbel, L. (1998). Palsa bogs as a climate indicator - Examples from Dovrefjell, southern Norway. *Ambio, 27*(4), 287-291.
Statistics Norway. (2015). *Utslipp av klimagasser.* Statistics Norway. Downloaded 05.05.15 from

https://www.ssb.no/statistikkbanken/selectvarval/Define.asp?subjectcode=&ProductId=&MainTable=UtslKlimaKildeR&nvl=&PLanguage=0&nyTmpVar=true&CMSSubjectArea=natur-og-miljo&KortNavnWeb=klimagassn&StatVariant=&checked=true.

St Jacques, J. M., and Sauchyn, D. J. (2009). Increasing winter baseflow and mean annual streamflow from possible permafrost thawing in the Northwest Territories, Canada. *Geophysical Research Letters, 36*. doi: 10.1029/2008gl035822

Svensson, H. (1961). Några iakttagelser från palsområden.

Svensson, H. (1969). A type of circular lakes in northernmost Norway. *Geogr Ann Ser A; Lund Stud Geogr Ser A Phys Geogr, 51*(1-2), 1-12.

Swets, J. A. (1988). Measuring the accuracy of diagnostic systems. *Science, 240*(4857), 1285-1293.

Tarnocai, C., Canadell, J., Schuur, E., Kuhry, P., Mazhitova, G., and Zimov, S. (2009). Soil organic carbon pools in the northern circumpolar permafrost region. *Global Biogeochemical Cycles, 23*(2).

Tveito, O.E., Førland, E.J., Heino, R., Hanssen-Bauer, I., Alexandersson, H., Dahlström, B., Drebs, A., Kern-Hansen, C., Jónsson, T., Laursen, E.V. and Westman, Y. (2000). *Nordic temperature maps (Nordklim)*. DNMI KLIMA Report 09/00.

Vallee, S., and Payette, S. (2007). Collapse of permafrost mounds along a subarctic river over the last 100 years (northern Quebec). *Geomorphology, 90*(1-2), 162-170. doi: 10.1016/j.geomorph.2007.01.019

van Everdingen, R. (1998). Multi-language glossary of permafrost and related ground-ice terms, Natl. *Snow and Ice Data Cent., Boulder, Colo*.

Vaughan, D. G., Comiso, J. C., Allison, I., Carrasco, J., Kaser, G., Kwok, R., Mote, P., Murray, T., Paul, F., Ren, J., Rignot, E., Solomina, O., Steffen, K., and Zhang, T. (2013). Observations: Cryosphere. In T. F. Stocker, D. Qin, G.-K. Plattner, M. Tignor, S. K. Allen, J. Boschung, A. Nauels, Y. Xia, V. Bex and P. M. Midgley (Eds.), *Climate Change 2013: The Physical Science Basis. Contribution of Working Group I to the Fifth Assessment Report of the Intergovernmental Panel on Climate Change* (pp. 317–382). Cambridge, United Kingdom and New York, NY, USA: Cambridge University Press.

Vorren, K. (1972). Stratigraphical investigations of a palsa bog in northern Norway. *Astarte, 5*(1-2), 39-71.

Vorren, K. D. (1979). Recent palsa datings, a brief survey. *Norsk Geografisk Tidsskrift, 33*(4), 217-219.

Vorren, K. D., and Vorren, B. (1975). THE PROBLEM OF DATING A PALSA 2 ATTEMPTS INVOLVING POLLEN DIAGRAMS DETERMINATION OF MOSS SUB FOSSILS AND CARBON-14 DATINGS. *Astarte, 8*(2), 73-81.

Walsh, C. and Mac Nally, R. (2013). Package "hier.part". Downloaded 10.05.15 from http://cran.r-project.org/web/packages/hier.part/hier.part.pdf.

Walvoord, M. A., and Striegl, R. G. (2007). Increased groundwater to stream discharge from permafrost thawing in the Yukon River basin: Potential impacts on lateral export of carbon and nitrogen. *Geophysical Research Letters, 34*(12). doi: 10.1029/2007gl030216

Washburn, A. (1980). Permafrost features as evidence of climatic change. *Earth-Science Reviews, 15*(4), 327-402.

Wilson, D., Hisdal, H., and Lawrence, D. (2010). Has streamflow changed in the Nordic countries? Recent trends and comparisons to hydrological projections. *Journal of Hydrology, 394*(3-4), 334-346.

Wramner, P. (1965). Fynd av palsar med mineraljordkärna I Sverige: En preliminär rapport. *Geologiska Föreningen i Stockholm Förhandlingar, 86*(4), 498-499. doi: 10.1080/11035897.1965.9626399

Zhao, L., Wu, Q., Marchenko, S., and Sharkhuu, N. (2010). Thermal state of permafrost and active layer in Central Asia during the International Polar Year. *Permafrost and Periglacial Processes, 21*(2), 198-207.

Zimov, S., Davydov, S., Zimova, G., Davydova, A., Schuur, E., Dutta, K., and Chapin, F. (2006). Permafrost carbon: Stock and decomposability of a globally significant carbon pool. *Geophysical Research Letters, 33*(20).

Zoltai, S. C. (1993). CYCLIC DEVELOPMENT OF PERMAFROST IN THE PEATLANDS OF NORTHWESTERN ALBERTA, CANADA. *Arctic and Alpine Research, 25*(3), 240-246. doi: 10.2307/1551820

Zuidhoff, F. S. (2002). Recent decay of a single palsa in relation to weather conditions between 1996 and 2000 in Laivadalen, northern Sweden. *Geografiska Annaler Series a-Physical Geography, 84A*(2), 103-111. doi: 10.1111/1468-0459.00164

Zuidhoff, F. S., and Kolstrup, E. (2000). Changes in palsa distribution in relation to climate change in Laivadalen, northern Sweden, especially 1960-1997. *Permafrost and Periglacial Processes, 11*(1), 55-69. doi: 10.1002/(sici)1099-1530(200001/03)11:1<55::aid-ppp338>3.0.co;2-t

Zuidhoff, F. S., and Kolstrup, E. (2005). Palsa development and associated vegetation in northern Sweden. *Arctic Antarctic and Alpine Research, 37*(1), 49-60. doi: 10.1657/1523-0430(2005)037[0049:pdaavi]2.0.co;2

Åhman, R. (1977). *Palsar i Nordnorge: en studie av palsars morfologi, utbredning och klimatiska förutsättningar i Finnmarks och Troms fylke*: Department of Geography, The Royal University of Lund.

Appendix

A.1: Information about aerial images over Lakselv utilized in this thesis. ND = No Data.

Lakselv (15-60 m a.s.l.)		
Date of capture:	20.07.1959	11.09.2008
Mission name:	Alta-Banak	Finnmark 2008
Coverage number:	WF-2120	13668
Image number:	W-19, W-21, X-15, X-17, Y-14	03-90, 02-93, 02-94, 02-95, 01-100
Source:	Aerial image archive*	Norgeibilder.no
Owner:	The Norwegian Mapping Authority	The Norwegian Mapping Authority
Firm/producent:	Widerøes Flyveselskap	TerraTec AS
Film type:	Panchromatic (black-white)	Digital RGB
Focal length [mm]:	210	ND
Camera:	Wild RC5	Not available
GSD/spatial resolution [m]:	0.26	0.5
Image scale:	1:20 000	ND
Altitude [m a.s.l.]:	4600	ND
Bits per pixel (digital sensors):		24
* http://159.162.103.4/geovekst/Flybildearkiv/		

A.2: Information about aerial images over Suossjavri utilized in this thesis. ND = No Data.

Suossjávri (310-360 m a.s.l.)				
Date:	16.08/08.09 - 1956	21.07.1959	01.07/15.07 - 1982	
Mission name:	Masi	Kautokeino	Finnmarksvidda, Jiesjav`ri	
Coverage number:	WF-0819	WF-2121	NLF-07523	
Image number:	K-2, K-3, M-1,	K-47, J-50	K-3, K-4, K-6, J-4, J-5	
Source:	Aerial image archive*	Aerial image archive*	Aerial image archive	
Owner:	The Norwegian Mapping Authority	The Norwegian Mapping Authority	The Norwegian Mapping Authority	
Firm:	Widerøes Flyveselskap	Widerøes Flyveselskap	Norsk luftfoto og fjernmåling	
Producent:	Widerøes Flyveselskap	Widerøes Flyveselskap	Norsk luftfoto og fjernmåling	
Film type:	Panchromatic (black-white)	Panchromatic (black-white)	Analog RGB-film	
Camera:	Wild RC5	Wild RC5	Wild RC10	
Focal length [mm]:	210	210	152	
GSD/spatial resolution [m]:	0.24	0.24	0.36	
Image scale:	1:20000	1:20000	1:25000	
Altitude [m a.s.l.]:	4600	4600	ca. 5000	
Bits per pixel (digital sensors):				

* http://159.162.103.4/geovekst/Flybildearkiv/

Suossjavri (310-360 m a.s.l.)	
01.07.2003	17.08.2011
Suossjavri 1933_1	Finnmark 2011
3067	13990
ND	04-65, 04-66, 03-66, 03-67, 04-68, 05-68, 04-69, 05-69, 04-70
Norgeibilder.no	Norgeibilder.no
The Norwegian Mapping Authority	Omløpsfoto
Fotonor AS	TerraTec AS
The Norwegian Mapping Authority	TerraTec AS
Panchromatic (black-white)	Digital RGB
ND	ND
ND	ND
0.5	0.4
ND	ND
ND	ND
8	24

A.3 Information about aerial images over Goatheluoppal utilized in this thesis. ND = No Data

Goatheluoppal (440 m a.s.l.)			
Date:	21-22.08.1958	18-20.07.1980	01.07.2003
Mission name:	Kautokeino	Finnmarksvidda vest	Addjit 1832_4
Coverage number:	WF-2033	NLF-06442	3067
Image number:	C-14, C-16	P-6, Q-4	ND
Source:	Aerial image archive*	Aerial image archive*	Norgebilder.no
Owner:	The Norwegian Mapping Authority	The Norwegian Mapping Authority	The Norwegian Mapping Authority
Firm:	Widerøes Flyveselskap	Norsk luftfoto og fjernmåling	Fotonor AS
Producent:	Widerøes Flyveselskap	Norsk luftfoto og fjernmåling	The Norwegian Mapping Authority
Film type:	Panchromatic (black-white)	Analog RGB-film	Panchromatic
Camera:	Wild RC5	Wild RC10	ND
Focal length [mm]:	210	153	ND
GSD/spatial resolution [m]:	0.24	0.31	0.5
Image scale:	1:20000	1:25000	ND
Altitude [m a.s.l.]:	4700	4300	ND
Bits per pixel (digital sensors):			8

* http://159.162.103.4/geovekst/Flybildearkiv/

Goatheluoppal (440 m a.s.l.)
14.08.2012
Finnmark 2012
14055
13-5, 13-6, 14-5, 14,6
Norgeibilder.no
Omløpsfoto
TerraTec AS
TerraTec AS
Digital RGB
ND
ND
0.4
ND
ND
24